EFFECT OF DYNAMIC THERMAL BOUNDARIES ON RESIDUAL STRESSES IN INJECTION MOLDING

by

DAVID D. SHA

B.S., Mechanical Engineering, University of California, Berkeley, 1992

B.A., Applied Mathematics, University of California, Berkeley, 1992

Submitted to the Department of Mechanical Engineering
in Partial Fulfillment of the
Requirements for the Degree of

MASTER OF SCIENCE

at the

Massachusetts Institute of Technology

August 1995

Signature of Author.....
Department of Mechanical Engineering
August 31, 1995

Certified by.....
David E. Hardt
Professor of Mechanical Engineering
Thesis Supervisor

Accepted by.....
Ain A. Sonin
Chairman, Graduate Committee

EFFECT OF DYNAMIC THERMAL BOUNDARIES ON RESIDUAL STRESSES IN INJECTION MOLDING

by
David D. Sha

Submitted to the Department of Mechanical Engineering on August 31, 1995,
in partial fulfillment of the requirements for the Degree of Master of Science

Abstract

The thesis objective was to determine the effect of mold thermal spatial variations on the reduction of polymer residual stresses in injection molding. An aluminum mold with a rectangular cavity constructed with lamination layers and Plexiglas windows was employed. The spatial thermal variations were manipulated with cartridge heaters and cooling channels perpendicular to the direction of the melt flow front. The polystyrene melt temperatures were directly measured to determine the effects of the thermal profiles.

In conventional molding, without heating or cooling, direct melt temperature measurements showed that the temperature profile of the melt had a skewed parabolic thermal profile. In a rectangular part the middle (flowlength) region had the highest temperatures, the sprue region cooler, and the end of the cavity coldest. A mold thermal profile inverse to this skewed parabolic melt thermal profile should balance the cooling, thereby reduce residual stresses. Experimental results validated this hypothesis.

Furthermore, correlations were developed which use the latent heat of fusion as a basis of the thermal analysis. These correlations calculate the skin layer thickness during injection and the solidification front speed after filling. Warpage calculations were based on those calculations.

The melt temperature distribution in the injection unit nozzle was nonuniform and had temporal and spatial variations of 10°F and 15°F, respectively. Additionally, thermal inertia imbalance between mold halves was established to be as great as 30°F. These nonuniform initial conditions represent a hazard to rapid thermal cycling of the mold that may create greater variations in melt temperatures. Thus, the application of low thermal inertia injection molding with rapid temperature cycling heavily relies on an in depth analysis and understanding of heat transfer mechanisms in injection molding. Such a treatment is presented in this thesis.

Furthermore, an alternate method of observing thermal spatial variations on the mold was developed. Photoelastic methods were employed to observe the development of birefringence patterns (caused by stresses in the melt) in a rectangular cavity constructed with a transparent window on each side. These birefringence patterns can be correlated with the residual stresses in the part that caused the warpage. The evolution of the birefringence patterns facilitates the generation of appropriate thermal profiles to balance these fringe patterns, thereby reducing residual stresses.

Thesis Supervisor: Dr. David E. Hardt
Title: Professor of Mechanical Engineering

Dedication

To my wife and best friend,
Sandra Sha,
the little one to come,
and my family.

Thank you for your encouragement,
love, and support.

Acknowledgments

I would like to acknowledge the support of the Leaders for Manufacturing research assistantship, a partnership between MIT and major US manufacturing firms.

I am grateful to the following people:

Professor David E. Hardt for his guidance and patience. His kindness and generosity will always be remembered and appreciated.

Earl Sun and Ed Wylonis for their time in helping me run the injection molding machine.

Fred Cote for various maching projects.

Andrew Parris and Peter Noymer for their careful thesis reading and insightful suggestions on how to improve this thesis.

Various portions of this thesis incorporate information written by Byung H. Kim, J.R. Rinderle, J.N. Border, Earl Sun, and Ed Wylonis.

Ken Amoruso, Benny Budiman, Upendra Ummethala, and Dan Walczyk for their unique and interesting personalities that made our lab an enjoyable experience.

CONTENTS

List of Figures

List of Tables

Nomenclature

A	Cross sectional area
c	Relative stress-optic coefficient (c_2 - c_1)
c_1	Stress-optic coefficient
c_2	Stress-optic coefficient
C	Stress-optical coefficient of the material
Cp_m	Specific heat of the mold
Cp_p	Specific heat of the plastic
d	Maximum deflection of the plate or warpage
Dim	Dimensions of the product
E	(1) Activation energy for viscosity
	(2) Elastic modulus of the plastic
$\bar{E}$	Average value of the elastic modulus
Geom	Mold geometry
h_{sfp}	Latent heat of fussion for the plastic
I	Moment of inertia in bending
Ja	Jacob number
k_m	Thermal conductivity of the mold
k_p	Thermal conductivity of the plastic
L	length
L_1	Length of cavity (length of part)
L_2	Half thickness of mold cavity thickness
M	Bending moment
$\dot{m}$	Mass flow rate
n	Index of refraction
n_0	Index of refraction in unstressed state
n_1	Stressed state index of refraction associated with σ_1
n_2	Stressed state index of refraction associated with σ_2
n_3	Stressed state index of refraction associated with σ_3
N	Fringe order
p_0	Specific pressure
$\hat{p}$	Material property
P	Pressure
P_{atm}	Atmospheric pressure
P_b	Back pressure
P_f	Final pressure
P_{fill}	Cavity filling pressure
P_i	Initial pressure
P_p	Packing pressure

P_r	Asymptotic value of pressure
q	Heat flux
$\dot{Q}$	Cooling rate
R	(1) Material property (2) Gas constant
s(t)	Thickness of the solidified melt
Struct	Structural part qualities
$\frac{ds}{dt}$	Speed of solidification front growth
t	(1) Thickness (2) Time
t_c	Total contact time of the mold and plastic interface
t_{cool}	Time when the cavity's center has reached the glass transition point
t_{cure}	Time when thermal equilibrium in the part is reached
t_{fill}	Time when cavity is filled
t_{fp}	Time between filling and packing
t_{gf}	Time when gate "freezes-off"
t_R	Relaxation time constant of the skin layer
t_0	Time when the melt first enters the mold
t_1	Intermediate filling time
T	Temperature
T_{ave}	Bulk temperature of the melt
T_c	Temperature at the mold and melt interface
T_i	Initial temperature
T_f	Final temperature
T_g	Glass transition temperature
T_m	Temperature of the melt
T_o	Initial temperature of the mold
$\hat{v}$	Material property
v	(1) Velocity (2) Specific volume
v_i	Initial volume
v_{inj}	Wave front speed in the mold (melt flow speed in the x direction)
v_f	Final volume
W	Width of cavity or optical path (= 12 mm or 15 mm)
x	Coordinate axis for flow along the mold's length (flow direction)
x_{front}	Leading edge of the fountain flow front in contact with the cavity
y	Coordinate axis for flow perpendicular to the mold's length flow (origin located from the centerline of the cavity)
z	Same as y except the origin is located from the mold's surface
α_m	Thermal diffusivity for the mold
α_p	Thermal diffusivity for the plastic
$\delta(t)$	Thickness of the mold
δ_{flux}	Diffusion length of heat flux

δ_{99}	length of thermal penetration in the mold such that $\frac{T_m(\delta,t)-T_c}{T_c-T_o}=0.99$
λ	Wavelength of the light source ($\lambda_{He\text{-}Ne}$ = 632.8 nm)
ρ	Density
ρ_m	Density for the mold
ρ_p	Density for the plastic
η	Viscosity
σ	Shear stress
σ_1	Principle stresses at a point in the first axis
σ_2	Principle stresses at a point in the second axis
σ_3	Principle stresses at a point in the third axis
γ'	Shear rate
π	(1) Material property
	(2) Numerical value = 3.14159....
ω	Material property
μ	Poisson's ratio
Λ	Warpage induced by the final solidification front thickness
Λ_{net}	Net warpage of a part.

CHAPTER I

Introduction

I.1 Motivation

Injection molding is one of the most commonly used methods of processing polymers. The process uses plastic pellets or powders that are melted and formed in a mold to allow rapid, automated production of a wide variety of complex, three-dimensional parts in large production volumes at low cost. The process is capable of producing compound curvatures, snaps, hinges, bosses, threaded holes, gear teeth and many other features. With proper design, these complex parts can be produced in a single molding operation, automated to increase production rates, and replace heavier and more costly metal components.

The injection molding process was patented by John and Isaiah Hyatt in 1872, but the process was not used extensively until World War II. The low cost and high production rate have made the injection molding process a very important manufacturing method. From 1972 to 1978[1], the volume of injection molded materials grew 15 fold or at an average rate of 57% per year. In 1980 injection molding was used to produce more than 5.4 billion pounds of thermoplastic parts with a material cost of more than $2.8 billion[2]. In 1981 more than 7.8 billion pounds of thermoplastic material was injection molded in the United States[3]. It is estimated that in the U.S. alone consumption of injection-molded polyethylene, polypropylene and polystyrene will rise to 11 billion pounds by 1997[4]. Critical to the expanding adoption of this high volume, low cost process technology is the ability to consistently produce quality parts. At the same time

---

[1] Frados, Joel, ed., Plastics Engineering Handbook, fourth edition, Van Nostrand Reinhold Co., New York, 1976, p. 89.
[2] Modern Plastics, Vol. 58, No.1, (January, 1981) pp. 67-73.
[3] Modern Plastics, Vol. 59, No.1, (January, 1982) pp. 77-87.

the need to improve the process to allow it to be applied to an ever increasing range of parts will become more important.

Although the rapid growth of this industry is a reflection of the benefits to be gained from injection molding, there are also some costs and some limitations on the application of the process. The direct costs of injection molding are the costs of the machines, molds, operators, materials, and energy. Injection molding tools (molds and related equipment) vary greatly in cost from perhaps $1,000 for a simple tool up to hundreds of thousands of dollars for multi-cavity molds for complex parts. Machines are also expensive and vary in price according to the maximum mold clamping force. Mold manufacturing time, final part quality and energy usage must also be considered when evaluating the costs versus benefits of injection molding. The typical temperature mold control start-up costs are $45,000 for a standard Zone Controller unit (provides three zones of control), $112-190 for mold temperature sensors, and $375-750 for induction heating elements.[5]

Therefore, the expense of the mold and the increasing demands on production cycle time reduction require a careful evaluation of all improveable processes. However, the research focus should be on the mold half, because the art of mold temperature control has only been recently investigated and the majority of the cycle time is on the mold cooling phase. This thesis demonstrates that dynamic mold temperature boundaries reduce residual stresses and warpage in the part while also improving the optical properties and quality repeatability of the part. This is a departure from the conventional thought and practice of injection molding that strives for an isothermal mold condition. The isothermal mold concept drastically increases the cycle time of the part and induces distortions in most parts, except in spherical parts or infinitely long bars where the solidification conduction paths are equal. Furthermore, a reduction in cycle time and cavity pressure can be realized using dynamic mold temperature boundaries because lower melt temperatures can be used to achieve comparable quality levels in controls with higher melt temperatures. This will translate to increased productivity of the mold through both

---

[4] School, Rudy, "Markets for Thermoplastic Elastomers," presented at the Society of Plastics Engineers 52nd Annual Technical Conference, San Francisco, 1994.

greater output per length of time from the reduced cycle time as well as increased operational life of the mold due to lower cavity pressure. Most importantly, dynamic thermal boundaries can add robustness to the design of the mold by thermally controlling the part as it solidifies. This technique can be used to bring parts into the range of tolerance through thermal manipulation. This ability to control mold temperature and heat transfer to obtain desired cooling rates will reap large savings in mold design costs on top of the increased productivity due to the reduced cycle time.

I.2 The Injection Molding Process

The injection molding process is primarily a sequential operation that results in the transformation of plastic pellets into a molded part. In thermoplastic injection molding, the plastic pellets are melted then forced under pressure through the barrel, sprue bushing, runner, and a narrow gate section into a mold cavity that is clamped closed with subsequent material solidification to retain the shape of the mold. The material freezes in the cold mold and is then ejected.

Although the term injection molding is most often used referring to thermoplastic injection molding, thermosetting materials and ceramic materials can also be processed by injection molding. Throughout this thesis thermoplastic injection molding will be discussed even though many of the concepts presented apply not only to injection molding of other materials but also to many other molding processes such as blow molding, transfer molding, compression molding, and casting.

An injection molding machine is composed of an injection unit, a clamping unit, and a control unit. The injection unit consists of the hopper, the barrel, the barrel heaters, the reciprocating screw and the nozzle. The clamping unit consists of the hydraulic clamping mechanism and the mold platens. The hydraulic unit consists of the hydraulic pump and all the associated plumbing and valving required to actuate the injection unit and the clamping unit. The ways in which injection molding machines perform the functions of

[5] Mould Control, REP, "Total Mould Temperature Control Systems," Reader enquiry number 208.

heating, injecting and clamping are the basis for the classification of injection molding machines. There are two basic varieties of injection molding machines, the reciprocating screw and the plunger type. In recent years the reciprocating screw machine has been found to be much easier to control than the plunger machine and as a result the reciprocating machine is used much more than the plunger machine and the most common type of injection unit today is the reciprocating screw as shown in Figure I.2.1. The reciprocating screw machine will be treated as the conventional molding machine in this thesis.

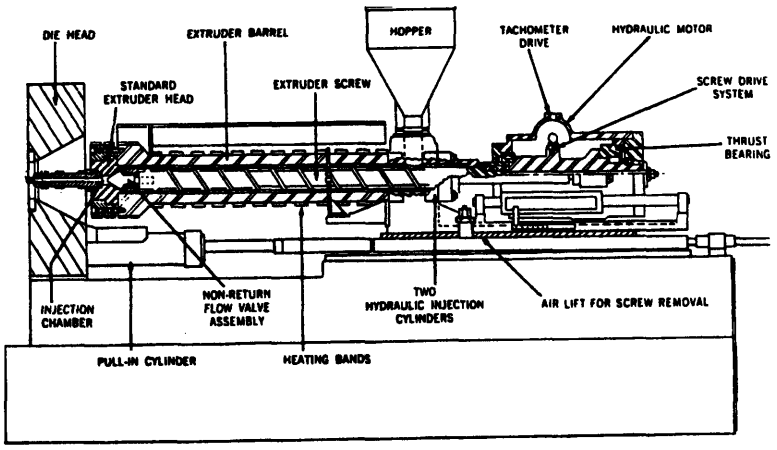

Figure I.2.1: Schematic of the injection end of a reciprocating screw machine.
(Courtesy Rubin, 1972 and the Van Nostrand Reinhold Company)

One major injection molding goal is to produce parts of consistently high quality. Part dimension consistency is the industry's standard measure of quality. This argues for controlling plastic part shrinkage, which is dependent on the molding variables of cavity pressure, mold temperature, melt temperature, and flow rate. Consequently, these variables should be controlled again with the focus on mold temperature manipulation.

The injection molding machine does not permit direct control over these variables but allows the operator to adjust machine settings that influence the molding variables. The inability to directly set and measure the molding variables that affect part shrinkage complicates the injection molding process. It is molding variables, properly defined and measured, not necessarily machine settings, that can be correlated with part properties.

For example, if one increases barrel temperature, melt temperatures do not necessarily also increase. Melt temperature is also influenced by screw design, rpm, back pressure and residence time. It is much more accurate to measure melt temperature and correlate it with properties than to correlate barrel settings with properties. Thus, the melt temperature distribution cannot be easily determined. This hampers the determination of the initial condition of the melt in the mold.

An injection molding process is characterized by four successive stages: plastication, injection of molten polymer, packing, and part cooling. The cycle that the machine executes is critical to understanding the molding process. During plastication, polymer pellets are fed by gravity from the feed hopper to the screw. The rotating screw causes material to be conveyed and to circulate in the screw flights. The conveyance and circulation of the material causes viscous heating and melting of the plastic pellets. The molten material collects in front of the screw as the screw is pushed backwards. The pressure on the screw is then increased, which causes the rotating screw to move forward by a hydraulic ram and the molten polymer is pushed through the barrel, sprue bushing, runner, and gate into the mold cavity. At the end of the screw the material passes through a one way valve and collects in the front of the barrel. In order to make room for the melted material the screw moves back in the barrel against a back pressure. As the plastic is transported along the barrel, heat is generated from the shear work done on the material and heat is conducted into the material from electric heater bands which surround the barrel. The polymeric material melts mainly due to the viscous heating effects as it moves along the screw and the barrel heaters have a minor contribution to the melting. Thus, the melting of the material is not limited by the low thermal conductivity of plastics.

The screw moves back because of the accumulation of plasticated material in front of the screw. Then the screw stops turning and is pushed forward by the hydraulic ram. The motion forward closes the one way valve near the screw tip which limits the polymer back flow so that the screw effectively becomes a plunger and forces the molten plastic into the mold. Plastication has transformed the solid plastic pellets into a melt which is at an elevated and nonuniform temperature, and nonuniform viscosity.

Plastication affects the repeatability of the molding process by influencing the viscosity of the melt. As previously discussed, viscosity is dependent on melt temperature and flow rate. During plastication, these molding variables are influenced by barrel temperatures and screw speed. Heat transferred from the barrel to the plastic results in the melting of the plastic pellets. The screw speed controls the shear force applied to the material. Shear force results in further heating—i.e., viscous dissipation—of the plastic. Back pressure also influences repeatability of the molding process because it determines the quantity of plastic in the barrel (it compresses the plastic). Ranges for these temperature, speed and pressure settings are usually provided by the material suppliers, and should be repeated accurately set-up to set-up.

During the injection the pressure applied to the hydraulic ram is very high. When the injection timer times out the pressure is reduced to a lower hold pressure. The hold pressure is maintained on the hydraulic ram until the hold timer times out. At this time the screw begins turning, preparing the melted material for the next shot as the part in the mold cools.

The injection rate must be carefully chosen. If the mold cooling effect is much greater than the screw viscous heating effect, the plastic will solidify before the mold is filled, resulting in a short shot. If the heating effect dominates, some of the material can degrade. A pressure in the range of 5,000 to 20,000 psi is usually required to obtain this rate. At the end of the injection period the flow fills the mold and stops, the pressure rises rapidly and the material begins to cool. As the material cools it shrinks slightly and more material is forced into the cavity by the hold pressure acting on the melt. This portion of the molding cycle is called the hold or the packing stage and continues until the hold pressure is released or until the gate freezes. After the gate has frozen the material continues to cool, which at first causes a reduction in pressure (to atmospheric) and then shrinkage of the material in the cavity. When the part has solidified sufficiently to remain dimensionally stable during ejection and to retain the shape of the cavity (accounting for shrinkage), the mold is opened and pins eject the part, runner, and sprue from the mold. The mold then closes and the next injection cycle begins.

A more complete introduction to the injection molding process has been written by Rubin[6] and a detailed analysis of this type of plastization is given by Tadmor and Klein[7].

The clamping units on injection molding machines are either hydraulic or mechanical. Hydraulic clamps use the pressure in a large cylinder to hold the mold halves closed. The largest molding machines use hydraulic clamps. Mechanical clamps consist of an arrangement of moving bars that lock the mold halves together. The clamping forces are very high which makes the clamping unit the most expensive part of the molding machine.

A typical mold cavity pressure curve for an injection cycle is shown in Figure I.2.2. The cavity pressure is an important process variable since it affects the state of the molding part directly. The four stages of the injection molding cycle can be readily inferred from the cavity pressure curve.

The Spencer Gilmore equation[8] relates pressure and temperature as follows:

$$(p_0 + \hat{p})(v - \hat{v}) = RT \qquad (1)$$

The equation indicates that a pressure variation causes spatial temperature variations in the melt with the bulk melt temperature to be lowest near the front. Furthermore, because the mold cavity pressure curve indicates that the pressure is both a spatial and temporal function, the temperature within the melt must have this functional form.

The pressure trace of a molding cycle recorded directly in the cavity is shown below in Figure I.2.2.[9]

---

[6] Rubin, Irvin I., Injection Molding of Plastics, John Wiley and Sons, Inc., New York, 1973.
[7] Tadmore, Z., Engineering Principles of Plasticating Extrusion, Van Nostrand Reinhold Co., New York, 1970.
[8] Spencer, R.S., and D.G. Gilmore, "Equations of State for High Polymers," J. Of Applied Physics, Vol. 21, (June 1950).
[9] Greener, J., and G.H. Pearson, "Orientation Residual Stresses and Birefringence in Injection Molding," Journal of Rheology, 27(2), 115-134 (1983).

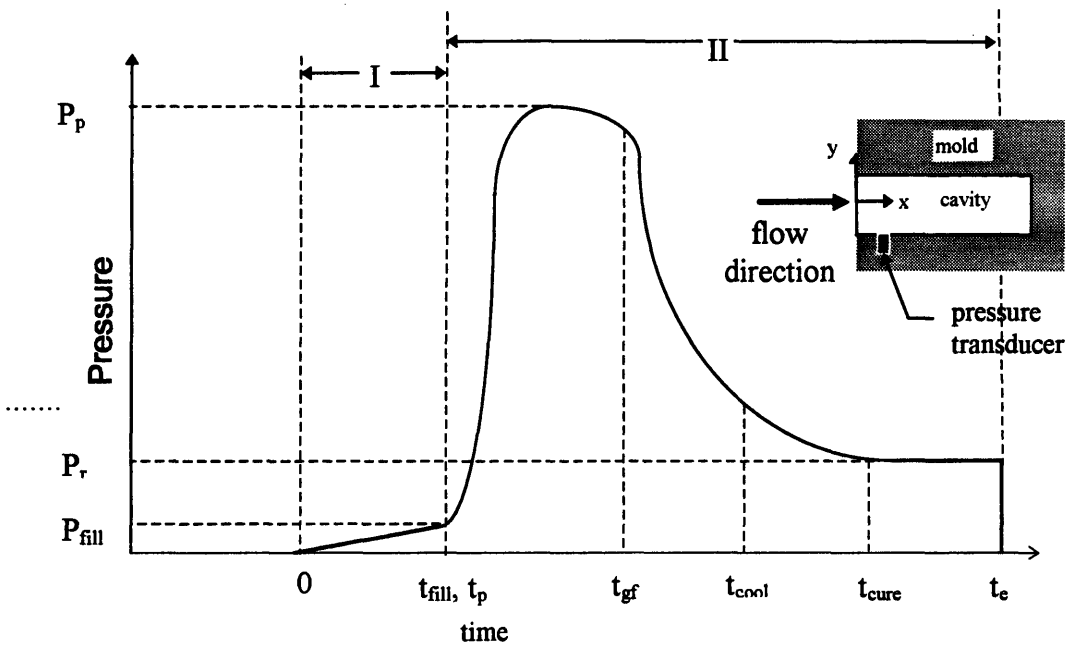

Figure I.2.2: Thin cavity filling pressure trace of one injection molding cycle. (Courtesy Greener and Pearson, 1983)

The cycle begins at time $t_0 = 0$ when the hot melt enters the cavity through a narrow gate. During filling ($t_0 \rightarrow t_{fill}$), the shear rate and the velocity decrease with increasing time in the vicinity of the wall as a result of mold cooling. Therefore, to maintain a constant flow rate, the velocity increases in the hot core region, with the associated maximum shear rate moving continually inward from the wall with increasing time. At time t_{fill}, as the cavity is just filled, the flow in the mold virtually stops and the pressure begins a rapid increase. This time marks the end of the mold-filling phase (I) and beginning of the packing-and-cooling or postfilling phase (II). P_{fill}, the pressure at the end of phase I, is the cavity-filling pressure, i.e., the pressure expended on filling the cavity with molten polymer under the set conditions. To maintain a high pressure in the cavity during phase II (to counteract shrinkage caused by cooling) some inflow through the gate must continue beyond t_{fill}. However, for low packing pressures (P_p), this flow is confined to the neighborhood of the gate and is expected to have limited effect on the overall level of molecular orientation in the molded part. P_p is kept roughly constant until, at t_{gf} the gate "freezes-off." After t_{gf} the pressure is controlled by the dynamics of cooling, whereupon it decays unimpeded toward some asymptotic value P_r, the material in the

cavity is already solid. In fact, at t_{cool} the center of the cavity has reached the glass transition point, beyond which no further long-range molecular reordering is possible. Nearly complete thermal equilibrium is reached at some later time t_{cure}. Finally, at time t_e the cycle is arbitrarily terminated when the mold is opened and the part is exposed to ambient temperature and pressure. However, the pressure profile varies along the length of the mold with lower pressure at the end of the mold due to greater shrinkage and the reduced effect of packing. Since pressure is directly proportional to temperature the temperature distribution will likely follow this trend. A typical pressure gradient profile is shown below.

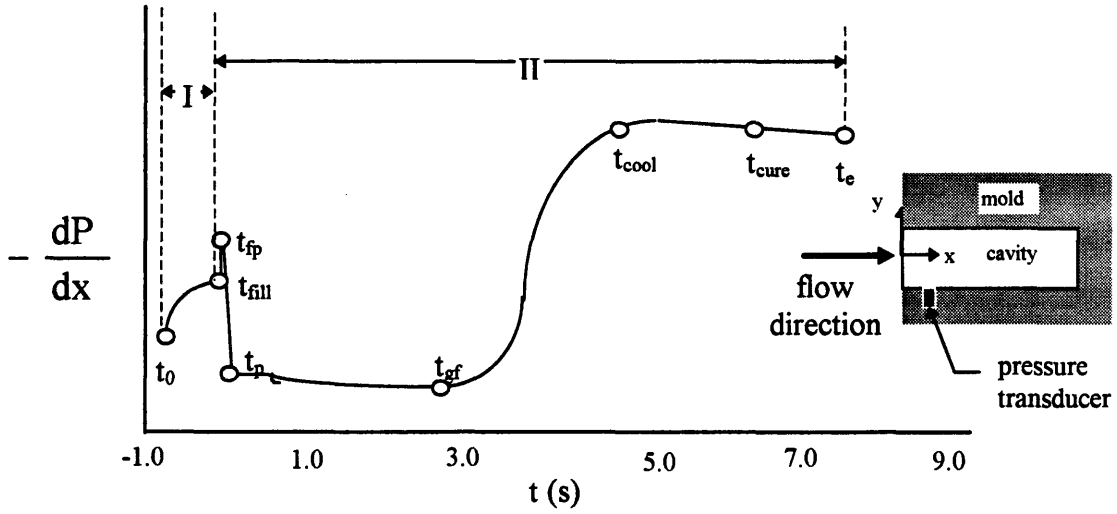

Figure I.2.3: Thin cavity filling pressure gradient trace of one injection molding cycle.

Development Of Residual Stresses In Molding

The buildup of stress components will now be discussed using the above figure by dividing the process into the discrete time levels indicated in the above figure. During filling ($t_0 \rightarrow t_{fill}$), the shear rate and the velocity decrease with increasing time in the vicinity of the wall as a result of mold cooling. Hence, to maintain a constant flow rate, the velocity increases in the hot core region, with the associated maximum shear rate moving continually inward from the wall with increasing time. This leads to an increase in the pressure gradient and consequently also to an increase in the normal stress and the

shear stress. The shear stress is linear in the thickness direction. Owing to the decreasing temperature in the wall region, the skin layer relaxation time constants increase and the developed stresses cannot relax anymore. This results in the stress profiles at the end of the filling stage, t_{fill}. The normal stress increases from the center of the channel to the wall until a maximum is reached. From this maximum, which lies in the neighborhood of the solidified layer, the normal stress decreases again. The major part of the stress in this region is frozen in. The characteristic normal-stress profile close to the wall is completely determined by the choice of the boundary condition at the melt front during the filling stage. The normal stress increases in value toward the wall, with a maximum value at the wall. When the front is passed, the normal stress starts to grow in that region where the temperature is still high enough.

Just after filling, when the system changes to the packing stage, the high pressure at the entrance of the cavity causes a sharp increase in the pressure gradient during a short period of time ($t_{fill} \rightarrow t_{fp}$). This results in a small increase of the normal stress and the shear stress, at least in that region where the temperature allows changes. In approximately 3×10^{-2} s ($t_p - t_{fp}$), the pressure gradients smooth out in the entire cavity because of the supply of extra material. The normal stress, as well as the shear stress, relaxes in the regions where the temperature is still high enough.

The decay of pressure, which starts at the end of the cavity, is determined by the competition between cooling and additional material flow, caused by a developing pressure gradient. The difference in the slope of the pressure decay of the transducers shows that more material is supplied in the neighborhood of the entrance. The increase in the pressure gradient, which starts at roughly t_{gf}, causes an increase in the stresses. During this increase the stresses are frozen in at a certain level because of the decreasing temperature. The stresses at t_{cure} are the final frozen-in values, which also determine the final frozen-in birefringence.[10] The correlation between the pressure gradient and the residual stresses might explain the observed disappearance of the birefringence patterns shortly after filling ($t_p \rightarrow t_{gf}$).

---

[10] Flaman, A.A.M., "Buildup and Relaxation of Molecular Orientation in Injection Molding, Part I: Formulation," Polymer Engineering and Science, 33, 4, (February 1993), p. 193-201.

I.3 Plastic Properties

The polymeric materials used in this process can reduce corrosion, can provide electrical insulation, and can greatly reduce weight and cost. Polymers are generally lighter (20%) than metals, less stiff (1%-5%), less thermally conductive (3%), not as strong (10%), and more ductile (10,000%). They also have a greater coefficient of thermal expansion (400%) than metals. Plastics are also less expensive than metals. On a weight basis plastics cost about 25% of what metals cost and on a volume basis are only 5% as expensive. Plastic materials do have severe limitations at high temperatures or under concentrated loads. [11]

The polymer chains that comprise the plastic intertwine with each other and are held together by covalent and van der Waals bonding forces. Thermoplastics are classified as either amorphous or crystalline depending on their molecular structure at room temperature. Amorphous plastics have a random structure. Crystalline plastics have an ordered structure, which takes up much less space than the amorphous state. Actually, no material is perfectly crystalline; amorphous sections will occur throughout a crystalline material. At melt temperature, all plastics are amorphous. The structure of the plastic is important because it affects the plastic's properties.

Because the amount of crystallinity varies with the material and molding conditions, it is much more difficult to hold tolerances in crystalline materials than in amorphous ones. Plastics have several additional properties that influence the repeatability of the molding process (Table I.3.1)[12]. First, plastics are compressible. The pressure in the mold cavity determines how much the melt is compressed. If all other variables are held constant, a higher hydraulic pressure results in a higher cavity pressure and will force more plastic into the mold cavities. Second, plastics shrink significantly when cooled. Together these properties indicate the need for the packing stage during the molding

---

[11] Rinderle, James R., "A Method for Precision Injection Molding," Master of Science Thesis, M.I.T., June 1979.

[12] Budill, K.T.., "A Systematic Approach to Tool Qualification for Injection Molding," Master of Science Thesis, M.I.T., p. 32, June 1993.

cycle. After the mold cavity is filled, continued pressure on the piston connected to the screw forces more melt into the cavity to compensate for part shrinkage due to initial cooling.

Table I.3.1: Plastic Properties which Influence Molding.

Properties	Influences	Critical Process Variables
1. Plastics are compressible	• Higher hydraulic pressures force more plastic into the mold cavity • Reduced viscosity allows more efficient compression	• Cavity pressure
2. Plastics shrink when they cool	• Higher compression results in less shrinkage • Faster cooling rates result in less shrinkage • Less orientation results in less shrinkage	• Cavity Pressure • Mold Temperature • Melt Temperature • Flow Rate
3. Plastic viscosity is dependent on temperature and flow rate	• Higher flow rates produce greater shear thinning and consequently lower viscosity • Higher temperatures are an indication of greater molecular motion and consequently lower viscosity	• Melt Temperature • Flow Rate

The accuracy and the tolerances that are obtained in injection molding serve to characterize parts that are molded. Polymer material shrinkage is compensated for by building the mold oversize. Shrinkage varies from about 0.7% for PMMA molded at 20,000 psi to about 7% for Polyethylene molded at 5,000 psi[13]. It is simple in theory to compensate for shrinkage, but the shrinkage depends on molding conditions and cannot be calculated exactly. The shrinkage of nylon, for example, depends on the degree of crystallinity which in turn depends on flow pattern and cooling rate. A faster cooling rate--i.e. colder mold temperature--results in less shrinkage. When a part is cooled very quickly, the dimensions are "frozen-in" and, therefore, the part will shrink less. A slower cooling rate gives more time for the molecules to align and, consequently, the part will exhibit greater shrinkage. Tolerances of 0.001" over short sections and 0.009" over 6"

[13] Middleman, Stanley, Fundamentals of Polymer Processing, McGraw Hill Book Co., New York, 1977.

lengths can be obtained when molding nylon[14]. Graphs of obtainable accuracy are included in many molders handbooks. The variations in shrinkage and other properties cause a distortion of shapes. Distortions show up as sink marks (surface depressions), bending, and parts out of round. It is difficult to hold a roundness dimension closer than 0.7% or a concentricity dimension closer than 0.5%[15].

Finally, shrinkage is affected by polymer orientation—the alignment of the molecule and molecular segments in the direction of flow. Shrinkage is a result of two factors—a normal decrease in volume due to temperature change and relaxation of the stretching caused by carbon-carbon linkages. As there are more carbon-carbon linkages in the direction of the oriented flow, there will be greater shrinkage. Any parameter that affects the mobility of the molecular segments will affect orientation and consequently part shrinkage. This indicates the need for accurate temperature control for a repeatable molding process. Orientation is also affected by melt flow rate. A fast fill rate increases orientation on the part surface and decreases orientation in the center of the part. A slow fill rate results in a less locally intense but more evenly distributed orientation through the whole cross section of the part.

The third property of plastic is that its viscosity is dependent on temperature and flow rate of the melt. Viscosity is a measure of a material's resistance to flow and is defined as the ratio of shear stress to shear rate:

$$\eta \equiv \sigma/\gamma' \qquad (2)$$

where η = viscosity

σ = shear stress

γ' = shear rate

The viscosity of the plastic melt decreases as the shear rate increases. Fluids that behave in this way are said to be shear thinning. Based on high shear rate data for a number of polymers, an empirical "power law" expression has been suggested to describe the dependence of viscosity on shear rate:

---

[14] Frados, Joel, ed., Plastics Engineering Handbook, fourth edition, Van Nostrand Reinhold Co., New York, 1976, p. 89.
[15] Ibid.

$$\eta \equiv \sigma / \gamma'^{n-1} \qquad (3)$$

The shear stress is then given by:

$$\sigma = K\gamma'^{n} \qquad (4)$$

A Newtonian liquid is special case for which n=1. For molten polymers, n is usually observed to be in the range of 0.3 to 1.0[16].

The viscosity of the melt also decreases with an increase in temperature. A simple expression often used to describe this effect is given by the equation:

$$\eta(T) = A\, e^{E/RT} \qquad (5)$$

where: T = temperature

R = gas constant

E = activation energy for viscosity

Mold filling software packages must model the dependence of viscosity on both shear rate and temperature. One example of such an expression is :

$$\eta(T) = A\, e^{E/RT}\, |\gamma'|^{n-1} \qquad (6)$$

A qualitative explanation for why an increase in temperature lowers viscosity is related to the concept of free volume. This is the volume of space in the melt that is not actually occupied by molecules and is thus available to permit the mobility of the molecules. The greater the free volume, the easier it is for molecules to adjust to deformations, and this will be reflected in a lower viscosity. An increase in temperature results in thermal expansion and thus an increase in free volume. This explains the decrease in viscosity as the temperature increases.

Therefore, increases in either flow rate or temperature reduce viscosity. An increase in flow rate results in greater shear thinning and consequently lower viscosity. Higher temperatures are an indication of greater molecular motion and consequently lower viscosity. Constant viscosity is required to produce parts of consistent quality. Viscosity affects how much the polymer is compressed in the cavity and therefore how much shrinkage will take place. Lower viscosity results in smaller pressure drops along the flow

[16] Dominick V. Rosato and Donald V. Rosato, Injection Molding Handbook (New York: Van Nostrand Reinhold Company, 1986), p. 637.

path (runner and gate) and consequently higher cavity pressure. Higher cavity pressure results in greater compressibility and consequently less shrinkage.

Although higher temperatures produce parts with reduced residual stresses and molecular orientation, the part shrinkage induces distortions which needs to be accounted for in the mold design.

I.4 Evaluation of Thermal Controls in Injection Molding

The suitability of injection molding to producing large numbers of parts at high production rates resulted in an increasing use of the injection molding process. As the process was applied to more and more products the demand to improve the consistency of product quality grew. This thesis explore the role that spatially and temporally varying mold temperature profiles have on process consistency. Thus, the focus of the analyses will be on the various methods of mold temperature control.

J.N. Border[17] attempted to control the viscosity by changing the back pressure to produce a change in melt temperature. He found the relationship between a change in back pressure and a change in viscosity to be independent of material. Although his viscosity control scheme was inconclusive because of problems in obtaining a consistent measurement of the viscosity, his control scheme can be used to make an intelligent injection molding machine.

J.R. Rinderle[18] has indicated that a high quality, precision part can be produced if the mold is preheated, filled at high pressures, and cooled at a variable rate. He presented a possible mold configuration and techniques for constructing such a mold. His method of heating the mold surface is by encapsulated resistance heaters. He tested a volume-controlled variable-conductance heat pipe as a means of providing controlled mold cooling. Since his mold surface is made of electroformed shell, the mold will deform

[17] Border, J.N., "Intelligent Injection Molding," Master of Science Thesis, M.I.T., June 1981.
[18] Rinderle, James R., "A Method for Precision Injection Molding," Master of Science Thesis, M.I.T., June 1979.

inevitably under the molding pressure. He presented an analysis of mold deflections as a guide for the design of the mold structures.

Research has been done on the advantages of low thermal inertia injection molding. It has been determined that frozen-in stresses are considerably reduced when molds are thermally cycled[19,20]. There is also the reduced injection pressure, lower plastic injection temperature, lower cycle times, and potential energy savings.

On rapid temperature cycling of molds, however, there has been a limited amount of research done. The approach used so far has been with the use of electric heaters[21]. This approach uses a thin layer of carbon resin as the heater element, sandwiched by two layers of insulating material. One of these layers insulates the electric heater from the molten plastic, while the other electrically and thermally insulates the metal mold from the electric heaters. The thickness of this second layer is critical, because it balances heat response in heating versus cooling response.

These molds have a very high initial thermal response at their surface, about 80°C increase in temperature in a few tenths of a second. A subsequent increase to a 100°C (an additional 20°C) takes a few seconds. The opposite applies in cooling, where after the power is turned off, a similar temperature decrease rate is observed[22]. These molds, however, have a surface hardness (i.e., wear resistance) only as high as that of the insulation layer applied. There is also the fact that high temperature response sacrifices maximum temperatures. Variations in electric heating element causes variations in power density, and therefore, in surface temperature[23]. Therefore, rapid nonuniform thermal manipulations can lead to increased thermal distortions.

---

[19] Kim, Byung H., "Low Thermal Inertia Injection Molding," Doctor of Philosophy Thesis, M.I.T., July 1983.
[20] Jansen, K.B., and A. Flaman, "Construction of Fast-Response Heating Elements for Injection Molding Applications", Polymer Engineering and Science, 34, 7, mid-April 1994, p. 894-899.
[21] Ibid.
[22] Ibid, pp. 898.
[23] Ibid.

I.5 Project Goal

The goal of this project is to focus on controlling the mold thermal spatial variations in the reduction of residual stresses and warpage. The research effort has been focused on development of a stepped lamination layer mold, whereby melt temperatures can be measured directly and of a real time flow and solidification optical analyzer to observe the effects of spatially varying temperature profiles on residual stress patterns to achieve the goal. The heat transfer sensitivity of the two distinct solidification processes-during filling and cooling will also be analyzed to determine which is the more dominant residual stress contributor.

CHAPTER II

PROBLEMS IN INJECTION MOLDING

II.1 Introduction

Although the injection molding process has many advantages, there are some inherent process problems. Distortions, warping, and excessive shrinkage are problems of shape reproduction. However, due to its low cost of operation and ease of application to large production volumes injection molding is being applied to parts which place ever increasing demands on the process. Higher production rates reduce production costs. It is at high production rates that problems are most prevalent. At low production rates most problems can be solved using a conventional machine. However to be economically competitive it is necessary to operate at the highest production rate possible. Thus, dynamic temperature control was created to satisfy the required additional degree of freedom to produce quality high production rate parts.

The experiments and models lead to a statement of the general injection molding problem: The performance of a molded part depends on the processing history of each element of material within the part. The processing history includes pressure, temperature, and strain history of each material element during the entire molding process. These variables affect the molded condition of the part and therefore the geometrical, mechanical, optical and environmental performance of the part. Because premold thermal melt history during molding determines the initial plastic state in the mold, the entire plastic thermal history during molding should be considered and is described below.

The first step of the process is the melting of the material. This step can be described as a material having certain material properties flowing into the system at a certain flow rate. The output of the process is a mixed material at a certain pressure and viscosity. The pressure on the material is related to the back pressure on the screw. The back pressure affects the viscosity of the melt produced so the viscosity and back pressure

are coupled. However, by changing the temperature of the screw barrel different viscosities can be obtained that effectively uncouples the back pressure and melt viscosity. Finally the rate of rotation of the screw affects the rate of material transport through the process.

The next step of the injection molding process as seen by the material is the injection. The material output from the injection can be described by its viscosity, velocity, continuity and the mass flow rate. The mass flow rate, the viscosity and the continuity of the material were fixed by the previous step, but the velocity of melt must be chosen for the process.

As the material flows into the mold cavity it takes the shape of the mold cavity, so that there is a geometry associated with the material. The degree to which the material takes the shape of the mold cavity is controlled by the peak pressure exerted on the material before the pressure is reduced to the hold pressure and the shrinkage index of the plastic. The material in the mold at the time the mold is filled can then be described by the pressure, temperature and mold geometry or dimensions which together take the place of the mass flow rate. Since the material at the surface of the part freezes as the mold is still filling the characteristics of the surface are established by the time the mold is filled.

After the mold is filled the material cools. The commonly used state equation for polymers is similar to the gas law. The form used in this thesis is the Spencer-Gilmore equation which is shown as equation (7).

$$(P+\pi)(V-\omega)=RT \qquad (7)$$

where P = pressure
T = temperature
v = specific volume
π, ω, R = material properties

From equation (7) it can be seen that during cooling the reduction in temperature is accompanied by a change in both pressure and specific volume. If the mass of material in the mold is constant, a change in specific volume exhibits itself as a change in volume or dimensions of the part. Conventionally, after the mold is filled a hold pressure is maintained on the screw so that as the material shrinks more material is pushed into the mold. The change in specific volume from the additional material results in a mass

increase rather than a volume change. There is a limit to the effectiveness of this type of control because once the gate has frozen no further material can be added to the mold. At this point the mold cavity becomes a closed system and the pressure, temperature and volume become coupled.

The last step in the process is the final cooling of the part to the point where the structural qualities of the part are developed. The structural qualities of the part come out of the properties and the degree of homogeneity of the material itself. At this point since the pressure, volume and temperature cannot change, the three variables can be combined into one variable, the mass of the part. When the process is examined over more than one cycle the mass of the part can be replaced by a mass flow rate. Putting all the steps together it is possible to trace the development of the different parameters of the injection molding process (Figure II.1.1)[24]. However, the warpage or residual stresses cannot be accounted for because these two parameters are determined by the interaction of many points or the pressure and temperature fields.

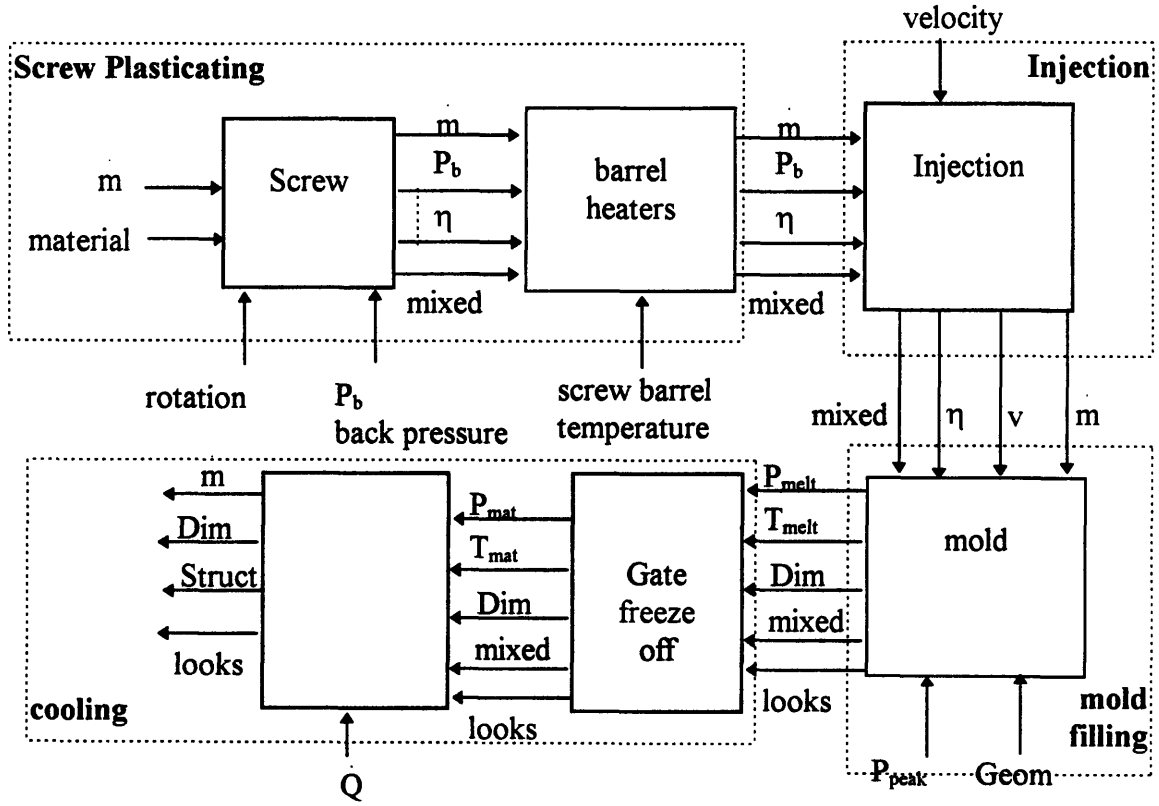

Figure II.1.1: Functional Diagram for the Injection Molding Process

[24] Border, J.N., "Intelligent Injection Molding," Master of Science Thesis, M.I.T., p. 29, June 1981.

Throughout the process the temperature is not listed as a characteristic parameter, instead the viscosity is given as the characteristic parameter. This is because both the plasticating and injection are controlled by the way the material flows. The temperature does not directly determine how a material flows. The viscosity describes the losses associated with a flow of a material. Therefore, viscosity is the characteristic parameter and not the temperature.

At this point further cooling of the part results in a reduction in both pressure and volume. Furthermore, the cooling of the part does not occur at a uniform rate across the part. Because of this nonuniform cooling, pressure gradients form[25] and secondary flows produce alignment of molecules and localized areas of large volume change which result in residual stresses and a loss of dimensional accuracy. To control the secondary flows the pressure gradients must be eliminated. Uncoupling the control of pressure, temperature and volume of the material in the mold would allow the part to be cooled while maintaining pressure and dimensions constant. As the section thickness gets smaller the time the material is molten while in the mold decreases and the initial conditions as the mold is filled become more important. From information obtained at Eastman Kodak[26] there are indeed variations in the melt flow index for the incoming material of as much as ±30%. The large variation range, the high production rates which necessitates high flow velocities, the high plastic melt thermal inertia resisting rapid temperature control, and the majority of the cycle time is the plastic cooling in the mold indicate that the most effective control would be the dynamic control of mold thermal boundaries.

The filling process is coupled with the cooling process. As the molten polymer fills the cold mold cavity it starts to cool from the mold surface where the melt comes in contact. Since the polymer cannot be injected into the mold instantaneously, the melt at every point undergoes different thermal history because of cooling while it is being injected. This temperature change within the melt changes the thermodynamic state of the melt. Because of the coupling it is difficult to control the state of the melt in the

---

[25] Rinderle, James R., "A Method for Precision Injection Molding," Master of Science Thesis, M.I.T., June 1979.

conventional injection molding process. This coupling, therefore, directly results in inconsistency of the molded part. One method for shrinkage and distortion compensation is the alteration of the cavity shape. Unfortunately, the mold designer cannot accurately predict the final shape of the part to fully compensate for dimensional inaccuracies.

Another major problem is that injection molding requires high temperature and pressure to mold thin parts. As the melt comes in contact with a cold mold surface during the injection stage, a thin layer of frozen plastic "skin" is formed. In molding a thin part the thickness of the skin layer approaches the half thickness of the part. To overcome the freezing of the melt, which blocks the flow path, extremely high pressure and temperature are used so that the cavity is rapidly and completely filled.

The high temperature causes high thermal shrinkage and therefore requires high packing pressure to compensate elastically the thermal shrinkage. The high pressure causes high flow-induced molecular orientation which in turn increases residual stresses, and the orientation freezes as the melt vitrifies. This frozen-in molecular orientation imparts anisotropic residual stresses. Molded parts with anisotropic residual stresses exhibit not only anisotropic mechanical and optical properties, but also poor impact strength and poor resistance to heat-shrinkage. Moreover, the condition of parts can change for weeks after molding as residual stresses relax. Eliminating these molding problems comes about from understanding how the properties of a molded part depend of the condition or state of a molding. This topic is discussed in the next section.

II.2 The Effect Of The Molding Condition On Mold Part Properties

The relationships between the condition of a molded part and the properties of the part have been the object of study for decades. An understanding of the way in which the state or condition of a molded part determines the properties of that part is useless without also understanding how materials and processing affect the state, and ultimately how to alter the state of a molding.

---

[26] Border, J.N., "Intelligent Injection Molding," Master of Science Thesis, M.I.T., June 1981.

In 1943 Alfrey, Golfinger and Mark[27] proposed two mechanisms to explain the thermal expansion of polymers. One mechanism is almost instantaneous and the other acts at a rate proportional to the difference between present volume and equilibrium volume.

In 1949 and 1950, Spencer and Gilmore published a series of papers based on the Alfrey work. In the first paper[28], Spencer discusses the effect of heating and cooling rates on the second order transition temperature, T_G , and the resulting effects on volume. He presents a model for predicting volume using temperature-time data. In the second[29] and third[30] paper Spencer and Gilmore propose a state equation to relate the temperature, pressure, and volume of polymer materials through measurable material properties. Equation (7), $(P + \pi)(v - \omega) = RT$, was presented in the third paper with the values of the material properties π, ω and R for five polymers that are commonly injection molded. This equation is only valid for amorphous materials above the glass transition temperature, but it can be used to estimate volumes of semi-rigid bodies in certain conditions and to estimate the pressure required to compensate for thermal shrinkage. The authors discussed the origin of residual strain in injection molded pieces, means of relieving or preventing residual strains, and their effect on crazing and on the mechanical properties of the molding. They stated that reduction in the amount of frozen orientation resulted in improved crazing resistance, dimensional stability on heating, and consistency.

In the same year, Spencer and Gilmore published a paper[31] on residual strains in polystyrene. The authors discuss the origin of residual strain and show that the state of stress during cooling is often unstable and either the surface collapses forming a sink mark or a void forms within the piece. They also state that residual strains are caused by molecular orientation and that by reducing orientation (by reducing packing and discharge) in the parts, crazing resistance, dimensional stability and consistency are all

---

[27] Alfrey, T., G. Goldfinger and H.J. Mark, J. of Applied Physics, 14, 700, (1943).
[28] Spencer, R.S., "Volume-Temperature-Time Relationships for Polystyrene," J. of Colloid Science, 4, 229, (1949).
[29] Spencer, R.S., and D.G. Gilmore, "Equation of State for Polystyrene," J. of Applied Physics, 20, (1949), p. 502-506.
[30] Spencer, R.S., and D.G. Gilmore, "Equation of State for High Polymers," J. of Applied Physics, 21, (June, 1950).
[31] Spencer, R.S., and D.G. Gilmore, "Residual Strains in Injection Molded Polystyrene," Modern Plastics, (Dec., 1950)

improved. They developed a procedure to predict filling time and maximum pressure in a disk shaped mold[32]. They were able to predict the effects of mold temperature and material viscosity on these variables. Spencer and Gilmore viewed the mold filling through windows in the mold and observed the fountaining effect during mold filling. They noted that the central region where flow occurred was only 40% of the total thickness.

Two decades later Kamal and Kenig[33],[34] published a model of the injection molding process and an experimental test of the model. The model predictions for spreading radial flow of a power law fluid are in good agreement with the experiments. The results for progression of the melt front, flow rate, velocity, temperature and pressure profiles are good except during the filling stage near the gate where viscoelastic effects are important.

Wu, Huang, and Gogos[35] developed a model based on slightly different assumptions. They present simulation results for PVC molding that show the effect of mold temperature and filling time on temperature distribution through the cavity.

Neither Kamal and Kenig nor Wu, Huang, and Gogos considered the strain history of the melt or attempted to predict the state of molecular orientation of the melt. Tadmor[36] did consider some of these effects in a semiquantitative model that he proposed. Tadmor incorporates flow and heat transfer mechanisms with molecular theories to model the shear and elongational flow that causes molecular orientation. The elongational flow results from having a steady melt front and a velocity gradient behind the melt front as described by Rose[37] and because the flow is accelerated toward the wall after passing

---

[32] Spencer, R.S., and D.G. Gilmore, "Some Flow Phenomena in the Injection Molding of Polystyrene," J. of Colloid Science, 6, (1951), p. 118.
[33] Kamal, M.R. and S. Kenig, "The Injection Molding of Thermoplastics Part 1: Theoretical Model," Polymer Engineering and Science, 12, 4, (July, 1972).
[34] Kamal, M.R. and S. Kenig, "The Injection Molding of Thermoplastics Part II: Experimental Test of the Model," Polymer Engineering and Science, 12, 4, (July, 1972).
[35] Wu, P.C., C.F. Huang and C.G. Gogos, "Simulation of the Mold Filling Process," Polymer Engineering and Science, 14, 3, (March 1974).
[36] Tadmor, Z., "Molecular Orientation in Injection Molding," J. Of Applied Polymer Science, 18, (1974). p. 1753.
[37] Rose, Walter, "Fluid-Fluid Interfaces in Steady Motion," Nature, 191, (1961), p. 242.

between solidified layers. Tadmor considered this "fountain effect" and the shear effects with a temperature dependent relaxation process to estimate the final frozen orientation.

White[38] presented a hydrodynamic analysis of the filling of a rectangular cavity. He considered the temperature dependence of the rheological properties and the effect of rheological properties on jetting and channeling during mold fill.

Williams and Lord[39],[40] used a numerical scheme to model flow in runners, sprues and the cavity. Modeling runner and sprue flow freed them from a common assumption of an isothermal melt entering the cavity. The model can be used in the design and modification of molding equipment and for problem diagnosis. They demonstrated the utility of their model by redesigning the runner system of a multicavity mold so that simultaneous filling of the cavities occurs.

Kamal, Kuo and Doan[41] presented two models, the second of which allows the application of potential theory and the determination of streamlines and melt front shapes during the filling of a thin rectangular cavity.

Stevenson, Wang et al[42],[43],[44] developed numerical schemes to estimate clamp force, injection pressure and temperature distribution during molding of ABS. They presented the model in a nondimensional form and developed a graphical method for estimating injection pressure and clamp force during the molding of amorphous polymers into thin disks.

---

[38] White, James L., "Fluid Mechanical Analysis of Injection Mold Filling," Polymer Engineering and Science, 15, 1, (January, 1975).

[39] Williams, G. and H.A. Lord, "Mold Filling Studies for the Injection Molding of Thermoplastic Materials Part I: The Flow of Plastic Materials in Hot and Cold Walled Circular Channels," Polymer Engineering and Science, 15, 8 (August, 1975).

[40] Lord H.A., and G. Williams, "Mold Filling Studies for the Injection Molding of Thermoplastic Materials Part I: The Transient Flow of Plastic Materials in the Cavities of Injection-Molding dies," Polymer Engineering and Science, 15, 8 (August, 1975).

[41] Kamal, Musa R., Youti Kuo and P.H. Doan, "The Injection Molding Behavior or Thermoplastics in Thin Rectangular Cavities," Polymer Engineering and Science, 15, 12, (December, 1975)

[42] Stevenson, J.F., C.A. Hieber, A. Galskoy and K.K. Wang, "An Experimental Study and Simulation of Disk Filling by Injection Molding," presented at the Society of Plastics Engineers 34th Annual Technical Conference, Atlantic City, New Jersey, April 26-29, 1976.

[43] Stevenson, James F., "A Simplified Method for Analyzing Mold Filling Dynamics, Part I: Theory," Polymer Engineering and Science, 18, 7, (May 1978).

[44] Wang, K.K., S.F. Shen, J.F. Stevenson and C.A. Hieber, "Computer Aided Injection Molding System," Progress Reports nos. 1-4, Cornell University for NSF under grant APR74-11490.

Of these modeling efforts, only Tadmor considered the molecular orientation and relaxation which greatly influences mechanical properties and part shrinkage. In an experimental study using hot molds, Johnson[45] noted that high mold temperatures allow relaxation of the melt during the molding cycle.

In 1976, Menges, Thienel, and Wubken[46] carried out experiments on relaxation of molecular orientation. They found that relaxation of orientation in injection moldings is governed by the Williams, Landel, Ferry Equation[47] and that the state of orientation could be estimated from a knowledge of the temperature-time history of the material. In another paper[48] the authors suggest that the computation of orientation relaxation can be used in conjunction with other models to determine the final state of the molding.

In 1960, Jackson and Ballman[49] conducted experiments on injection molded specimens to determine the magnitudes of the effects of orientation on mechanical properties. Their results show the influence of orientation on tensile strength, elongation at failure, and notched impact strength. The data do not show a systematic effect of orientation on modulus.

Johnson[50] investigated strain free injection molding and published his work in 1963. Using molds that had been heated to near the melt temperature and by using very high pressures, he was able to produce relatively strain free parts that were crack free. The parts molded at high pressures had a smaller change in density during aging than other parts which implies that the parts had greater long term dimensional stability. Johnson used birefringence measurements to determine the condition of the moldings. He determined that improved properties of the part result when orientation is allowed to relax in the mold and when the part has greater density.

---

[45] Johnson, L.I., "Strain-free Injection Molding," Modern Plastics, 40, (June 1963), p. 111.
[46] Menges, G., P. Thienel and G. Wubken, "A Method to Estimate the Relaxation of Molecular Orientation in Plastics," Kunstoffe, 66, (January 1976), p. 42-48.
[47] Williams, M.L., R.F. Landel and J.D. Ferry, J. of American Chem. Soc., 77, (1955), p. 3701.
[48] Thienel, P. and G. Menges, "Mathematical and Experimental Determination of the Fields of Temperature, Velocity and Pressure During the Filling Stage in Injection Molding: Determination of Disorientation During the Cooling Stage," presented at the Society of Plastics Engineers 34th Annual Technical Conference, Atlantic City, New Jersey, April 1976.
[49] Jackson, G.B. and R.L. Ballman, "The Effect of Orientation on the Physical Properties of Injection Moldings," SPE Journal, (October 1960), p. 1147.
[50] Johnson, L.I., "Strain-free Injection Molding," Modern Plastics, 40, (June 1963), p. 111.

Koda[51] studied the effects of molding conditions on properties of polycarbonate. He found that reduced orientation improved abrasion resistance and decreased heat shrinkage at 180°C. Koda also found that hotter molds produced moldings with greater solvent crack resistance and hardness, lower density and less heat shrinkage at 120°C. Increased holding pressure decreased shrinkage but increased density and caused a decrease in solvent resistance.

Koda hypothesizes that moldings with low residual stresses could be molded at a high mold temperature and at a low holding pressure. The hotter mold reduces temperature gradients in the melt but the hot mold also allows relaxation of oriented molecules. Molecular orientation has a strong effect on solvent resistance.

Menges and Wubken[52] studied the influence of processing conditions on molecular orientation in injection moldings. They concluded that the main direction of orientation in plane-shaped moldings is the flow direction. They also found that the orientation is highly biaxial at the surface of the molding and that there is very little orientation in the center of moldings. The frozen orientation is reduced when the melt temperature is increased. Increasing cavity wall temperature has a similar effect in relaxing the orientation. An increase in injection rate results in a slightly higher surface orientation while the internal orientation is significantly reduced.

Y.T. Koita[53] considered the effect of packing and discharge on the injection molded parts. Photoelastic stress patterns suggested that packing and discharge give rise to high frozen stresses due to molecular orientation in the gate area. Degradation of mechanical properties of the specimen resulted from the high frozen stress region at the gate.

---

[51] Koda, Hiroyuki, "Effects of Molding Conditions on Properties of Injection Molded Polycarbonates," J. of Applied Polymer Science, 12, (1968), p. 2257.

[52] Menges, G. And G. Wubken, "Influence of Processing Conditions on Molecular Orientation in Injection Moldings," presented at the Society of Plastics Engineers 31st Annual Technical Conference, Montreal, May 1973.

[53] Koita, Y.T., "Packing and Discharge in Injection Molding," Polymer Engineering and Science, 14, 12, (Dec. 1974).

Tadmor[54] proposed a semiquantitative model to explain the complex molecular orientation distribution observed in injection molding of amorphous polymers. The bead and spring macromolecular theory was used to calculate root mean end to end distances of macromolecules in the various flow fields and the relaxation process. The model assumes that the orientation in the surface skin is related to steady elongational flow in the advancing front and the orientation in the core is related to the shear flow.

Burkle[55] used a modified milling method to measure inherent stresses in U-shaped moldings of fourteen different thermoplastic materials. His data on fourteen different samples does not correlate well with the theory he presents to estimate residual stress from the temperature gradients in the mold. He states that the inherent stress decreases with increasing mold temperature. He also states that mold temperature has a significant effect on residual stress but that the injection temperature does not. This seems contradictory to earlier works[56].

In 1976, Menges et al.[57] published a study on relaxation of molecular orientation in plastics. They found that the relaxation process in an injection molding die is governed by the WLF (Williams, Landel, Ferry) equation[58]. They reported a method to estimate the relaxation of molecular orientation from a knowledge of the temperature-time history of the material.

Han and Villamizar[59] carried out an experimental study to investigate the development of stress birefringence patterns of molten polymer during the mold filling and cooling operation. Their study showed how molding conditions influence the distribution of stress birefringence patterns. They showed that mold temperature influences the

---

[54] Tadmor, Z., "Molecular Orientation in Injection Molding," Journal of Applied Polymer Science, 18, (1974), p. 1753.
[55] Burkle, Dieter, "Measurement of Inherent Stresses in Plastic Mouldings," Kunstoffe, 6, (January 1975).
[56] Menges, G. And G. Wubken, "Influence of Processing Conditions on Molecular Orientation in Injection Moldings," presented at the Society of Plastics Engineers 31st Annual Technical Conference, Montreal, May 1973.
[57] Menges, G., P. Thienel and G. Wubken, "A Method to Estimate the Relaxation of Molecular Orientation in Plastics," Kunstoffe, 66, (January 1976), p. 42-48.
[58] Williams, M.L., R.F. Landel and J.D. Ferry, Journal of the American Chem. Soc., 77, (1955), p. 3701.
[59] Han, C.D. and C.A. Villamizar, "Measurement of Pressure and Stress Birefringence Patterns During the Mold Filling and Cooling Operation," presented at the Society of Plastics Engineers 35th Annual Technical Conference, Montreal, 1977.

amount and distribution of residual stress in the molded part and that the residual stress is intimately related to its mechanical properties and dimensional stability of heating.

In 1977, Bakerdjian and Kamal[60] completed an extensive investigation of the three dimensional variation of density, heat shrinkage, birefringence and tensile strength in molded thermoplastic rectangular parts. They show that birefringence through the thickness of polystyrene plaques is maximum at the surface and falls to a minimum at a small distance from the surface. A local maximum of birefringence occurs at a distance of about 15% through the section. Polyethylene moldings did not exhibit a local maximum of birefringence. The density of polyethylene samples was minimum at the surface because of low crystallinity in the quickly chilled region and was greater near the gate than at the far end of molding. The tensile strength of polystyrene samples along the direction of orientation was 45.6% greater than in the transverse direction. Polyethylene was 16.6% stronger in the direction of orientation. The lowest heat shrinkage values, for example, are found near the center of the molding, where the polymer chains have the greatest chance to relax and assume a more random configuration.

Hoare and Hull[61] attempted to describe properties of moldings in terms of molecular structure. They studied the effect of orientation on the mechanical properties of injection molded polystyrene and regarded the molding as a composite structure of materials with different degrees of anisotropy and orientation. They present data relating crazing stress and fracture stress to the angle between loading and orientation and to the magnitude of birefringence. The authors data are in good agreement with a model they propose for estimating properties of molded parts with complex orientation distributions. The model is based on estimating the properties of a lamination of unidirectionally oriented layers by applying experimental results for tensile behavior of oriented plaques to each layer. They concluded that the crazing behavior and crack mechanism can be predicted from the properties of hot drawn sheet.

---

[60] Bakerdjian, Z. And M.R. Kamal, "Distribution of Some Physical Properties in Injection Molded Thermoplastic Articles," Polymer Engineering and Science, 17, 2, (February 1977).
[61] Hoare, Linda and Derek Hull, "The Effect of Orientation on the Mechanical Properties of Injection Molded Polystyrene," Polymer Engineering and Science, 17, 3, (March 1977).

Dietz, White, and Clark[62] presented a study of the development of orientation distribution and relaxation of the orientation in injection molding of amorphous polymers. Their predictions of orientation development are based on the assumption that the stress-optical laws are valid in the molten state. They also assumed that the melt relaxes in a Maxwellian manner. Their analysis predicts the birefringence distribution in injection molded parts fairly well.

In 1982, Isayev[63] reported a study of a coupled effect of the flow induced and thermally induced orientation in the molded part. He measured three components of birefringence and related these to the processing conditions. His work is based on the constitutive equation of Leonov[64]. The experimental results are in good agreement with Leonov's theory.

Crouthamel et al.[65] studied the effects of processing conditions on the residual stresses of the molded part using the layer-removal technique of Treuting and Read[66]. They found that residual stresses in the molded part depend on the orientation with respect to flow during cavity filling, and on the distance from the gate. They concluded that injection rate and mold temperature have a minor effect on the level and distribution of molding stress, while melt temperature has a significant effect. Their mold temperature, however, varies only from 40°C to 60°C.

Hubbauer[67] stated that physical properties of a molded part can be improved by optimizing processing conditions such as injection pressure, melt temperature, injection rate and mold temperature. He did not, however, mention a method of optimizing processing conditions.

---

[62] Dietz, White, and Clark, "Orientation, Development and Relaxation in Injection Molding of Amorphous Polymers," Polymer Engineering and Science, 18, 4, (March 1978), p. 273.
[63] Isayev, A.I., "Orientation Development in the Injection Molding of Amorphous Polymers," presented at the Society of Plastic Engineers 40th Annual Technical Conference, San Francisco, 1982, p. 288.
[64] Leonov, A.I., Rheol. Acta, Vol. 15, 1976, p. 85.
[65] Crouthamel, Isayev, and Want, "Effect of Processing Conditions on the Residual Stresses in the Injection Molding of Amorphous Polymers," presented at the Society of Plastics Engineers 40th Annual Technical Conference, San Francisco, 1982, p. 295.
[66] Treuting and Read, Journal of Applied Physics, Vol. 22, 1951, p. 130.
[67] Hubbauer, P., "Effects of Processing Conditions on Plastic Parts," presented at the Society of Plastics Engineers 40th Annual Technical Conference, San Francisco, 1982, p. 302.

Fritch[68] studied the effect of mold temperature on impact strength. He concluded that mold temperature influences the molded part properties to a significant degree. However, he pointed out a need to compromise in raising mold temperature and in minimizing cycle time. He showed that the improvement of impact strength is greatest at low melt temperature and at high mold temperature.

Burke and Newcome[69] made an assessment of the mold temperature influence on molded part quality of semicrystalline polymer. Mold temperature can directly influence the physical properties of semicrystalline material since it affects the degree of crystallinity. They recommended higher mold surface temperature for a thinner part to ensure full crystallinity.

Woebcken[70] investigated the effects of processing on the dimensional accuracy of parts. He shows that shrinkage and orientation depend strongly on the gating pattern. Woebcken also measured the warping of molded specimens during annealing. He found that less warping occurred when the parts were molded in a hotter mold. Woebcken discusses the effects of the mold on corner shrinkage and warping in the vicinity of variations in wall thickness.

In 1973 Menges and Wubken[71] published a study of plane rectangular moldings. Shrinkage measurements of microtomed samples show that the orientation is highly biaxial at the surface of the molding and that there is very little orientation in the center of the section. Increasing stock temperature decreases the orientation. Increasing the mold wall temperature has a similar but smaller effect.

---

[68] Fritch, L.W., "How Mold Temperature and Other Molding Variables Affect ABS Falling Part and Izod Impact," presented at the Society of Plastics Engineers 40th Annual Technical Conference, San Francisco, 1982, p. 332.

[69] Burke and Newcome, "Essential Parameters for Molding Modified PET Resins: An Assessment of Their Influence on Molded Part Quality," presented at the Society of Plastics Engineers 40th Annual Technical Conference, San Francisco, 1982, p. 336.

[70] Woebcken, W., "The Effects of Processing on the Dimensional Accuracy of Thermoplastic Injection Molded Articles," Kunstoffe, 67, 4, (1977), p. 179-183.

[71] Menges, G. And G. Wubken, "Influence of Processing Conditions on Molecular Orientation in Injection Moldings," presented at the Society of Plastics Engineers 31st Annual Technical Conference, Montreal, May 1973.

Gutfinger, Broyer, and Tadmor[72] worked on the problem of static melt solidification and also considered the problem of solidification during flow in a narrow gap. This problem is analogous to the mold filling stage in injection molding where rapid cooling and solidification can result in a short shot and frozen-in orientation. Their numerical scheme predicts solid layer thickness and temperature profiles as a function of time and position in a cavity and is useful for designing flow paths in molds.

II.3 Current State Of Thermal Control

Review of the mentioned literature indicate that temperature control of the molds is crucial to mold operation and part quality; however, mold temperature is currently not directly controlled. As the plastic flows into the mold cavity, it begins to solidify. Heat that has been transferred to the mold by the molten plastic is carried away by a coolant that circulates through cored passages in the mold. This affects part quality in several ways. The first and most apparent is the fact that mold temperature is a balance between the cooling time and the melt length of flow. Colder mold temperatures results in shorter cooling times, but it shortens the plastic melt path length because of solidification induced flow termination. Since cooling time is a major fraction of the total cycle time of the part, determination of an appropriate temperature of operation of the mold is crucial and most effective when directly here.

The design of the mold cooling passages affects the ability to remove heat from the mold. The mold surfaces closest to the cored water passages will cool first causing the solidification of the outer regions of the part, while the inner regions remain molten. Since plastic have relatively large coefficients of expansions, when the inner regions solidify, they contract in a fixed volume, determined by the already solid outer regions. Hook-up of the external hoses to the mold inlets and outlets will also influence cooling rate. Furthermore, coolant temperature and flow rate determine the efficiency of heat removal.

---

[72] Gutfinger, C., E. Broyer and Z. Tadmor, "Melt Solidification in Polymer Processing," Polymer Engineering and Science, 15, 7, (July 1975).

Differences in mold temperature or mold temperature distribution will affect reproducibility of part moldings. Consequently, repeatability in molding requires optimizing and controling the temperature distribution in the mold to balance the temperature distribution in the plastic.

Mold temperature also affects built-in stresses and geometric accuracy in the part. As the plastic fills the mold, it experiences high shear in the velocity boundary layer. But since it is also freezing, the long polymer molecules solidify in the stretched state, without being allowed to return to its natural coiled form. This is one of the causes of built-in stresses caused by mold filling. This also produces molecular orientation in the part[73].

The sources of built-in stresses explained above detract from part quality. The more residual stresses in the part, the weaker the part. There is also the fact that sink marks can develop in poorly cooled plastic parts.

There are basically three ways that mold temperatures are currently chosen to minimize cooling time,[74]:

1. Trial and error. Mold temperature is varied until a satisfactory compromise is reached.

2. The formula of Ball and Shusman is used. It is the solution of the transient heat equation in one dimension using infinite series and constant plastic properties. Although it is a simple solution, it is used since it has been included in injection molding textbooks in graphical form for a variety of plastics.

3. Proprietary solutions provided by specialized engineering firms. Since details are not released, it would be a reasonable assumption that these solutions entail both analytical and finite element methods.

The major flaw in current thermal control is the focus on maintaining a constant mold surface temperature when what is desired is the uniform decay of plastic temperatures. According to Cannock, UK-based mold cooling specialists REPS[75], many molders are using cooling systems that have changed little in the past 20 years. The

---

[73] Brydson, J.A., *Plastics Materials*, fifth edition, pp. 252-282, Butterworth Books, London 1989.
[74] Mekkaoui, A., and K. O'Brien, "Accurate Determination of Set-up Time for Faster Cycles," Injection Molding of Plastics: Proceedings of the Injection Molding Conference, p. 26, El Segundo, California, December 3-5, 1980.

company claims that 85% of molds in use today could run on a 10-25% shorter cycle time and 98% could produce more consistent parts. The reason that such systems are still in common use is simply that few, up until now, have questioned what goes on in the mold during the molding process.

II.4 Research Applicable To Thermal Control

Kurosaki and Satoh[76] investigated the relation between the development of stress in a molded polymer and the injection molding conditions. They also estimated the frozen skin thickness layer caused by the flow on the basis of the relation between the relaxation time of the birefringence resulting from shear stresses and the solidifying time of injected polymer melt. Their concept of flow visualization was adapted for this thesis. Another important contribution was their observed disappearance of birefringence in the melt core once flow terminated.

Jacques[77] illustrated that warpage is more sensitive to differences in cooling fluid temperatures between mold sides than for differences in metal thickness between mold sides and that their effects are additive. His computational analysis was restricted to flat parts and requires experimental verification. He suggested that mechanisms that affect warpage are differences in cavity pressure, differential orientation, differential crystallinity, inhomogeneous thermal stresses caused by irregular geometry, and stresses frozen during packing.

Bur, Wang, Thomas, and Rose[78] measured the onset of polymer solidification during injection molding. They used an optical sensor to detect characteristic fluorescence radiation intensity, which are different between the solid and melt phases.

---

[75] Mould Control, REP, "Total Mould Temperature Control Systems," Reader enquiry number 208.
[76] Kurosaki, Y. And I. Satoh, "Visualization of Flow and Solidification of Polymer Melt in the Injection Molding Process," 1989 National Heat Transfer Conference, HTD-Vol. 113, Heat Transfer in Manufacturing and Material Processing, p. 63.
[77] Jacques, Michael St., "An Analysis of Thermal Warpage in Injection Molded Flat Parts Due to Unbalanced cooling," Polymer Engineering and Science, 22, 4, (March 1982).
[78] Bur, A.J., F.W. Wang, C.L. Thomas, and J.L. Rose, "In-Line Optical Monitoring of Polymer Injection Molding," Polymer Engineering and Science, 34, 8, (April 1994).

Jansen and Flaman[79],[80] designed a fast-response heating element. They claim that heating during, and shortly after, the filling stage will result in the highest amount of orientation relaxation with minimum power consumption.

Sun[81] used fluid passages conformal to the mold cavity surface to try to uncouple the mold plastic filling stage from the plastic cooling stage. He investigated different liquids to be used as heating/cooling working fluids. He observed a greatly reduced stress pattern under birefringence with parts produced by the thermal cycling of his low thermal inertia mold as compared to molds without thermal cycling.

Wylonis[82] used three dimensional printing to create complex internal cooling passages. The purpose of these passages were to maintain an uniform mold surface temperature. He observed a variation of 7°C with straight cooling channels as opposed to only 4°C variation with his internal cooling channel.

II.5 Summary

In the previous section, literature regarding the effects of processing conditions on the properties of injection molded parts was surveyed. Most of the researchers indicated that processing conditions are interrelated to molded part properties in a complex manner. Common processing variables were mold temperature, melt temperature, and injection rate. Most of the works related molded part properties to the level and distribution of molecular orientation. Many investigators attempted to predict an anisotropic residual stress distribution resulting from the flow-induced orientation. Although the relationship

---

[79] Jansen K.M.B., and A.A.M. Flaman, "Construction of Fast-Response Heating Elements for Injection Molding Applications," Polymer Engineering and Science, 34, 11, (Mid-June 1994), p. 894-897.
[80] Jansen K.M.B., and A.A.M. Flaman, "The Influence of Surface Heating on the Birefringence Distribution in Injection Molded Parts," Polymer Engineering and Science, 34, 11, (Mid-June 1994), p. 898-904.
[81] Sun, E.S., "Implementation Of Low Thermal Inertia Injection Molds Using Conformal Passages," Master of Science Thesis, M.I.T., May 1995.
[82] Wylonis, E.M., III, "Production Of Injection Molding Tooling With Conformal Cooling Channels Using The Three Dimensional Printing Process," Master of Science Thesis, M.I.T., May 1995.

between part properties and processing conditions is complicated, increasing mold temperature was established to improve molded part quality.

Mold temperature, of all the process variables, can have the greatest influence on reducing residual stresses of molded parts. The general properties of the molded part are improved when the residual stress is reduced. In other words, an isotropic and homogeneous part has, in general, improved part qualities. The main cause of the residual stresses is the frozen-in molecular orientation in the molded part. Therefore, the minimization of residual stress through the relaxation of molecular orientation improves the molded part quality.

Detailed examination of the recent technical literature will show that there are two major contributors to residual stresses. One is the portion of the melt that solidifies during the filling stage; the "skin layer". This layer is highly oriented similar to a strectched rubber band and when heated this layer will relax and contract. The other contributor results from the necessary polymer temperature gradient in order to solidify the melt during the cooling stage. The question of which is the major contributor to residual stresses remains highly controversial. The skin layer thickness is associated with the contact duration between the polymer and the mold; thus, the skin layer is thickest near the sprue hole and thinnest at the end of the cavity. Therefore, maximal residual stress reduction requires temporal and spatial thermal variation between the filling and the subsequent cooling stages.

These two stages - filling and cooling - represent unique challenges to thermal control. The filling stage is only a fraction of the entire solidification stage; therefore, the thermal response has to be rapid. On the other hand, the cooling stage comprises the majority of the solidification stage. However, solidification causes the polymer to shrink away from the mold wall thereby forming air gaps between the surfaces that increase the thermal contact resistances. In this case time is less a factor than is the lack of perfect contact that prevents efficient heat transfer. From just these considerations one can appreciate the difficulty and infeasibility of accurately predicting warpage analytically. Even the best models will serve mainly as guides because material properties are hard to pin down, and the complex shapes limit the applicability of simplified models.

The general application of temporal and spatial thermal control requires that the process be deterministic. Otherwise, thermal control is of little use because the final part dimensions cannot be predicted, much less be manipulated. Mr. Dick Barlik[83] and other workers from Hasbro have observed that warpage is a deterministic phenomenon as measured by same degree of warpage at consistent locations. If residual stresses are the major causes of warpage, then residual stresses can be thought of as deterministic as well.

[83] Barlik, Dick; Hasbro, personal conversation.

CHAPTER III

METHODS OF IMPROVING THE MOLDED PART QUALITY

III.1 Introduction

In reviewing literature on injection molding (Chapter II), it is clear that anisotropic residual stress in the molded piece is the single most important cause of degraded part quality. For example, impact strength, crazing resistance, dimensional stability, abrasion resistance, and resistance to heat shrinkage will be improved by minimizing the residual stress. In order to eliminate many molding problems, the residual stress must be minimized.

Development of stresses via molecular orientation during the injection stage is unavoidable. Reduction of the developed stress can be achieved by heating the mold; thereby allowing the relaxation of the stress before the vitrification of the melt. Since the same mold must be heated and cooled quickly to shorten the injection cycle time and to improve the molded part quality, a low thermal inertial mold with spatially and temporally varying temperature is needed.

Two special cases of isothermal filling and differential cooling will provide the background for the discussion of a realistic case of nonuniform melt solidifying in a nonisothermal mold.

III.2 Isothermal Filling Process

When the surface of a mold is at the same temperature as the incoming molten polymer, the filling process can be done isothermally. Upon the completion of filling, the surface temperature of the mold is lowered to cool the part. A plot of the temperature

curve of the mold surface for an isothermal filling process is shown in Figure III.2.1. When the parts are produced this way, the quality of the molded part is improved because of the relaxation of the flow-induced molecular orientation. In conventional molding, however, the molecular orientation is frozen before it relaxes completely, thereby producing an anisotropically oriented part. This anisotropical molecular orientation degrades the mechanical and the optical properties of the molded part. Therefore, an isothermal filling process can improve the general quality of the part.

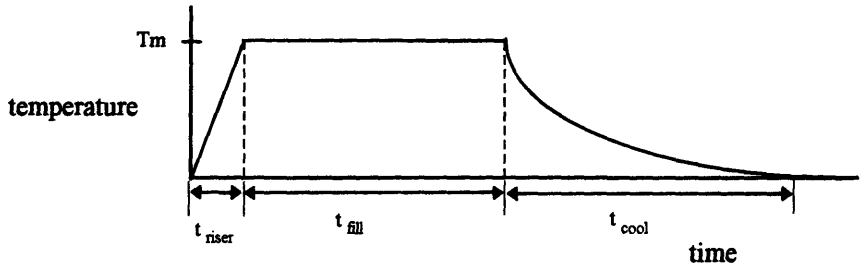

Figure III.2.1: A plot of a mold surface temperature curve for an isothermal filling process.

There are other advantages in injection molding with the isothermal filling process. For example, the process is capable of producing a high quality optical part. An optical part must have a uniform index of refraction across the whole section of the part. In conventional injection molding, however, molding a part with a uniform index of refraction is very difficult to achieve because of frozen-in molecular orientation near the surface of the part. Figure III.2.2 depicts a schematic comparison between the conventional process and the isothermal filling process in molding an optical part. In conventional molding, the macromolecules, elongates because of shear stresses near the surface, freeze when they come in contact with the cold mold surface; consequently, the index of refraction at the surface and the core section is different as shown in Figure III.2.2 a). In order to make a part without frozen-in molecular orientation, it is necessary to relax the orientation. The relaxation process can occur simultaneously as the molten polymer fills the cavity isothermally. A complete relaxation of the flow-induced orientation is possible if the surface temperature of the mold remains the same for some time after the isothermal filling has been completed.

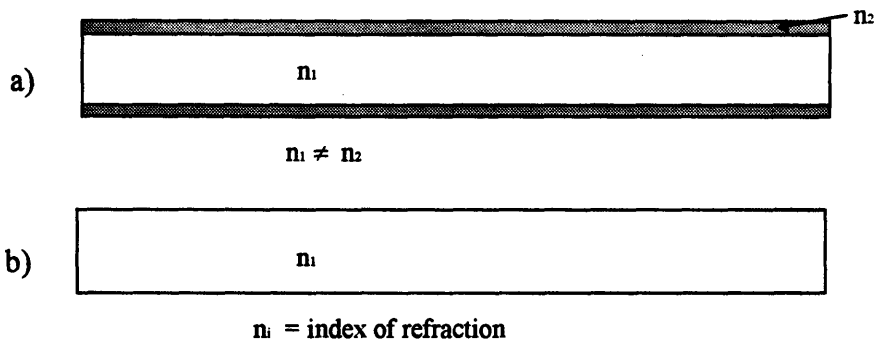

Figure III.2.2: Schematic comparison between a) conventional and b) isothermal filling process in molding an optical part.

Since there is no solidification layer along the surface of the mold during the isothermal filling process, the required pressure to fill the mold is less than that of the conventional mold filling process. As the L/t ratio (L = length, t = thickness of the part) increases, the solidification layer buildup increases in the conventional process and thus the area that the molten polymer passes through to fill the mold decreases. The reduction of the area directly results in an increase of the pressure requirement to fill the mold at the same filling rate. When the L/t ratio is too large such that the reduction of the area completely closes off the polymer passage, the mold cavity cannot be filled completely; this is termed "short shot." In the isothermal filling process there is no pressure drop resulting from the area reduction in the mold cavity. Moreover, shear stress will be reduced because of the lesser pressure gradient. The reduced shear stress results in a decrease of flow-induced molecular orientation.

Another advantage of the isothermal filling process is the lower packing pressure requirement for zero thermal shrinkage. The density of polymeric material at solid state is higher that that of molten polymer. In other words, the volume of polymeric material becomes smaller when the molten polymer solidifies. Therefore, in injection molding a high packing pressure needed for elastic deformation to compensate for thermal shrinkage can be reduced if initial melt temperature can be lowered.

Rinderle[84] has considered the elastic and thermal expansion of steel molds and plastics, and concluded that the volume changes of the mold can be neglected to obtain an approximate solution of the volume changes in plastics during the molding process. Rearranging the Spencer-Gilmore equation (7), and substituting the injection temperature, Ti, and the average final temperature, T_f, the following two equations can be written:

$$P_i = RT_i / (v_i - \omega) - \pi \qquad (8)$$

$$P_f = RT_f / (v_f - \omega) - \pi \qquad (9)$$

For zero volume change:

$$v_i = v_f \qquad (10)$$

and

$$P_f = P_{atm} \qquad (11)$$

$$P_f << \pi \qquad (12)$$

Equations (2) and (3) can be combined to determine the injection pressure for zero volume change in terms of the injection temperature and the average final temperature:

$$P_i = \left(\frac{T_i}{T_f} - 1\right) \pi \qquad (13)$$

The pressure required, P_i, can be reduced in the isothermal filling process because the injection temperature, T_i, in equation (13) can be lowered since the freezing of plastic during the filling stage is no longer an issue. With the decreased injection temperature, the time required to cool the part is correspondingly shortened.

One more advantage of the isothermal filling process is the consistency of the part. Since the temperature of the molten polymer in the mold cavity is the same throughout the entire cavity upon cessation of the flow and the cavity volume does not change, the pressure of the polymer melt must remain the same everywhere within the cavity. If the injection temperature and the mold surface temperature can be controlled from one injection cycle to the next, then the state of polymer in the cavity can be controlled thereby enabling one to produce consistent parts.

---

[84] Rinderle, James R., "A Method for Precision Injection Molding," M.S. Thesis, M.I.T., June 1979.

A disadvantage of this conservative method is the increased cycle time, the added complication of the mold design, and the waste of energy. This model also makes the unrealistic assumption that the melt is at a uniform temperature which is not the case as determined by experiments which probed the plastic temperatures in the nozzle and barrel. These problems represent an upper limit to the cycle time and the dimensional consistency of continually more complex parts.

III.3 Differential Cooling Process

A differential cooling process is defined as a controlled cooling process in which every section of the molded part is cooled uniformly (part temperature is independent of the spatial coordinate) so as to maintain a constant pressure throughout the molded part. In reality, the part can not be cooled uniformly by conduction since the heat transfer by conduction itself requires a temperature gradient. Although completely homogeneous parts can not be molded, one can minimize the deleterious effects of the secondary flow caused by density variations within the part. A concept of a differential cooling process that can eliminate the secondary flow of plastic from the thick to the thin sections is illustrated in this section.

Consider molding the part shown in Figure III.3.1. The part consists of a thin and a thick section. When the part is cooled from the molten state in a constant temperature mold, the thick section cools more slowly than the thin section because of the thermal insulation properties of the plastic. The average temperature in the thick section, therefore, is higher than that in the thin section during the cooling process. From the Spencer-Gilmore equation (1), it can be seen that the pressure of plastic is higher at higher temperatures of the plastic provided that the volume remains constant. Consequently, there is a secondary flow of plastic from thick to thin sections during the cooling process due to the pressure gradient. The secondary flow results in surface depressions known as "sink marks".

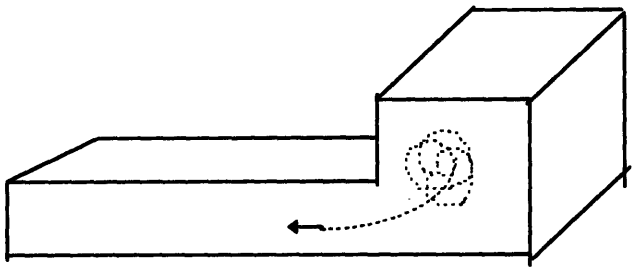

Figure III.3.1: A difficult part to mold because of the change in part thickness.

The differential cooling process minimizes the secondary flow of plastic from one section to another. There are two approaches to differential cooling of the part. One is to change the heat transfer rate by controlling the surface temperature of the mold. The other is to change the heat transfer coefficient through the thickness variation of the insulation that surrounds the part. The first method will be referred to as an active control method, and the latter will be referred to as a passive control method. Each method has its own advantages and disadvantages.

When the vitrification rates are the same, the temperature gradient between the two sections is minimized and thereby the pressure gradient is reduced. Consequently, the secondary flow from thick to thin sections can be minimized. The surface temperature at the thin section is lowered more slowly than that at the thick section in order to minimize the vitrification rate difference between the two sections. This reduction in the pressure gradient can be achieved with uniform part temperature rather than uniform mold temperature. This is an example of an isothermal mold inducing distortions rather than preventing them.

It is advantageous to use an active control method for a part of continuously varying cross section. For example, optical parts such as lenses must have a smoothly varying cross section. The vitrification rates in the varying cross section can be actively controlled at the thinner sections. The cycle time, therefore, does not increase since the thickest section of the part must also vitrify before ejecting the part.

The effects of an isothermal filling and a differential cooling process on the quality of the molded part have been discussed in this chapter. The part quality can be improved with active thermal mold control; otherwise, the isothermal filling and the differential cooling processes cannot be achieved with the mold. These processes affect the residual

stresses in the final part. A detailed study of the stress relaxation is presented in the next chapter.

III.4 Detailed Description Of The Filling And Cooling Stage

A detailed model will be developed that incorporates all essential information building from the molecular structure which influences the macroscopic properties of polystyrene. The models developed here can be used to determine warpage as well as heating duration and intensity requirements to achieve the desired product dimensions. The relation of these models with those discussed previously will illuminate the essential discrepancies of the models currently employed in industry as well as in technical journals. Furthermore, energy requirements to produce a part with temperature histories independent of position will be formulated.

Polystyrene was the polymer used. It was chosen for its transparent optical properties that will be exploited for later birefringence studies. Furthermore, polystyrene is one of the most researched polymers; thus, formulations developed in this section can be readily compared to the existing experimental data in the technical literature.

Figure III.4.1 provides the molecular structure of polystyrene. The benzene ring side groups adds stability to the molecule.

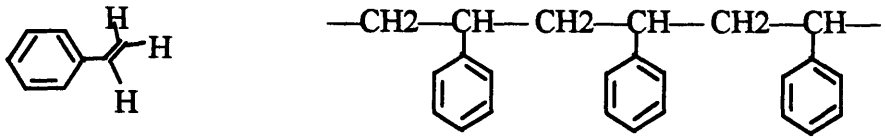

styrene
$C_6H_5CH=CH_2$

polystyrene

Figure III.4.1: The molecular structure of styrene and polystyrene.

Heat induces polymerization of styrene to polystyrene. During the filling stage the polystyrene is highly oriented with subsequent relaxation once flow terminates.

Figure III.4.2 shows the spatial and temporal dependance of the skin layer thickness as it develops during the filling stage.

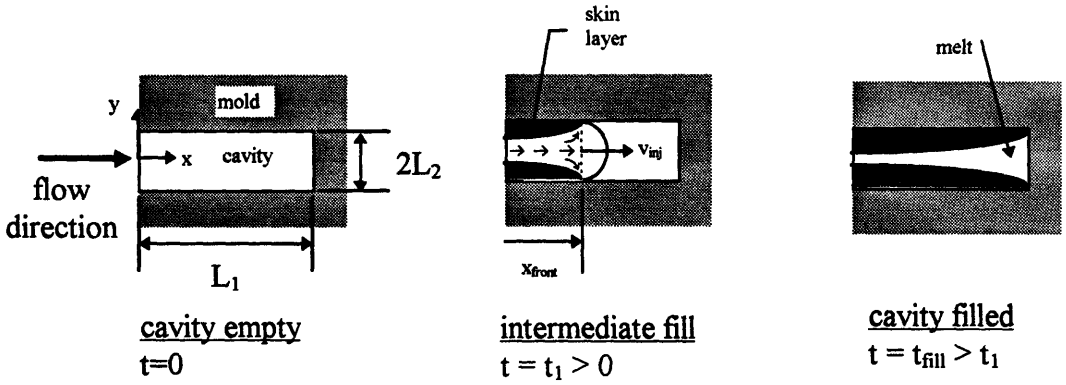

Figure III.4.2: Development of the skin layer.

The intermediate fill shows the dependence of the frozen skin layer thickness on the injection speed that roughly correlates with the wave front speed in the mold, v_{inj} (melt flow speed in the x direction). The total contact time of the mold and plastic interface (t_c) and the leading edge of the fountain flow front in contact with the cavity (x_{front}) (assuming melt solidifies at instant of contact) is given by:

$$t_c(x) = \frac{x_{front} - x}{v_{inj}} \qquad \text{for } x_{front} \geq x \qquad (14)$$

During the filling stage the plastic and the mold should have perfect contact $\Rightarrow$ no thermal contact resistance.

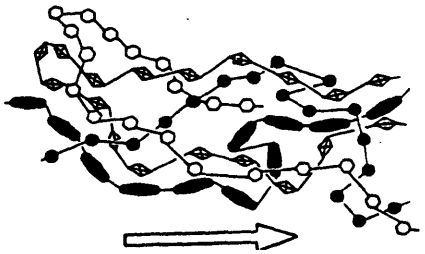

Figure III.4.3: Molecular orientation induced by injection.

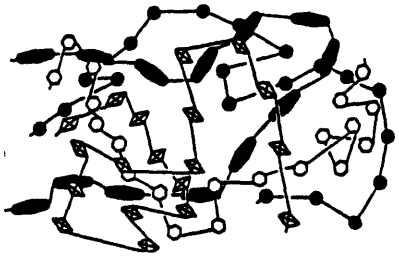

Figure III.4.4: Relaxation of orientation.

Injection induces preferential orientation of the polystyrene polymer chain. This stretching and kinking induces warpage when relaxation occurs because the amount of stretching is unbalanced between different solidification layers. The different solidification

layers are created by the inherently different solidification properties between the polymer solidifying while flowing during injection and filling and further solidification once flow terminates in the post filling stage.

There are three major parameters that characterize the energy requirement necessary for part quality and produce a part thermal history that is independent of the spatial coordinate. They are:

- skin layer thickness
- solidification front speed
- warpage tolerance

They are detailed below.

(a) Skin Layer Thickness and The Solidification Front Speed

Figure III.4.2 displayed the spatial and temporal variation in the skin layer thickness. Because the energy requirement to uniformly reduce these thicknesses are a function of the thickness, then the optimal energy requirement must also have the same functional relationship as that of the skin layer thickness. Thus, the energy requirement for skin layer reduction has both a spatial and temporal functional form.

Experimental evidence (Section VI.2(b)) has shown that a temperature gradient along the path length exists in the part and that the initial melt temperature injected into the mold is nonuniform. Therefore, the two melt solidification fronts (growing from $y = \pm L_2$ towards $y = 0$) will not meet at the rectangular body's plane of symmetry. This is another source of noniformity with has the same functional dependence as the skin layer thickness that results again with a spatial and temporal energy requirement function. The analyses quantifying these parameters are detailed below.

Semi Infinite body analysis of heat conduction in a region bounded by a moving surface (phase change of a solidifying body) is given in Mills[85] and is summarized below. These formulations provide an order of magnitude estimate of the skin layer thickness and the solidification front speed.

The formulations assume constant properties. The properties are: α_I (thermal diffusivity), ρ_I (density), k_i (thermal conductivity), and Cp_i (specific heat), for i = m (mold) and p (plastic) and both bodies initially at uniform temperatures.

Figure III.4.5 displays the heat transfer thermal circuit treating the mold as a semi-infinite body and the melt as a moving flow front. The coordinate $y = L_2 - y'$

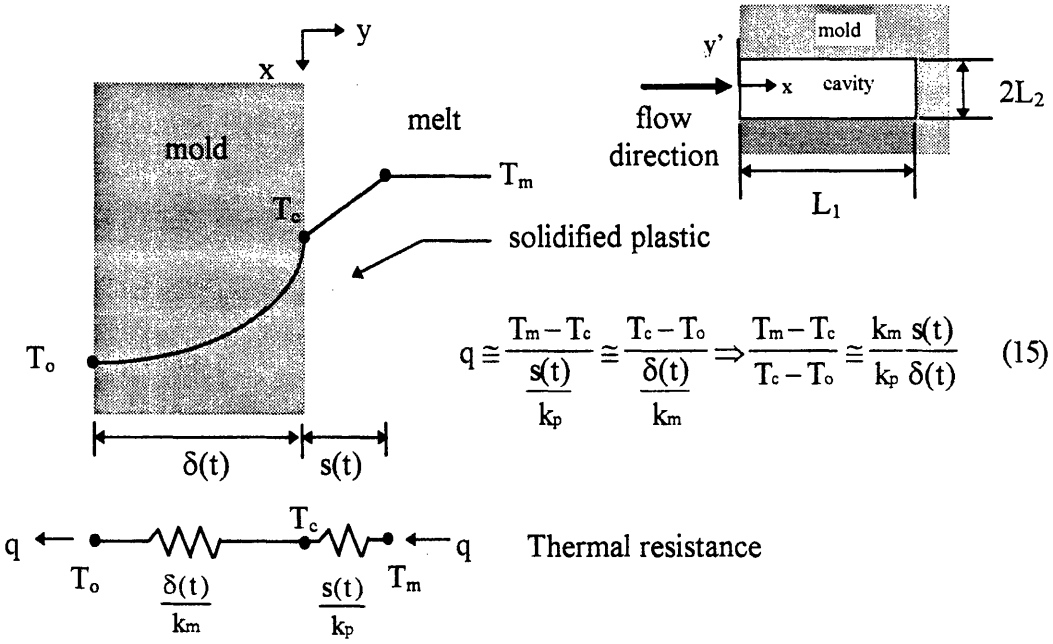

Figure III.4.5: Thermal circuit representation of the mold and the solidifying melt.

An estimation of $\frac{s(t)}{\delta(t)}$ is needed to determine the relative thermal resistance between the mold and the solidifying polymer where $\delta_{99} \equiv$ length of thermal penetration in the mold such that $\frac{T_m(\delta,t) - T_c}{T_c - T_o} = 0.99$ (16)

[85] Mills, A.F., Heat Transfer, Richard D. Irwin, Inc., Boston, MA, 1992.

Figure III.4.6 shows the temperature increase in the mold at an arbitrary time. Figure III.4.7 shows how energy transfer to the mold causes the moving flow front.

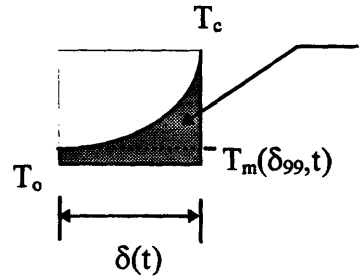

shaded area represents the energy taken up by the mold per unit area

$$\cong \rho_m C_{pm} \frac{T_c - T(\delta_{99},t)}{2} \delta_{99} \leq \rho_m C_{pm} \frac{T_c - T_o}{2} \delta_{99} \quad (17)$$

for $T(\delta_{99},t) \geq T_o$

Figure III.4.6: Energy balance on the heat absorbed by the mold.

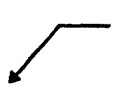

melt

energy given up by plastic to the mold $= \rho_p h_{sf\,p} s(t)$

Figure III.4.7: Energy balance on the heat released by the melt forming skin layer.

Thus, by conservation of energy, and reinserting and rearranging (15):

$$\rho_m C_{pm} \frac{T_c - T_o}{2} \delta(t) \geq \rho_p h_{sfp} s(t) \quad (18)$$

$$\Rightarrow \frac{\delta(t)}{s(t)} \geq \frac{2 \rho_p h_{sfp}}{\rho_m C_{pm} (T_c - T_o)} \Rightarrow \frac{T_m - T_c}{T_c - T_o} \leq \frac{k_m}{k_p} \frac{\rho_m C_{pm} (T_c - T_o)}{2 \rho_p h_{sfp}} \quad (19)$$

There are three thermal resistance considerations. These cases provide insight into the requirements of a specific low thermal inertia mold to the particular plastic being molded.

Case I: $\frac{T_m(\delta,t) - T_c}{T_c - T_o} << 1$ all the thermal resistance is in the mold $\Rightarrow T_m(\delta,t) \approx T_c$

$\Rightarrow q \cong \frac{T_m - T_o}{\frac{\delta(t)}{k_m}} \Rightarrow$ constant wall heat flux solution

$$\Rightarrow \qquad q \cong \frac{T_m - T_o}{\frac{\delta_{flux}}{k_m}} \qquad (20)$$

where $\delta_{flux} = \sqrt{\pi \alpha_m t}$ and $\frac{\delta_{flux}}{\delta_{99}} = \frac{\sqrt{\pi}}{3.65}$

Solidification:

$$q = \frac{\dot{m}}{A} h_{sfp} = \frac{\rho_p A(-\frac{ds}{dt})}{A} h_{sfp} = -\rho_p h_{sfp} \frac{ds}{dt} \qquad (21)$$

Equating the q's and integrating to solve for $\frac{ds}{dt}$ and s:

$$\frac{ds}{dt} = -\frac{k_m(T_m - T_o)}{\rho_p h_{sfp} \sqrt{\pi \alpha_m t}} \qquad \Rightarrow \qquad s(x) = s(x(t=0)) + \frac{2k_m(T_m - T_o)}{\rho_p h_{sfp} \sqrt{\pi \alpha_m}} \sqrt{\frac{x_{front} - x}{V_{inj}}} \qquad (22)$$

$$\text{for } t \le \frac{L_1}{V_{inj}} \text{ and } \delta_{99} \le L_1$$

This s(x) overpredicts the thickness since the melt is at a temperature higher than the solidification or glass transition temperature T_m. At $t = \frac{L_1}{V_{inj}}$ the flow front has reached the end of the cavity and for $\delta_{99} > L_1$ the semi infinite body solution is no longer valid. After the plastic stops flowing and packing, the plastic will start to shrink; thus, perfect plastic and mold contact is no longer valid. These air gaps represent thermal contact resistant regions which hampers heat transfer. Therefore, warpage is a greater problem in a part with greater shrinkage capacity and possibly thinner section parts. Once the flow completely stops birefringence patterns disappear in the interior sections indicating a relaxation of stresses in the core region of the plastic. Intuitively this observation is reasonable since the core region is the unsolidified plastic no longer subjected to the shearing stress induced by the flow. Two additional cases are detailed below.

<u>Case II:</u> $\frac{T_m(\delta, t) - T_c}{T_c - T_o} >> 1$ all the thermal resistance is in the plastic $\Rightarrow T_o \approx T_c \approx$ constant

This case considers a thermally controlled mold surface temperature. The formulations developed for this case provides a heat transfer lower limit for low thermal inertia injection molding.

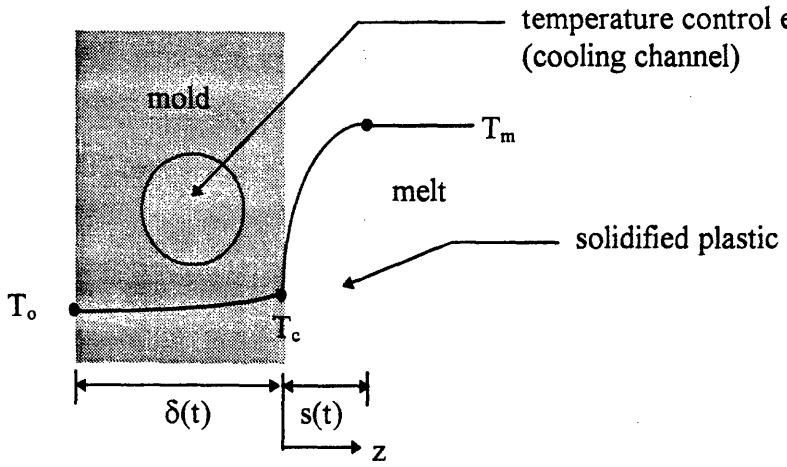

Figure III.4.8: Thermal profile of a thermally controlled mold surface.

Because to the size of the mold (infinite) relative to the rectangular part 1-D conduction may be assumed. Therefore:$\Rightarrow$ $\frac{d^2T}{dz^2} = \frac{1}{\alpha_p}\frac{dT}{dt}$ where $z = L_2 - y$ (23)

Boundary conditions: z=0: $T(0,t) = T_c$ Initial condition: t=0: $T(z,0) = T_m$

z=s: $T(s,t) = T_m$

Transforming to nondimensional variables: $\Theta \equiv \frac{T(z,t)-T_c}{T_m-T_c}$ and $\zeta = \frac{z}{\sqrt{\alpha_p t}}$ (24)

Transformed boundary conditions: $\zeta = 0: \Theta = 0$; $\zeta = \frac{s(t)}{\sqrt{\alpha_p t}}: \Theta = 1$

Transformed initial condition: $\zeta \to \infty : \Theta \to 1$

The interface surface balance between the melt and the solidified layer gives:

$$q \equiv \frac{\frac{T_m - T_c}{\delta_{flux}}}{k_m} = \frac{m}{A} h_{sfp} = -\rho_p h_{sfp} \frac{ds}{dt} \Rightarrow Ja \equiv \frac{Cp_p(T_m - T_c)}{h_{sfp}} = \sqrt{\pi}\left(\frac{\zeta}{2}\right) e^{\left(\frac{\zeta}{2}\right)^2} \operatorname{erf}\left(\frac{\zeta}{2}\right) \quad (25)$$

The plot of equation (25) is given in Figure III.4.9.

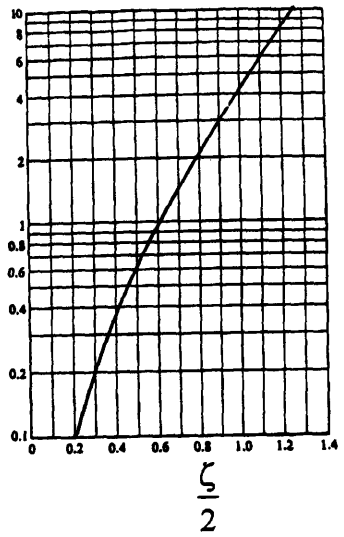

Figure III.4.9: Plot of equation (25), $Ja \equiv \frac{Cp_p(T_m - T_c)}{h_{sfp}} = \sqrt{\pi}(\frac{\zeta}{2}) \quad e^{(\frac{\zeta}{2})^2} \; erf(\frac{\zeta}{2})$.
(Courtesy Mills, 1992)

Therefore, $$\frac{ds}{dt} = (\frac{\zeta}{2})\sqrt{\frac{\alpha_p}{t}} \text{ and } s = \zeta\sqrt{\alpha_p t} \qquad (26)$$

which is valid for $t \geq 0^+$

$t=0^+$ when the front has reached that location in the mold ($x_{front} = x$)

The concept of variable wall temperatures can be applied to better simulate actual conditions of the thermally controlled mold surface. This case would best model thin sections where large ratios of thermal gradients to the thickness of the part exists.

<u>Case III:</u> $\frac{T_m(\delta,t) - T_c}{T_c - T_o} \cong 1$

thermal resistance of solidifying material $\cong$ thermal resistance of the mold

Assume $Ja << 1 \Rightarrow Ja \equiv \frac{Cp_p(T_m - T_c)}{h_{sfp}} = \sqrt{\pi}(\frac{\zeta}{2}) \quad e^{(\frac{\zeta}{2})^2} \; erf(\frac{\zeta}{2})$

$$\Rightarrow Ja \cong \frac{\zeta^2}{2} + \frac{\zeta^4}{12} + \frac{\zeta^6}{120} + \ldots \quad \text{as} \quad \zeta \to 0 \qquad (27)$$

$$\Rightarrow Ja \cong \frac{\zeta^2}{2} \Rightarrow \zeta \cong \sqrt{2Ja} \Rightarrow \zeta \cong \sqrt{\frac{2Cp_p(T_m - T_c)}{h_{sfp}}} \Rightarrow \rho_p h_{sfp}\sqrt{\frac{Cp_p(T_m - T_c)\alpha_p}{2h_{sfp}}} = \frac{k_m(T_c - T_o)}{\sqrt{\pi\alpha_m}} \quad (28)$$

$$\Rightarrow \frac{\pi\rho_p{}^2 h_{sfp} Cp_p \alpha_p (T_m - T_c)\alpha_m}{2k_m{}^2} = (T_c - T_o)^2 \quad (29)$$

$$\text{let } A \equiv \frac{\pi\rho_p{}^2 h_{sfp} Cp_p \alpha_p (T_m - T_c)\alpha_m}{2k_m{}^2} \quad (30)$$

Expand and solve using the quadratic equation:

$$T_{c1,2} = \frac{-b \pm \sqrt{b^2 - 4ac}}{2a} \quad \text{for} \quad aT_c{}^2 + bT_c + c = 0 \text{ where } a = 1 \quad b = A - 2T_o \quad \text{and} \quad c = T_o{}^2 - AT_m$$

A physical constraint on the temperature range of T_c ($T_o < T_c < T_m$) eliminates one of the two mathematical solutions to give the unique physical solution.

$$\text{So with } A > 0 \Rightarrow \frac{-b}{2a} = T_o - \frac{A}{2} < T_o \quad \text{and} \quad \frac{\sqrt{b^2 - 4ac}}{2a} \geq 0 \Rightarrow T_o - \frac{A}{2} - \frac{\sqrt{b^2 - 4ac}}{2a} < T_o$$

$$\Rightarrow T_c = T_o - \frac{A}{2}\left(1 - \sqrt{1 - \frac{4(T_m - T_o)}{A}}\right) \quad (31)$$

$$\zeta \cong \sqrt{\frac{2Cp_p(T_m - T_c)}{h_{sfp}}} \quad (32)$$

$$\text{Therefore,} \quad \frac{ds}{dt} = \left(\frac{\zeta}{2}\right)\sqrt{\frac{\alpha_p}{t}} \text{ and } s = \zeta\sqrt{\alpha_p t} \quad (33)$$

There will be two solidification fronts one from each of the mold surfaces along the y axis. It is proposed that warpage is induced by unbalanced cooling which manifests in these fronts meeting off center ($y \neq 0$).

(b) Warpage Development As Thermal Gradients Across The Part's Thickness

The objective of this section is to correlate a temperture gradient across the thickness of the part with the warpage induced by this gradient. The formulations can be used to determine the temperatuare gradient necessary to bring a given part warpage back into tolerance. Planar elastic theory was assumed and the skin layer thickness and solidification front speed calculated in one of the three above cases were employed.

The relevant background formulations are:

Hooke's Law (planar):

$$\varepsilon_x = \frac{1}{E}(\sigma_x - \nu\sigma_y) + \alpha\Delta T$$
$$\varepsilon_y = \frac{1}{E}(\sigma_y - \nu\sigma_x) + \alpha\Delta T \qquad (34)$$
$$\gamma_{xy} = \frac{\tau_{xy}}{G} \quad \text{where} \quad G = \frac{E}{2(1+\nu)}$$

Elasticity Theory (planar):

Force equilibrium (neglect body forces):
$$\frac{\partial}{\partial x}\sigma_x + \frac{\partial}{\partial y}\tau_{xy} = 0$$
$$\frac{\partial}{\partial y}\sigma_y + \frac{\partial}{\partial x}\tau_{xy} = 0 \qquad (35)$$

Compatibility of strain:
$$\frac{\partial^2}{\partial y^2}\varepsilon_x + \frac{\partial^2}{\partial x^2}\varepsilon_y = \frac{\partial^2}{\partial x \partial y}\gamma_{xy} \qquad (36)$$

combining the above equations give:
$$\left(\frac{\partial^2}{\partial x^2} + \frac{\partial^2}{\partial y^2}\right)\{\sigma_x + \sigma_y + \alpha E\Delta T\} = 0 \qquad (37)$$

For a rectangular part $L_1 >> 2L_2 (=2s) >> W$

where W is the width of the rectangular part into the page

Assuming the temperature gradient is in the y direction only ($\Delta T(y)$ only):

$\Rightarrow$ No stresses in the z direction $\sigma_z = 0$, $\sigma_{yz} = \sigma_{xz} = 0$, $\sigma_y = 0$, and $\sigma_x = \sigma_x(y)$

$$\Rightarrow \frac{\partial^2}{\partial y^2}\{\sigma_x(y) + \alpha E\Delta T(y)\} = 0 \qquad (38)$$

Integrating: $\Rightarrow \sigma_x(y) = -\alpha E\Delta T(y) + C_1 y + C_2 \qquad (39)$

When the mold halves open, the part's ends are unconstrained:

$$\text{Net force} = 0: \quad Fx = 0 = W \int_{-\frac{L_2}{2}}^{\frac{L_2}{2}} \sigma_x \, dy \qquad (40)$$

Net moment = 0: $$M = 0 = W \int_{-\frac{L_2}{2}}^{\frac{L_2}{2}} y\sigma_x \, dy \qquad (41)$$

$$\Rightarrow C_1 = \frac{12}{L_2^3} \int_{-\frac{L_2}{2}}^{\frac{L_2}{2}} \alpha E y \Delta T(y) \, dy \quad \text{and} \quad C_2 = \frac{1}{L_2} \int_{-\frac{L_2}{2}}^{\frac{L_2}{2}} \alpha E \Delta T(y) \, dy \qquad (42)$$

More accurately, s (skin layer thickness at the time the solidification fronts meet) should be used but $s \approx L_2$ (half thickness of the part) and $s = L_2$ for a completely balanced cooling. An accurate calculation of s is needed to compute the final warpage of the part.

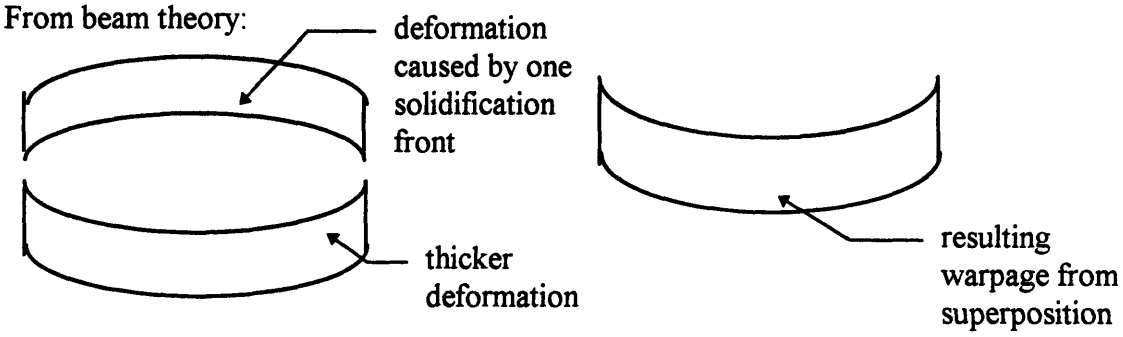

Figure III.4.10: Resulting warpage from the superposition of the two solidifiation fronts.

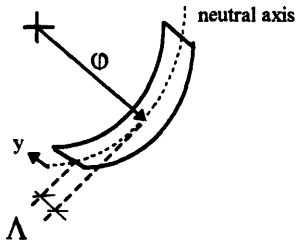

$$\varepsilon_x = \frac{\sigma_x}{E} + \alpha\Delta T = \frac{y}{\varphi} \qquad (43)$$

where φ is the radius of curvature

Figure III.4.11: Neutral axis deviation as a measurement of warpage.

$$\varphi \equiv \frac{\frac{\partial^2 y}{\partial x^2}}{[1+(\frac{\partial y}{\partial x})^2]^{\frac{3}{2}}} \cong \frac{\partial^2 y}{\partial x^2} \quad \text{for small distortions} \Rightarrow y = \frac{x^2}{2\varphi} \Rightarrow \Lambda = \frac{L_1^2}{8\varphi} \qquad (44)$$

$$\Lambda = \frac{L_1^2}{8y}(\frac{\sigma_x}{E} + \alpha\Delta T) \qquad (45)$$

where Λ is the warpage induced by the solidified skin layer and the additional solidified layer at the point when the two flow fronts meet. There is one Λ on each side of the mold just prior to the meeting of the two solidification fronts. (Λ is the y direction thickness measured from the surface of the mold)

This can be applied for assumed mold surface temperatures at $y = L_2$ and $y = -L_2$ and the location where the two flow fronts meet which is approximately at $y = 0$. Assuming linearity and using superposition give:

$$\Lambda_{net} = |\Lambda_1 - \Lambda_2| \qquad (46)$$

The above equation models the rectangular part as two halves each with individual warpages associated with the thermal gradient. The plastic melt zone present in the middle section (region around y = 0)after the mold fills allows this simplification. This analysis explains the phenomenon of the plastic bending towards the hotter side after the mold opens. The hotter side has a smaller Λ, so Λ_{net} pushes the plastic towards the hotter side.

(c) Comparison Of Formulations

The following are relations commonly used in recent technical literature. The formulations developed above can be compared to those currently used to estimate the skin layer.

The assumptions used for a semi-infinite slab solution are: (1) 1-D heat transfer and flow (end gated slab); (2) constant wall temperature T_o ; (3) uniform melt temperature T_m at the time of fill, t_{fill} ; (4) isothermal Poiseuille flow of a power law fluid; and (5) viscoelastic stress relaxation commencing at the instant of fill for a thermorheologically simple material. The equation does not account for the latent heat of fussion.

$$\frac{T-To}{Tm-To} = 2\sum_{m=0}^{\infty} \frac{(-1)^m}{(m+1/2)\pi} \times e^{-(m+1/2)^2\pi^2\alpha t/b^2} \cos[(m + 1/2)\pi / b] \qquad (47)$$

Implicit assumptions for the above equations are that the frozen layer next to the cavity walls is negligibly small and that the thermal properties of the polymer are independent of

temperature and pressure. Not accounting for the skin layer underestimates the heat requirement to reduce residual stresses and underestimates the level of warpage.

For a fully developed plane Poiseuille flow of a power law fluid, the velocity gradient is given by:

$$\left|\dot{\gamma}\right| = \frac{Qb(2n+1)}{2Wn(b-\delta)^3}\left(\frac{y}{b-\delta}\right)^{1/n} \tag{48}$$

where W is the width of the cavity and δ is the thickness of the frozen layer of polymer adjacent to the wall (the skin layer). Implicit in the above equation is that any extensional stresses that may arise in the gate area decays rapidly and practically vanish at some small distance downstream from the gate. The equation will not be able to account for the velocity gradient once the leading edge of the fountain flow has reached the end of the mold but the melt is continuing to fill the mold. The skin layer reduces the effective gap for flow and thus increases the wall shear stress and the pressure drop in the cavity. The skin layer (δ) may be calculated from the solution of the heat-conduction equation for a semi-infinite medium,

$$\delta = \frac{T_g - T_{mold}}{T_{melt} - T_{mold}}(4\alpha t_c)^{1/2} \tag{49}$$

where t_c is the time of contact of the melt wit the wall during the filling stage (Figure III.4.2). This time may be estimated from:

$$t_c = \frac{2bW(L-x)}{Q} \tag{50}$$

The shear stress for a power law fluid is:

$$\sigma_{12} = K\left|\dot{\gamma}\right|^n \tag{51}$$

where $K = \exp(a_0 + a_1/T + a_2 P + a_3 P/T)$

The first normal stress difference is then calculated from an empirical relationship:

$$N_1 = A\,\sigma_{12}^{\beta} \tag{52}$$

where A and β are material constants.

The residual stresses can be expressed in terms of birefringence (stress-optical law):

$$\Delta n \equiv n_1 - n_2 = C(N_1^2 + 4\sigma_{12}^2)^{1/2} \qquad (53)$$

where C is the stress-optical coefficient of the material.[86] ($C = 4.5 \times 10^{-10}$ cm^2/dyn Dow Styron 685D - commercial polystyrene)

Depending on the injection conditions the melt can either "jet" or form a front as it flows in the mold. This will affect the skin layer thickness calculation. Fountain flow deposits hot melt from the center of the mold onto the wall where it solidifies while jetting fills the cavity more irregularly.

In either case, the hypothesis is that thermal control should be input after the mold completely fills and immediately prior to the complete solidification of the melt in the mold. This is because some shear stress that has built up during filling can relax because there is a compliant melt core region. Relaxation of shear stress takes 0.1-1.0 seconds. The relaxation time t_R (the period required for the disappearance of stress birefringence in the flowing region) rapidly decreases with increasing melt temperature T_m, but is hardly affected by the injection velocity. From experimental results, an empirical correlation between the relaxation time and injection temperature for polystyrene is as follows:

$$t_R = 4980 \exp(-0.0416\, T_m) \text{ [sec]} \qquad (54)$$

where T_m is expresses in °C

This relaxation time can be used to estimate the filling thermal control time.

The thermal input should be applied with the appropriate thermal lag time accounted for such that the greatest energy input is imparted to that plastic region with the longest mold residence time.

Further solidification produces stress variations that should also be reduced to reduce warpage. The shrinking of the plastic produces gaps between the mold and the plastic, which complicates the thermal treatment because thermal contact coefficients must be calculated for the air gap between the plastic and the mold. A model of spatial and temporal shrinkage or melting the skin region so that it is always in contact with the mold may be possible solutions. The temperature gradients established during solidification

[86] VanKrevelen D.W., and Hoftyzer, P.J., Properties of Polymers, Elsevier, Amsterdam, 1976.

have the greatest effect on warpage. For symmetric cooling the solidification fronts meet at the center of the part; therefore, the forces are balanced with tensile strain in the center and compressive strain near the surfaces. For asymmetric cooling the solidification fronts meet off center of the part causing a shift in the strain distribution. Upon release, the part will bend in the direction of the hotter side.

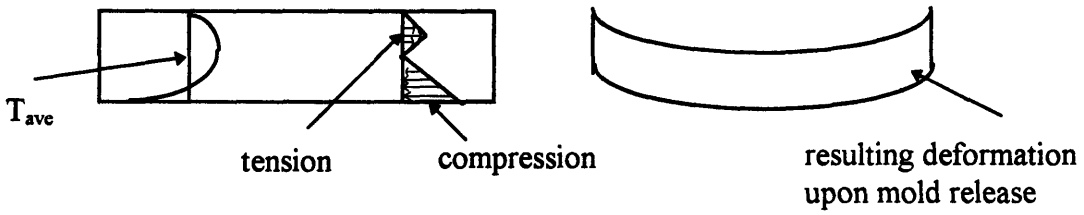

Figure III.4.12: Effect of unbalanced thermal control on the part.

The final deformation of the part or the warpage can be calculated in a simplified way if it is assumed that the elastic modulus of the material takes on a constant average value at the specified glass transition temperature and that viscoelastic effects are negligible.[87] That is:

$$E = 0, \quad T > T_g \qquad (55)$$

$$E = \bar{E}, \quad T \leq T_g \qquad (56)$$

where E is the elastic modulus, T is the temperature, T_g is the glass transition temperature and $\bar{E}$ is the average value of the elastic modulus. The stress distribution is evaluated in the following way.

$$\sigma_n = \alpha \bar{E} (T_n - \bar{T}) \qquad (57)$$

where σ_n is the normal stress at the n^{th} layer after all temperatures have reached ambient temperature, T_n is the temperature of that layer at the time when the maximum plastic temperature reaches the glass transition point, $\bar{T}$ is the average temperature at the same time and α is the average thermal expansion coefficient (assumed constant). A positive value of σ_n indicates tension.

The stress distribution is then converted to an equivalent bending moment by:

---

[87] Jacques, Michael St., An Analysis of Thermal Warpage in Injection Molded Flat Parts Due to Unbalanced cooling.

$$M = \sum_{n=1}^{m} \sigma_n A_n \delta_n \qquad (58)$$

where M is the bending moment, A_n is the cross sectional area of the n^{th} layer and δ_n is the distance of the n^{th} layer from the center of the part.

Finally, the deformation is obtained using pure bending theory:

$$d = M L^2 (1 - \mu^2) / (8 \bar{E} I) \qquad (59)$$

where d is the maximum deflection of the plate or warpage, L is its length, μ is Poisson's ratio, and I is the moment of inertia in bending.

It must be noted that ignoring viscoelastic effects results in a more severe deformation than actual. As the difference in cooling fluid temperatures between mold halves increases, the predicted warpage increases linearly. The thinnest part warps the greatest amount, because of its relatively small moment of inertia in bending. The sensitivity of part warpage is greater for the design condition of asymmetric cooling fluid temperatures than for the case of different distances of the cooling channel to the surface of the cavity and the effects are approximately additive. Experimental verification is required before the accuracy of the model can be conclusively evaluated.

The major difference between the correlations employed in current technical literature and the correlation written in this thesis is that the latent heat of fusion is used here, whereas, other literatures ignore the skin layer in their analysis.

After the solidification and ejection of the part, the cycle repeats as before. The mold cavity is briefly exposed to the air which can be neglected in the heat transfer analysis. Under the assumption of rapid cycle times and the high thermal inertial of the typical mold, the time duration of ambient exposure is negligible compared to the time constants of the mold temperature decay. The mold temperature decay time constants obtained from experimentation indicate that this is a reasonable assumption.

CHAPTER IV

ANALYSIS OF STRESS RELAXATION

IV.1 Introduction

In order to predict the residual stresses in the injection molded part, a rheological constitutive equation that can characterize the nonlinear viscoelastic flow behavior of the polymer melt must be used. Wagner's[88],[89] integral type constitutive equation can predict the stress relaxation from the instant the mold is filled by fully developed simple shear flow. Leonov developed a differential type constitutive equation[90],[91] which successful describes the nonlinear viscoelastic behavior[92],[93]. However, both analyses are highly dependent on property values; thus, they will not used in this research.

The stress-optical law will be described in detail in Sections IV.2. Section IV.3 provides a prediction of isothermal stress relaxation upon cessation of fully developed simple shear. A nonisothermal stress relaxation of an injection molded part will be discussed in Section IV.4.

These formulations and considerations enable the molder to determine the duration and intensity of heating to remove the skin layer described previously as well as balancing the heating requirement during the post-filling stage.

---

[88] Wagner, M.H., Rheol. Acta, 15, 1976, p. 136.
[89] Wagner, M.H., Rheol. Acta, 16, 1977, p. 43.
[90] Leonov, A.I., Rheol. Acta, 15, 1976, p. 85.
[91] Leonov, A.I., E.H. Lipkina, E.D. Paskhin, and A.N. Prokunin, Rheol. Acta, 15, 1976, p. 411.
[92] Isayev and Hieber, Rheol. Acta, 19, 1980, p. 168.
[93] Wang, K.K., S.F. Shen, C. Cohen, C.A. Hieber, and A.I. Isayev, "Computer Aided Injection Molding Systems," Progress Reports Nos. 6-8, Cornell University for NSF under grant APR74-114990.

IV.2 The Stress-Optical Law

The theory that relates changes in the indices of refraction of a material to the anisotropical state of stress in the material is known as the stress-optic law. These laws are used to relate fringe patterns caused by phase shifting of the electric field to isostress contour lines. The isostress contour lines are used to determine the residual stresses in the part. Thus, the amount of orientation in an injection molded part can be determined by measuring the birefringence. Maxwell[94] reported that the changes in the indices of refraction were linearly proportional to the loads. The relationships are expressed as follows:

$$\begin{aligned} n_1 - n_0 &= c_1 \sigma_1 + c_2 (\sigma_2 + \sigma_3) \\ n_2 - n_0 &= c_1 \sigma_2 + c_2 (\sigma_1 + \sigma_3) \\ n_3 - n_0 &= c_1 \sigma_3 + c_2 (\sigma_2 + \sigma_1) \end{aligned} \qquad (60)$$

where

$\sigma_1, \sigma_2, \sigma_3$ = principle stresses at a point

n_0 = index of refraction in unstressed state

n_1, n_2, n_3 = indices of refraction in stressed state associated with principal stress directions

c_1, c_2 = constants known as stress-optic coefficients

Although equations (60) provide the complete state of stress at a point, practical application has been limited because of the difficulty in measuring absolute changes in the index of refraction. However, the more widely used method of photoelasticity makes use of relative changes in the indices. The following equations are obtained by eliminating n_0 from equation (60):

$$\begin{aligned} n_1 - n_2 &= c (\sigma_2 - \sigma_1) \\ n_3 - n_2 &= c (\sigma_2 - \sigma_3) \end{aligned} \qquad (61)$$

---

[94] Maxwell, J.C., "On the Equilibrium of Elastic Solids," Trans. R. Soc. Edinburgh, XX, part 1, 1853, p. 87-120.

$$n_1 - n_3 = c\,(\sigma_3 - \sigma_1)$$

where $c = c_2 - c_1$ is the relative stress-optic coefficient, usually expressed in terms of brewsters (1 brewster = 10^{-13} cm^2/dyn = 10^{-12} m^2/N = 6.895 x 10^{-9} in^2/lb) - c is taken as 4500 brewsters[95].

For plane-stress situations, equations (61) reduce to:

$$\Delta n = n_1 - n_2 = c\,(\sigma_2 - \sigma_1) \qquad (62)$$

From the Mohr's circle, the principal stress can be expressed in terms of normal stress and thus equation (62) can also be expressed as

$$\Delta n = c\,[4\tau_{12}^2 + (\tau_{11} - \tau_{22})^2]^{\frac{1}{2}} \qquad (63)$$

The relationship of birefringence (Δn) to the stress in amorphous polymers obeys the stress-optic law. Oda, White, and Clark[96] found that the molecular orientation in polymeric parts is quantitatively related to the principal stress difference acting at the time of vitrification.

IV.3 Isothermal Stress Relaxation

An isothermal stress relaxation after the termination of a fully developed one-dimensional shear flow is considered in this section. Analysis of this section is useful in describing the stress relaxation behavior of the injection molded part when the isothermal condition is maintained some time after the filling stage has been completed.

Consider the situation in which a polymer melt is initially at a uniform temperature T_m and flowing as a fully-developed flow between parallel plates. From time $t = 0^-$ to $t = t_{fill}$, the temperature of the plate remains the same as that of the melt, namely T_m. Thus, the fully developed isothermal flow condition is identical to the initial condition. At t =

[95] Dietz, White, and Clark, "Orientation, Development and Relaxation in Injection Molding of Amorphous Polymers," Polymer Engineering and Science, 18, 4, (March 1978), p. 273.
[96] Oda, K., J.L. White, and E.S. Clark, Polymer Engineering and Science, 18, no. 1, 1978, p. 53.

t_{fill}, the flow stops and the flow-induced stress starts to relax while the melt temperature remains constant at T_m, assuming that viscous heating is negligible.

The isothermal relaxation of shear stress, primary normal stress difference, and birefringence exhibit similar behavior.[97] A decrease in the pressure gradient results in the lower initial values of the three, but higher values for later times than the higher pressure gradient. The steady state values can be reached in about one fifth the time for the higher pressure gradient.

In this case no skin layer should form and a uniform melt temperature can be assumed for the initial condition. When solidification begins, however, the part corners cool faster than the middle of the part. This should not result in warpage, because residual stresses are relaxed shortly after filling phase. The thermal requirement would still be to maintain a nonuniform mold surface temperature trajectory because of the differing solidification environments encountered by the ends versus the middle of the part as discussed previously.

IV.4 Nonisothermal Stress Relaxation

In practice, the stress will relax in a nonisothermal environment. The molten polymer in the mold cavity must be cooled below the glass transition temperature before it can be ejected. The stress relaxation rate at a lower temperature is slower. In analyzing the nonisothermal stress relaxation, one must take this variation of the relaxation rate caused by temperature changes into account. In thermoplastic materials, however, the changes in temperature can be easily compensated for by the appropriate changes in the relaxation time using the WLF temperature-shift factor[98]. A variation of temperature corresponds to a shift in time scale; thus, all relaxation time changes with temperature are proportional to the shift factor.

---

[97] Kim, B.H., "Low Thermal Inertia Injection Molding," Ph.D. Thesis, M.I.T., p. 74-76, July 1983.
[98] Flaman A.A.M. "Buildup and Relaxation of Molecular Orientation in Injection Molding. Part I: Formulation"

Kim[99] found that the flow-induced stresses relax on the order of a second for the isothermal filling and nonisothermal cooling process, and the residual stresses can be minimized without difficulty. Because of the viscoelastic nature of the polymer melt, the more strain the melt undergoes during filling (within the longest relaxation time period) the faster it will relax. Hence the cavity should be filled as rapidly as possible for molecular relaxation and for decreasing total cycle time. If the molding machine cannot provide the rapid filling then the isothermal condition can be maintained beyond the completion of filling to allow orientation caused by small strain from the slow filling process to relax. Therefore, molding a part with the minimum residual stress can be achieved if molecular relaxation takes place before vitrification by using a heated mold surface. This heating restores the condition of the plastic to that of the isothermal stress relaxation shortly after filling. Thus, both the isothermal and the nonisothermal stress relaxation processes require the same mold temperature variation rather than a constant mold surface temperature.

[99] Kim, B.H., "Low Thermal Inertia Injection Molding," Ph.D. Thesis, M.I.T., p. 81, July 1983.

CHAPTER V

Development Of Injection Molding Tooling

V.1 Introduction

The first step in the design is to define the desired plastic part geometry and location of cooling channels and heater locations in the mold. The thermal control ideally should be close to the surface for two reasons. First, the relatively low thermal conductivity of mold materials could make heat diffusion through the metal walls longer than desired. Second, since the mold cavity is the only part of the mold that the plastic comes in contact with, any thermal cycling in the mold that does not happen at the surface of the mold cavity is wasted.

Determination of an optimal test part geometry was based on several required characteristics which are based on the objectives of this thesis. A geometry was sought that contained the following features:

1. The geometry of the part should lend itself to one-dimensional analysis and corroborate information published by other researchers using the same geometry.

2. The part geometry should be sensitive (in terms of warpage or distortion) to the mold surface temperature.

3. The geometry should have characteristic features that can be easily measured to distinguish the amount of distortion that may exist. In this case "distortion" refers to the deviation of the plastic part dimensions from the mold cavity shape accounting for shrinkage.

4. The effects of the dynamic thermal boundary inputs on residual stresses can be readily visualized.

The most common geometry used in the technical literature was a thin rectangular bar. Because this geometry satisfied all the research requirements, the thin rectangular bar was used.

The plastic chosen for the test parts is clear polystyrene (DOW 678). Polystyrene was chosen because it is the plastic used in numerous other research studies; thus, a comparative analysis can be made. Furthermore, it is commonly used in industry. Experimentally, it remains clear during both the flow and solidification stages of molding which is a prerequisite for flow visualization. Other properties are rigidity, good dimensional stability, good moldability and low moisture absorption, which precludes the need for predrying the plastic pellets[100].

Polystyrene, compared to other thermoplastics, is hard, rigid, and has a distinct metallic sound when dropped. Its specific gravity is around 1.06, it is brittle, has medium resistance to oil and is unable to withstand temperatures around that of boiling water. Polystyrene is widely used in injection molding and vacuum forming[101].

Table V.1.1: Thermophysical Data Of Polystyrene.

Temp. [K]	Thermal Diffusivity [m^2/s]	Linear Expansion [x 10^{-6} /K]	Temp. [K]	Thermal Diffusivity [m^2/s]
295	1.29×10^{-7}	71	420.3	8.4×10^{-8}
311.8	1.19	71	432.9	8.21
326.6	1.12	71	440.9	8.22
338.7	1.13	71	451.0	8.2
350.2	1.12	71	460.6	8.2
361.4	9.87×10^{-8}	71	473.2	8.2
383.2	8.85	71	485.4	8.19
393.2	8.57		493.1	8.21
403.2	8.41			

Melt Temp. [°C]	Mold Temp. [°C]	Specific Gravity	Specific Heat [J/Kg K]	Latent Heat of Fusion [J/kg]	Flow Path Ratio
200	20	1.05	1720	71,400	150

[100] Brydson, J.A., *Plastics Materials*, fifth edition, pp. 252-282, Butterworth Books, London 1989.
[101] Ibid.

The flow path ratio is a rough "rule of thumb" first approximation of the moldability of a plastic part. It is the ratio of flow distance / section thickness. If in a particular mold, the flow path ratio is less than the table values the part will fill. This assumes typical mold temperatures conditions and relatively constant cross sections.

Some factors that have to be considered when using polystyrene as a molding plastic are[102]:

1. Polystyrene has a comparatively low specific heat, which makes it easier to heat in the plasticizing cylinder. It therefore cools faster that other polyolefins, which means faster cooling times.

2. It has a strong viscosity dependence on shear rate. This means that care has to be taken when designing molds with comparatively narrow sections.

3. It has low shrinkage because of its lack of crystallization on freezing.

4. Since it is relatively rigid, it is difficult to produce parts free from internal stresses. Although this is true of all thermoplastics, it is especially so for polystyrene.

5. It is recommended, in order to obtain a polystyrene part with minimum strain, to inject the plastic in a homogeneous melt state into a hot mold, at an injection pressure that will drop to zero when the melt solidifies.

V.2 Design Considerations For The Dynamic Thermal Boundary Mold

The purpose of thermal spatial and temporal control is to reduce warpage or increase part consistency while maintain a reasonable injection molding cycle. The effect of these varying temperature profiles can be visualized using a specially built mold with windows. The birefringence can then be observed using photoelasticity. Different temperature profiles can be generated by using a heating surface.

The parameters to consider are the passage separation distances, and cooling channel and cartridge heater placements. From earlier analysis it was shown that the solidified plastic skin development during the filling stage resembles that of an boundary

[102] Ibid.

layer with the leading edge at the end of the cavity. Therefore , the optimal thermal input that strives to reduce the variation in the skin thickness or eliminate it entirely is a linear temperature gradient along the flowlength with the highest temperatures at the beginning of the cavity where the contact time is longest. However, once the plastic fills a rectangular cavity the ends of the part have a greater contact area to volume ratio with the mold than the center of the part. Heat conduction will be greatest at these ends, so the optimal thermal input is warm near the gate area, cold in the middle region, and hot at the end of the cavity. The reason for warm temperatures instead of hot temperatures is that the melt near the gate has a lower mold residence time in the cold mold than the plastic reaching the end of the cavity. Thus, the plastic at the end of the cavity has already solidified to some extent. Furthermore, there has been more heat transfer near the entrance so the mold temperatures near the entrance should be higher than those near the end of the cavity. However, a different temperature gradient is required for this combination effect for both the developed skin layer and the packed plastic. The new profile depends on which mode is more dominant. If the skin layer effects are more dominant, then a skewed parabolic profile with the gate region at the highest temperatures, the end of the cavity at medium temperatures, and the center of the cavity at the lowest temperatures should be used. Otherwise, the profile used for the packed plastic with an change in intensity of the thermal profile applies.

In order to maximize the heating rate of the mold, while minimizing the energy consumption, fluid passages are placed conformal to the mold cavity, as close as possible. As was already explained, this would allow a one-dimensional heat flow assumption possible, while increasing thermal response and decreasing energy expenditure.

Once mold dimensions are finalized, passage evaluation begins. The chosen fluid properties and cartridge heater power outputs can be manipulated to desired levels to produce reproducible and significant results.

CHAPTER VI

EXPERIMENTAL SETUP AND RESULTS OF DYNAMIC THERMAL BOUNDARY MOLDING

VI.1 Introduction

The objective of the thermal control experiments is to demonstrate its utility in reducing residual stresses, thereby reducing warpage. The evaluation of the thermal control efficacy consists of a conventionally molded part without thermal control compared to that of the same part molded with thermal control. Experimental procedures and results are discussed for the conventional molding and the molding under thermal control in Section VI.2 and Section VI.3, respectively.

The thought process behind the implementation is as follows:

1. Observe the warpage locations in a part without thermal control. This is measured directly from the part dimensions after ejection from the mold.

2. Correlate (if possible) the birefringence patterns (residual stresses) observed from the photoelasticity experiments to the observed warpage.

3. From correlation "guess" a possible thermal input with spatial and temporal variations that will reduce the number of birefringence patterns. Compare predicted reduction with observed.

VI.2 Conventional Molding

(a) Experimental Setup and Procedure

The experimental setup consists of three major parts: (1) the injection molding machine, (2) the test mold with transparent windows made of Plexiglas, and (3) the optical system.

(1) An Engel EC88, 30 ton injection molding machine located at MIT was used to mold the polystyrene parts with the aluminum molds. Melt temperatures were controlled by setting the nozzle and barrel temperatures to 450°F.

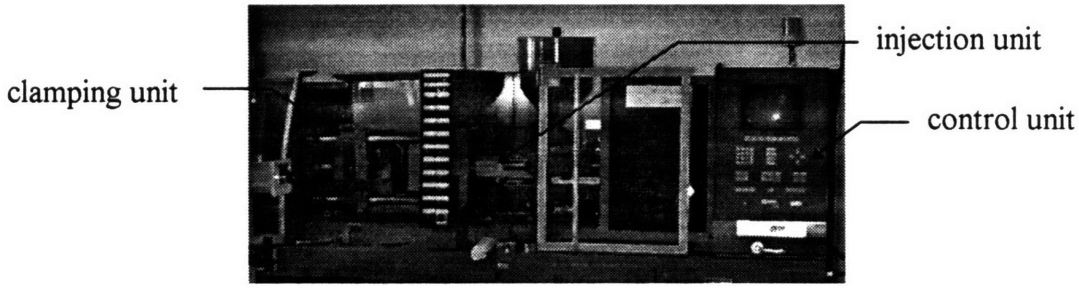

Figure VI.2.1: Engel EC88, 30 ton injection molding machine.

(2) The design of the mold avoids undulating flow for comparative experimental tests. Thus, the flow front advances in a straight line over the whole cavity breadth which gives parallel flow. A laminated aluminum mold for a thin and flat rectangular part was used with three components—female, male, and lamination layer. The details of the test mold are shown in Figures VI.2.2 through VI.2.4. The lamination layers vary in thicknesses from 2, 4, to 6 mm. The mold will produce parts that are 65 mm x 12 (15) mm x 2 (4 or 6) mm. Plexiglas windows will be used to view the 65 mm x 2 (up to 6) mm area that will be illuminated by the laser. If stress build-up and relaxation is understood in simple shaped injection molded parts, then the analysis can be extended to explain the thermorheological history of complex parts using the formulations and the method of birefringence observation developed in this thesis.

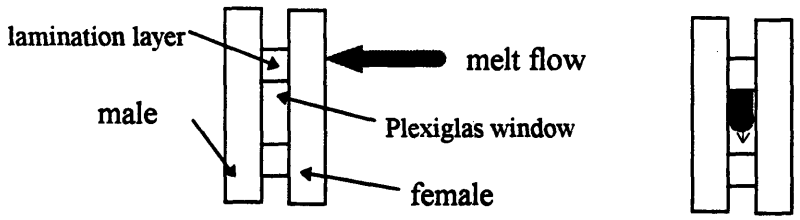

Figure VI.2.2: Components of the test mold.

The lamination layers and Plexiglas windows are sandwiched between the male and female blanks when the mold halves are in the closed position; however, both the lamination layers and Plexiglas windows are secured only to the male blank. Plastic shims where used to offset the windows from the lamination layers. Width flexibility was obtained by changing the orientation of the windows as shown in Figures VI.2.3. This increased the width range from 12 mm to 15 mm.

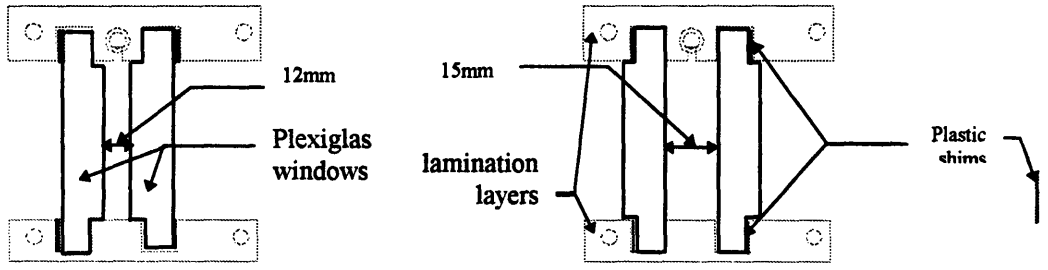

Figure VI.2.3: Two widths are possible by changing window orientation (plane view).

Further versatility was achieved by using the different thickness lamination layers in different combinations and/or stacking them for a maximum part thickness of 12 mm (6+4+2). For example, two different sizes of the lamination layers were used to allow placement of thermocouples within the melt stream as shown in Figure VI.2.4. The 6mm lamination layer was placed on the top mold end (near the sprue) and the 2 mm lamination layer was placed on the other mold end (near the end of the cavity) with 6 mm thick Plexiglas windows to complete the enclosure. The top region (where the plastic initially touches the cold mold) is entirely enclosed but the bottom portion of the mold now has a gap of 4 mm that allows a thermocouple to be placed between the molds.

A five inch ruler was placed in Figure VI.2.4 and was used in most of the pictures.

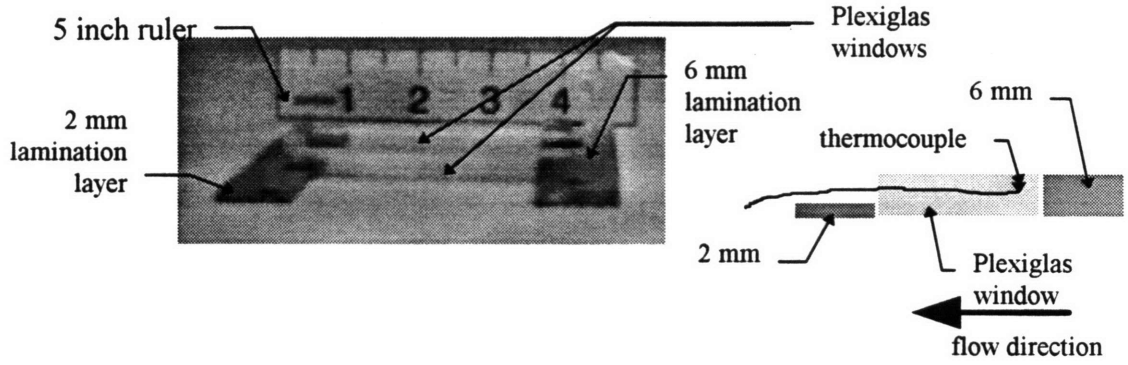

Figure VI.2.4: Stepped lamination layers for thermocouple insertion.

As the plastic fills the mold, the melt stream envelops the thermocouple placed along its path. The final position of the thermocouple is difficult to control but the "frozen in" coordinates can be determined precisely after the part is removed from the mold as shown in Figure VI.2.5. This allows the measurement of the thermal history of any spatial location can now be identified, and also the plastic surface temperature. The lack of packing pressure magnifies the effects of the residual stresses. Thus, the general applicability makes this a powerful technique to directly measure the effects of differing temperature profiles on the part. Recalling that perfect contact enhances heat transfer, then the increased number of air gaps and sink holes on the surface of the part formed due to lack of packing will decrease the heat transfer compared to the packed in polymer that has better contact with the mold. Thus, the difference in temperature readings between the packed in and the nonpacked as time increases but there is an limit to this error since the plastic has cooled down, which reduces the heat transfer, thereby, reducing the temperature range which directly translates into a temperature error range reduction.

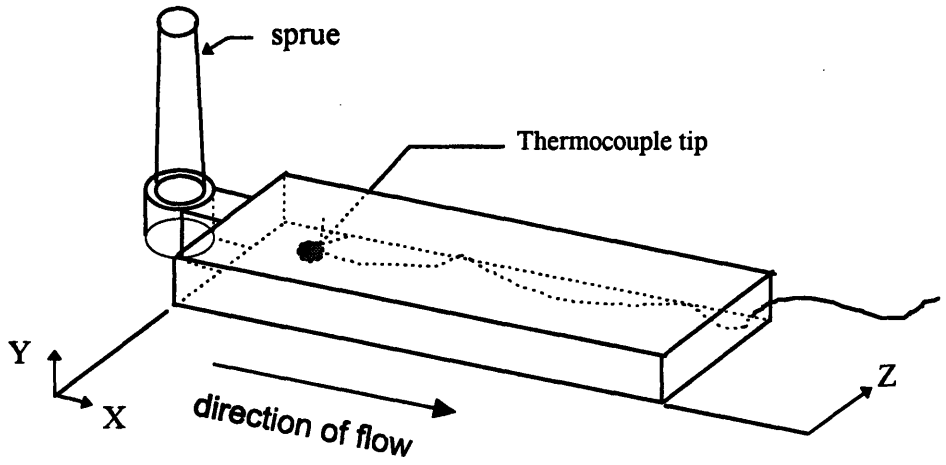

Figure VI.2.5: Thermocouple 'frozen in' using the stepped lamination layer method.

The thermocouple does not interfere significantly with the flow because its tip and diameter (0.020 inches ≅ 0.5 mm) are much smaller than the 6 mm thick part being molded. However, as the part thickness decreases the utility of this method becomes increasingly questionable as the thermocouple might obstruct the flow or become a significant heat sink for the molding part.

(3) Photoelasticity will be used to determine the distribution of residual stress in the injection molded specimen. A schematic of the setup is shown below in Figure VI.2.6.

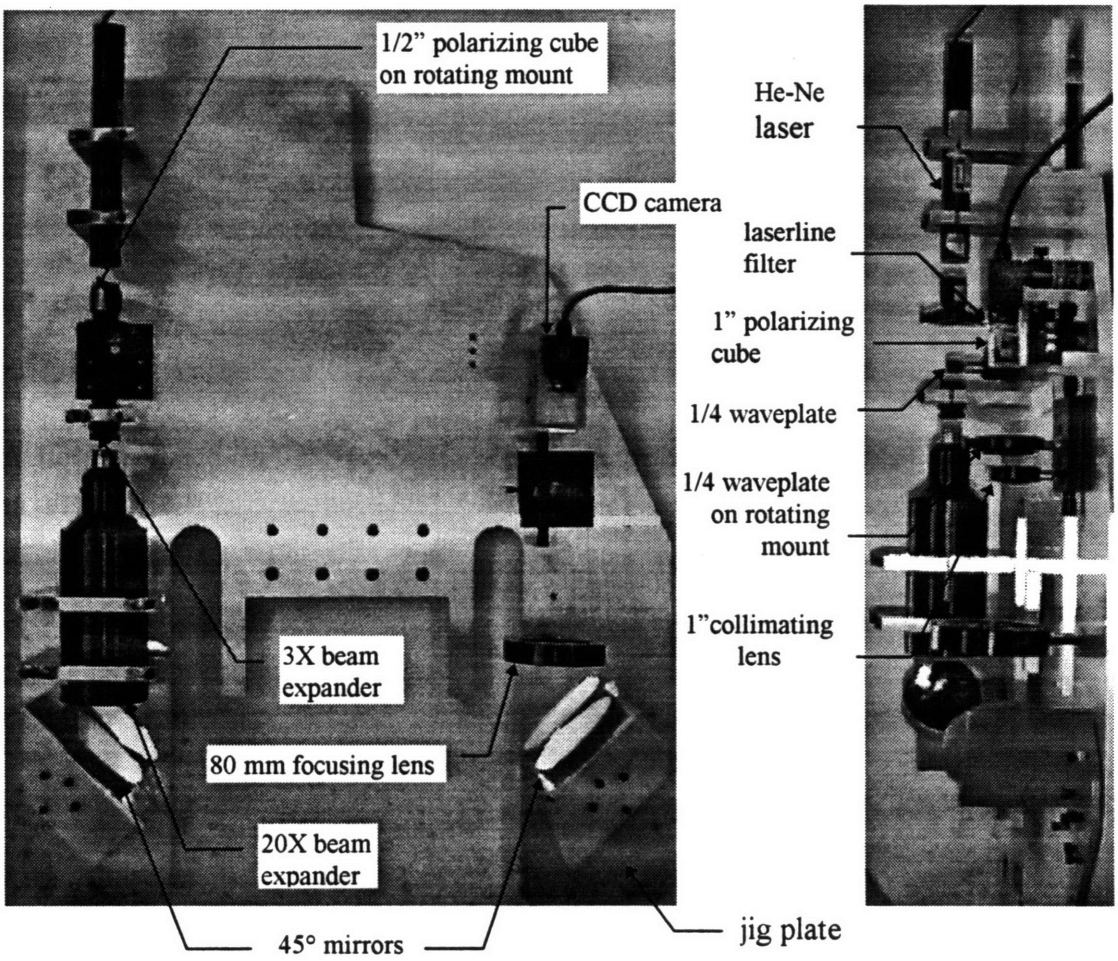

Figure VI.2.6: Laser setup used for birefringence illumination of the mold.

The He-Ne (632.8 nm) laser emits a randomly polarized 1 mm diameter beam. This beam goes through a polarizing cube that vectorizes the polarization into orthogonal vectors. The cube is oriented such that the purer form of the linearized beam is transmitted to the quarter waveplate. The quarter waveplate breaks the linearized beam into orthogonal vectors of equal magnitudes and out of phase by 90° (circularly polarized). This circularly polarized beam is then expanded 3X then another 20X to a 60 mm diameter beam. The beam is then redirected at 45° by a mirror. This 60 mm diameter beam now illuminates the sample. Vitrification of the polymer melt creates stresses in the

part. Differences in principle stresses are linearly proportional to differences in indices of refraction as discussed in Section IV.2. After the beam is transmitted through the part, it now has additional phase changes induced by the differences in the index of refraction. A two lens system is used next to reduce the image to the size of the CCD camera sensor area. The first lens focuses the beam to its focal point while the second lens placed at its focal length away from this focal point collimates the beam. This reduced image now strikes another quarter waveplate then a linearly polarizing cube that relinearizes the beam, causing amplifications for certain phases and total annihilation for those vectors 180° out of phase. This accounts for the alternating bands of light and darkness. Before the image is received by the CCD camera a laserline filter is used to screen out the ambient light. The CCD camera is connected to a monitor and the monitor is connected to a VCR. Images recorded on the VCR was retrieved using framegrabber.

Optical holders were machined to a tolerance of ±0.005 inches. These were specially designed such that the centerlines of all the components could be aligned and offset to properly illuminate the part. Rotation about the axis of the beam is required for the polarizers and the quarter waveplates to obtain the proper orientation for birefringence patterns. However, the rotation can also be accomplished by the relative difference in rotation of the polarizer set and the quarter waveplate set. Thus, only one polarizer and quarter waveplate need be rotated while the other can sit with a fixed rotation. Therefore, only two rotating mounts were used in the setup—one for the 1/2" polarizing cube and the other for the 1" quarter waveplate. Beam expansion of 60X on the left side of Figure VI.2.6 required the two expensive beam expanders. However, only a 10X reduction of the image was needed to fit the image onto the CCD camera sensor area; therefore, the inexpensive two lens system was employed.

Furthermore, all the optical components were secured onto a jig plate which was fashioned to fit onto the bolster and within the security doors of the injection molding machine. The upper right area of the jig plate was band sawed off so that the injection molding machine's security doors could close as seen in Figure VI.2.7 c) below.

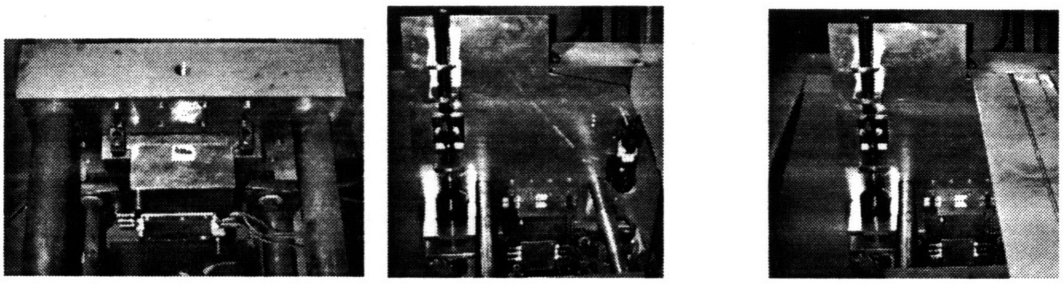

a) Bolster. b) Laser setup on bolster. c) Security door closed.

Figure VI.2.7: Laser secured to bolster with and without the doors closed.

Figure VI.2.7 a) shows the location where the optical equipment must sit. The shape of the jig plate was constructed to use the bolster, which is fixed to the injection molding machine, and the top two horizontal cylindrical bars as support.

The observed birefringence patterns can now be correlated to stresses. The calculated stress birefringence can be compared to the observed using the following relation: [103]

$$\Delta n = \frac{N \lambda}{W} \qquad (64)$$

where N is the fringe order, λ is the wavelength of the light source ($\lambda_{He\text{-}Ne}$ = 632.8 nm), and W is the optical path (= 12 mm)

(b) Results

The parts made below were molded without any thermal control and injections were spaced such that the mold temperatures reached the same initial conditions through natural convection (air) cooling. The waterline was shut off and the heaters were not turned on. Seven 6 mm thick parts were molded to exploit the thickness difference between the larger and the smaller lamination layers and to obtain enough data samples to characterize the temperature field in the entire part.

[103] Kurosaki, Y. And I. Satoh, "Visualization of Flow and Solidification of Polymer Melt in the Injection Molding Process," 1989 National Heat Transfer Conference, HTD-Vol. 113, Heat Transfer in Manufacturing and Material Processing, p. 63.

The coordinate system used to chart the location of the thermocouples is shown below. The approximate thermocouple final locations are labeled on a schematic of a typical part divided into three zones: entrance, middle, and end.

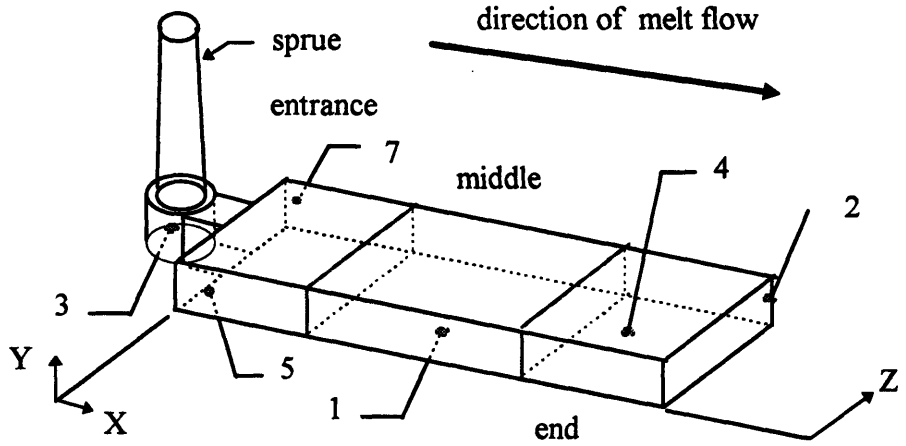

X x Y x Z

nominal part dimensions (inches): 2.553 x 0.236 x 0.654

Figure VI.2.8: Coordinate system used for thermocouple locations and final thermocouple locations for experiment sample numbers 1 to 7.

The part was sectioned into three equal volume regions as shown in Table VI.2.1. The top region accounts for the region near the sprue. The middle region accounts for the following one third region. The end region accounts for the last third region which includes the end of the cavity. The experiment numbers are included for reference, and coordinates of the thermocouple tip are also listed. Figure VI.2.9 shows the temperature decay of the respective thermocouples.

It has been observed that the majority of the residual stress buildup occurs during solidification (after filling). Therefore, the temperature of concern is the temperature after the polymer fills the mold.

Table VI.2.1: Coordinate of thermocouple tip in the conventionally molded parts.

Thermocouple final location	Comments	Region (entrance, middle, end)
1. 1.308 x 0.020 x 0.0220	extreme end	middle
2. 2.536 x 0.187 x 0.600		end
3. N/A	inner cone of sprue, not in part	N/A (sprue - above top)
4. 2.312 x 0.237 x 0.088	top surface in Y	end
5. 0.253 x 0.112 x 0.153		entrance
7. 0.212 x 0.170 x 0.537		entrance

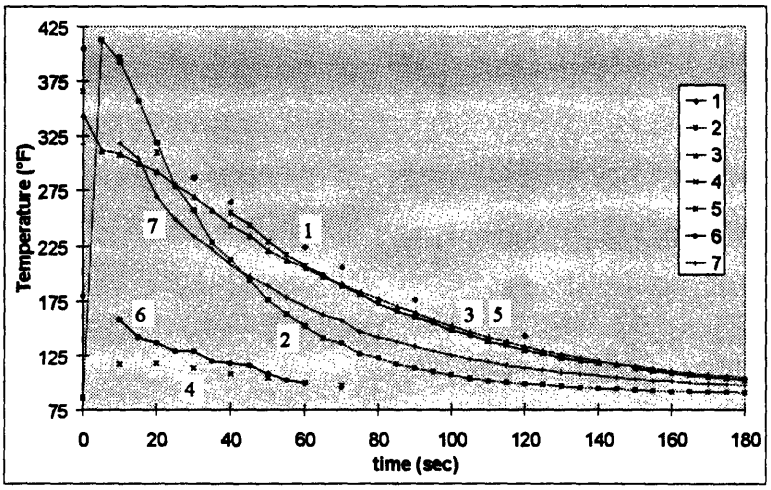

Figure VI.2.9: Thermal response of the solidifying plastic in conventional molding.

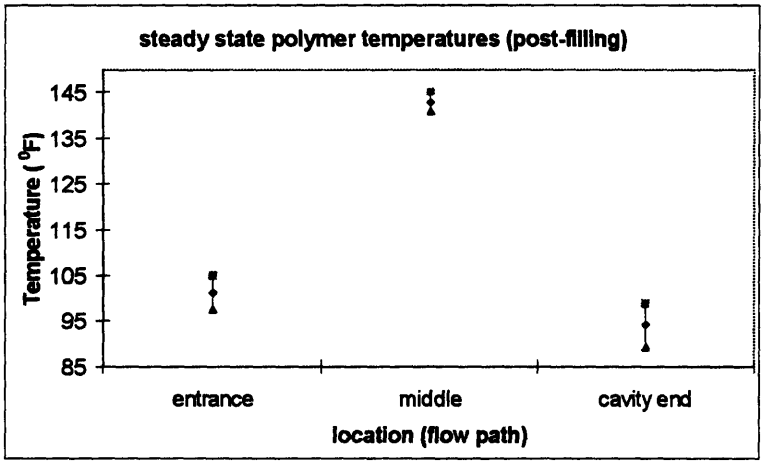

Figure VI.2.10: Polymer thermal response (Post filling) in conventional molding.

These experiments confirmed the need for the relatively warm temperatures near the gate region, relatively cold temperatures in the middle region, and relatively hot temperatures at the end of the cavity skewed parabolic thermal profile as discussed at the end of Section V.2. From Figure VI.2.10, the middle region of the polymer (Experiment 1) was observed to be the hottest of all seven trials (143±2°F) with the top region (Experiments 3, 5, and 7) (101.3±3.7°F) having significantly lower temperatures. Furthermore, the end region (Experiments 2, 4 and 6) (94.2±4.8°F) had the lowest temperatures which justifies maintaining the mold cavity end at the highest temperatures.

VI.3 Dynamic Thermal Boundary Molding

The type of dynamic control needed to produce part with uniform spatial temperatures depends on the determinacy of the process. The two options are closed and open loop control. If the process is random, then closed loop control is necessary. However, if the process is determinant (cyclic pattern) then open loop control is appropriate. The determinacy was determined both experimentally and experientially through consultation with Dick Barlik from Hasbro (Section II.5) to be relatively determinant depending on the tolerance.

Warpage was visually examined on parts made at Hasbro. The warpage was determined to be localized to the same general area; therefore, warpage appears deterministic. Because residual stresses are directly related to warpage; thus, residual stress distributions must also be a deterministic.

The determinacy was examined experimentally by assessing the uniformity of the incoming melt from the nozzle of the injection unit to the mold. The implication of a nonuniform incoming melt temperature is that maintaining the surface at a constant temperature will not reduce the stresses in the part. The premise is that if the melt temperature is not uniform prior to injection, then it cannot become uniform during injection.

A thermocouple was inserted into the nozzle of the injection molding machine and it was allowed to reach steady state. The first few measurements were taken by first feeding the plastic then inserting a thermocouple into the nozzle tip, then pulling out the thermocouple. After refeeding the plastic, the thermocouple was inserted to about 1/2" into the nozzle. This process was repeated except the thermocouple was inserted to about 1" into the nozzle. A second procedure where all three spatial measurements of tip, were recorded without refeeding between measurements was used. Therefore, the two procedures are:

- feed polymer to obtain a steady polymer stream from the nozzle
- record temperatures at (1) tip or 1/2", or 1" *OR* (2) tip and 1/2", and 1"

Procedures (1) and (2) tabulated and displayed in Table VI.3.1 and Figure VI.3.1 are labeled different and same, respectively.

Table VI.3.1 Polymer temperatures in the nozzle and barrel of the injection unit.

	Tip-different	Tip-same	1/2"-different	1/2"-same	1"-different	1"-same
Temperature [°F]	465±5	466±5	484±6	480±4	497±6	498±7

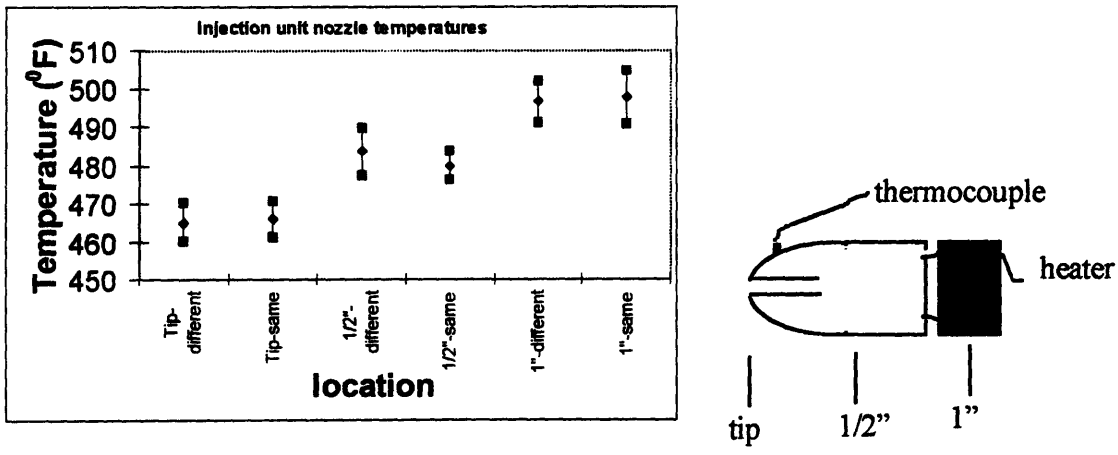

Figure VI.3.1: Steady state temperatures for the plastic melt in the injection unit nozzle.

The barrel and nozzle temperatures were all set to 450°F on the Engel injection molding machine computer controller with a tolerance of ±14°F. Temperatures higher

than 450°F resulted from the viscous heating effects of the reciprocating screw. The general trends are the increasing temperature going into the nozzle and towards the heater. The expected melt linear temperature variation is seen. The variation at any location (standard deviation) is a fixed variation of approximately 10°F. This is an indication of temporal random variations. The variation between locations (difference between mean values) is a linear profile with a gradient (slope) of approximately 15°F / 0.5". This nonuniformity becomes increasing critical as the tolerance decreases.

The experimental setup for dynamic thermal boundary manipulation includes the setup used for conventional molding as well as the cartridge heater/variac thermal control unit. Furthermore, the mudframe (Figure VI.3.4) was machined to obtain a smaller sprue hole for faster solidification and to create an access space to connect the cartridge heaters and the waterline to the mold.

The variable controlled is the duration and intensity of the cartridge heater energy flux imbedded within the mold for a given configuration. The cost of constructing a mold of this type is much less than those proposed with passive insulating layers or the typical mold start up cost given in Section I.1. For every application the cost versus benefit trade-off study should be examined on the basis of tolerance requirements, cost of fabricating a mold to satisfy the given tolerance, and the mold operational life. Some materials have a higher warpage index implying these materials will benefit more from the use of thermal control because of the greater efficiency in warpage reduction. Irregularities in shape and paper thin sections suffer severe temperature gradients which can be countered by thermal control. An understanding of the heat transfer between the part and the mold is vital to reducing residual stresses; otherwise, technologies such as low thermal inertial injection molds will worsen, not reduce, distortions. However, low thermal inertia injection molds must be used for thermal spatial and temporal manipulations required by the two distinct solidification modes.

(a) Experimental Setup

Three parallel passages were drilled and pipe tapped into each of the male and female die parts. Each passage can have either tap water flowing through it or a cartridge heater sitting in the core and there are three passages in each of the male and female molds for a total of six passages as shown in Figure VI.3.2; thus, there are $2^6 = 64$ different combinations accounting for only the interchange between the heater or the cooling line. If high, medium, and low levels of heat input or water pressure is considered, the number of different combinations increases to $6^6 = 46{,}656$ different combinations. However, balanced heating requires symmetry between the male and female mold temperatures, thereby reducing the number of different combinations to $6^3 = 216$. Previous arguments concerning the best cartridge heater and waterline arrangement and levels (waterline sandwiched between the heaters as shown in Figure VI.3.3) further reduce the number of different combinations to $3^3 = 27$. Further arguing that only two types of thermal profiles either linear (three combinations) or a skewed parabolic profile (four combinations) should be used reduces the number to seven.

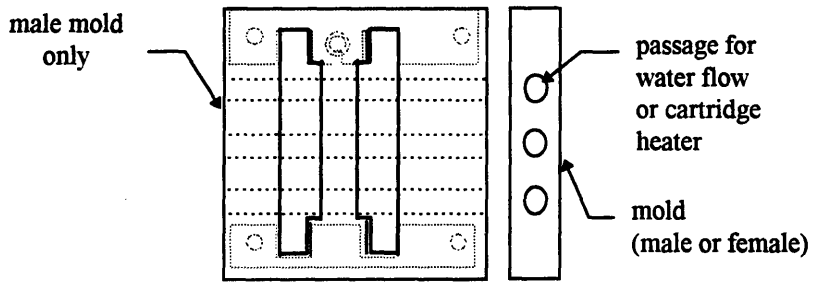

Figure VI.3.2: Mold with three passages for the cartridge heaters and waterline.

The water cooling channel is used as a heat sink to establish and maintain the steady state temperature gradient. The cartridge heaters used were 3/8" nominal diameter, 2 1/4" sheath length, 350 Watts, and 172 W/in^2. Each cartridge heater is connected to a separate variac set at 120V for independent variation of surface temperatures. At a particular voltage setting and flow rate the system will eventually reach steady state. Once

steady state has been reached a temperature probe will survey the initial surface temperature conditions.

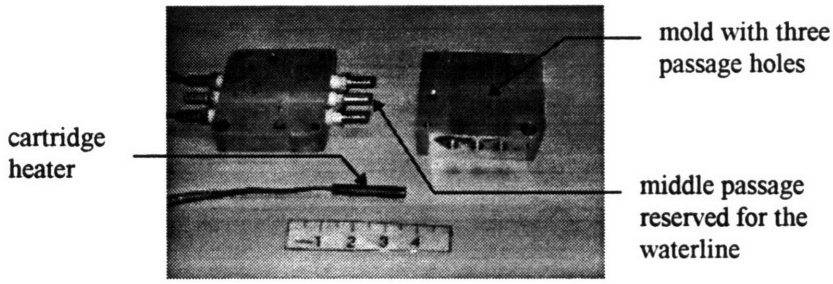

Figure VI.3.3: Mold passages for two cartridge heaters and a waterline cooling channel.

Figure VI.3.4 displays the male mold with the windows and lamination layers and the female mold placed in their respective mudframes.

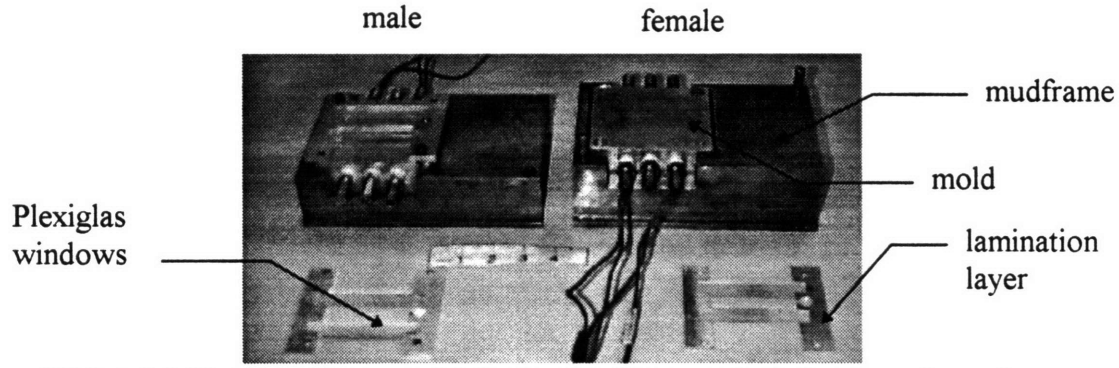

Figure VI.3.4: Molds in mudframes with lamination layers and windows on the male.

(b) Experimental Procedures and Results

It is desired to establish steady state thermal profiles and assume that they hold during the actual heat control experiments. The first thing that will be done is a test of the repeatability of thermal control. Next, any general profile can be generated from a linear combination of independently generated profiles which will form the bases for the space of all thermal profiles. The effects of these bases should be quantified and a novel technique of measure the plastic not mold surface temperature will be described. Ultimately, the desired uniform temperature distribution is that of the part not the mold. However, measurements of both the mold and the plastic temperature fields correlates the effects of a temperature profile to the subsequent part qualities.

Experimental description:

Each mold has three circular holes equally spaced and in cross flow with the flow path of the polymer. Two of the three holes have cartridge heaters inserted inside and the middle hole between the cartridge heater holes is reserved for water cooling. Each cartridge heater was attached to its own variac for independent heater control. The variac switch was set for 120 Volts which is the recommended maximum voltage specified for the cartridge heaters. The voltages was varied throughout the experiment to observe the effect of various energy requirements. The heat flux varies as the square of the adjusted voltage setting. For example, if a 50% variac setting was used then only 25% of the rated heat flux (172 W/in^2) is generated.

An independent test determined that the heat generated was concentrated at the center of the cartridge heater rather than evenly distributed along its sheath length; thus, the heat flux is nonuniform. However, the nonuniformity should have insignificant effect because the region of heating is 12 to 15 mm compared to the sheath length of 2.25 inches.

Part I: Repeatability of Thermal Control

Thermal decay of the mold temperature is an extremely slow process. It is also important to determine the system response and approximate thermal effects to facilitate experimental planning. Therefore, an initial thermal response test was performed to investigate the difference in measured temperatures of an easily controlled system. The results determine the number of trials needed to secure reproducible results and the expected differences in temperatures between runs for an identical setup.

One cartridge heater was placed in the female mold hole closest to the sprue hole. A linear profile was assumed; thus, only Two thermocouples were placed on the surface of the mold with each thermocouple placed at the ends spanning the entire length of where the molded rectangular part would contact the mold surface. The mold and thermocouples were sandwiched between two Nomex insulating boards to prevent heat

transfer out of the system. The thermal response should be approximately the same between the two molds although the male mold has a slightly greater thermal mass due to the addition of the lamination layers and the Plexiglas windows. Figure VI.3.5 shows the setup described above.

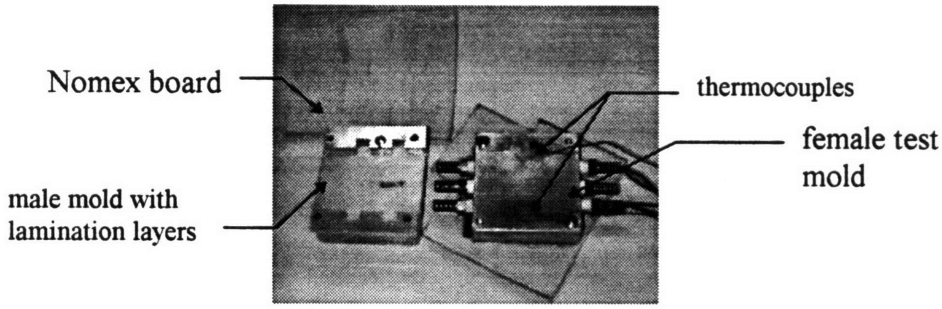

Figure VI.3.5: Female mold thermocouple sandwiched using two Nomex boards.

Figure VI.3.6 shows the thermocouple assignments. Channel A corresponds to the region near the sprue. This region is subjected to the highest temperatures because this thermocouple is placed directly above the only heater in the system. Channel B corresponds to the region at the end of the cavity.

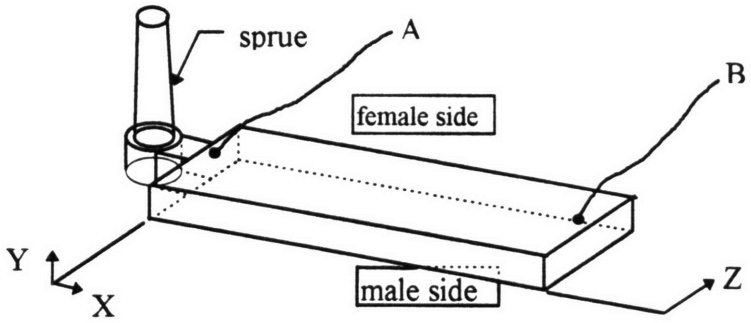

Figure VI.3.6: Thermocouple channel assignment of female mold surface.

The variac settings were 50%, 75%, and 100% of the rated 120 Volts. The power was left on until system reached steady state. The temperature decay was also measured. Figure VI.3.7 shows the results. In the legend the nomenclature is as follows:

'voltage level' - 'trial number' 'channel assignment'.

For example, 50%-3B represents 50% of the maximum voltage level (120V)set by the variac of trial number 3 on channel A which corresponds to the region near the sprue.

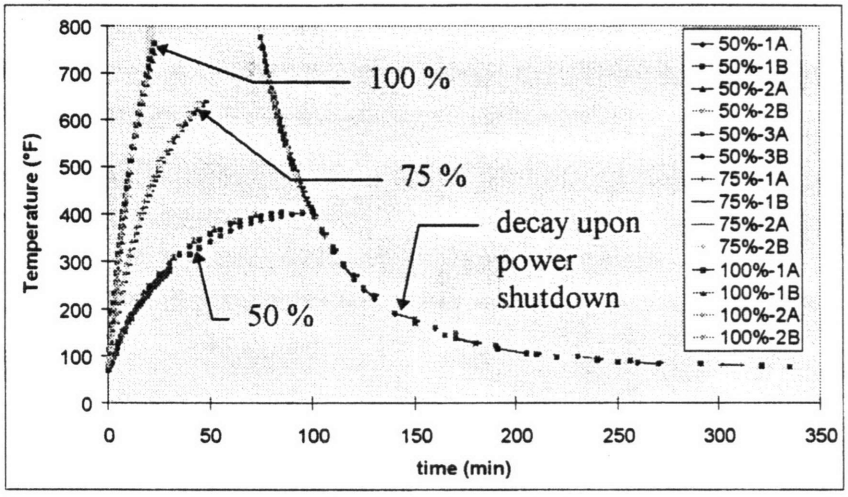

Figure VI.3.7: Repeatability of thermal response on the female mold.

The three trials at 50% show close agreement in the temperature response curves, as do the two trials for 75% and another two for 100%. Furthermore, the thermal inertia of the mold is relative small due to the close agreement in temperatures between channels A and B. This implies a rapid heat diffusion occurred within the mold. From these experiments, it can be assumed that the heater and mold assembly thermal controls are repeatable. Thus, reproducible results can be expected with only one run.

Part II: Determining Bases For Arbitrary Thermal Profiles

The dynamic thermal boundary thermal control implementation uses two cartridge heaters and a water line for each of the two molds as shown in Figure VI.3.8.

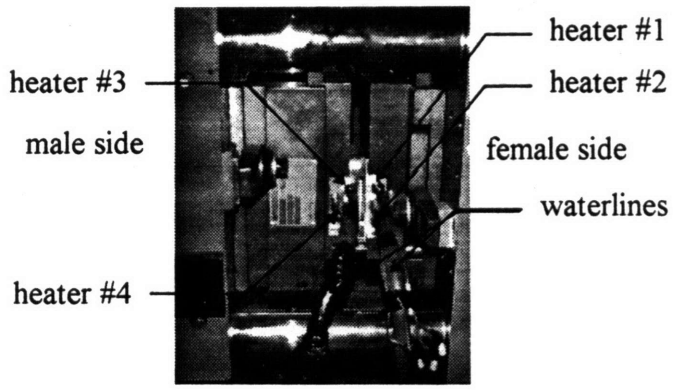

Figure VI.3.8: Cartridge heater and waterline arrangement.

Mold surface temperatures in the region where the plastic is molded were the objectives of the setup shown in Figure VI.3.9. Six thermocouples were used to analyze the thermal response. The thermocouples were sandwiched between a 6 mm Nomex insulating rectangular piece resembling the shape of the molded part. Three thermocouples were pressed against the surface of each mold face. Because each set of three thermocouples contacts different mold faces and is insulated from the others, the imbalance from inputting equal amounts of heat flux can be measured. The 6 mm lamination layer was used to create the necessary gap for the thermocouples and the Nomex rectangular piece to not be crushed during mold closing. This 6 mm lamination layer provided the only thermal bridge between the male and the female parts. The six thermocouple locations were the region nearest the sprue (where the plastic first forms), the region in the middle of the part, and the region near the end of the cavity.

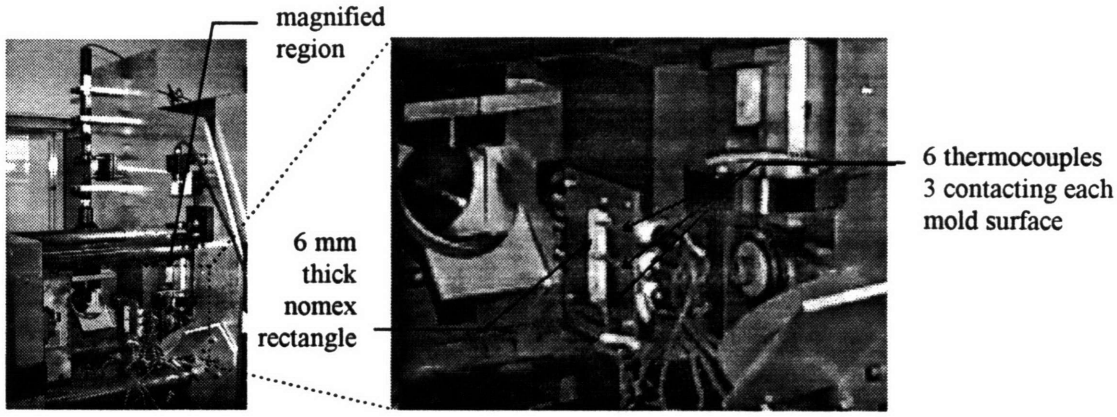

(a) Experimental setup. (b) Magnification of sample region.

Figure VI.3.9: Setup for characterization of steady state thermal profile bases.

Figure VI.3.10 displays the channel assignment on a molded part. The temperature readings are of the mold surface temperature, not the plastic surface temperature. The measured steady state mold temperatures can be correlated to its effects on part qualities. These temperatures were assumed to be those experienced by the melt flow during subsequent experimentation.

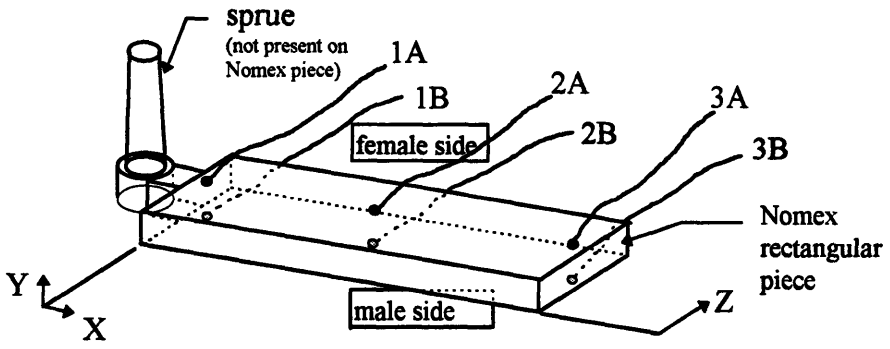

Figure VI.3.10: Thermocouple channel assignment of Nomex rectangular piece.

Figure VI.3.11 schematically combines the heater arrangement and thermocouple channel assignments. A channels register the surface temperature of the female mold while B channels register the male mold temperatures. Channel numbers 1, 2 and 3 correspond to the top, middle, and end regions of the plastic and mold contact surfaces, respectively.

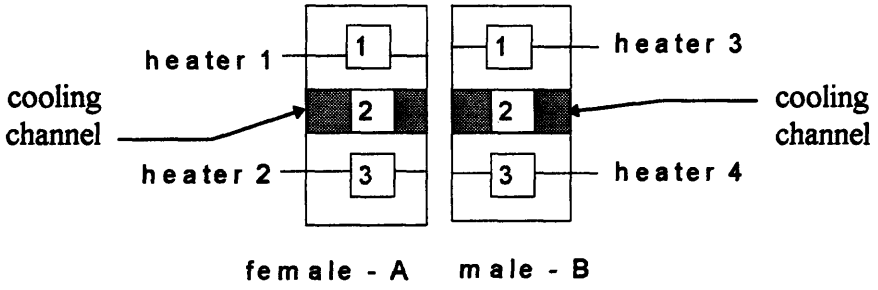

Figure VI.3.11: Cartridge heaters and waterline locations and channel assignments.

The following considerations were used in devising the type and number of experiments performed. The first consideration is how many variables are in the system and what are the controllable parameters. The controllable parameters were the heat flux as controlled by the variac, water flow rate, and which of the four heaters should be turned on. From earlier discussions (Section II.5) it was determined that two major modes of solidification schemes are involved in injection molding so to effect constant plastic temperature those areas cooled first should be heated by the heaters to effect a more uniform cooling of the part. The experiments performed below allow the determination of the necessary profiles needed for the objective of this thesis. The experiments were not repeated because repeatability was already established and only general trends are sought, not explicit formulas, so accuracy was sacrificed without loss to the fulfillment of the end experimental objective.

The initial conditions of the system are as follows. The initial uniform temperature of the entire system without heating or cooling was 78.9°F. Temperature with water flow rate at maximum was 77.4°F. Additionally, the polymer melt was manually injected at the feed speed of 20mm/sec and the nozzle and barrel temperatures were set to 450°F.

Nine experiments were performed to establish the required bases:

The nomenclature of Table VI.3.2 is as follows. The **experiment numbers** are incorporated in the same area as the varying flow rate and voltage settings in **boldface**. The data set consists of a 3X2 matrix corresponding to the experiment number directly above or horizontally adjacent. The thermocouple channel assignments are *1A*, *1B*, *2A*, *2B*, *3A*, and *3B* in italics and all steady state temperatures are in °F. The intersection of the horizontal voltage level and the vertical flow rate determines the settings used.
For example, **(area shaded in Table VI.3.2)**
The steady state temperatures 151.6, 161.2, 138.6, 147.8, 152.5, and 159 corresponding to channels *1A*, *1B*, *2A*, *2B*, *3A*, and *3B* are for experiment number 5 where intermediate flow rates and 100% variac setting were used.

The numbers in italics were steady state temperatures linearly extrapolated from the seven experiments.

Table VI.3.2: Steady state temperatures for various voltages and water flow rate.

			Water flow rate (Temperatures °F)							
			4. maximum		5. intermediate		6. minimal		7. no flow	
channel and region #			*A*	*B*	*A*	*B*	*A*	*B*	*A*	*B*
Variac voltage level (% of max.)	3. 100	*1*	131.6	136.9	151.6	161.2	225.7	238.5	362.1	395
		2	118	122.8	138.6	147.8	214.9	226.6	360	393
		3	133.1	136	152.5	159	223	230.2	362.1	384
	2. 75	*1*	109.5	114.5	*130*	*140*	*204*	*218*	*340*	*374*
		2	101.7	105.3	*122*	*130*	*194*	*207*	*339*	*373*
		3	110.8	112.9	*131*	*138*	*201*	*210*	*340*	*364*
	1. 50	*1*	94	96.9	*114*	*122*	*188*	*200*	*324*	*356*
		2	90	91.8	*110*	*117*	*176*	*192*	*321*	*355*
		3	94.9	95.7	*115*	*121*	*185*	*195*	*324*	*349*

Figure VI.3.12 shows that the maximum gradient that can be generated is 15°F. This gradient is insufficient to produce the spatially uniform part for the following reason. The temperature difference between the middle and the entrance section was observed to be approximately 40°F. Because the thermal resistance of the plastic is higher than that of the mold, then the minimum temperature gradient required is 40°F. Thus, the maximum of 15°F that can be generated with the current setup is insufficient.

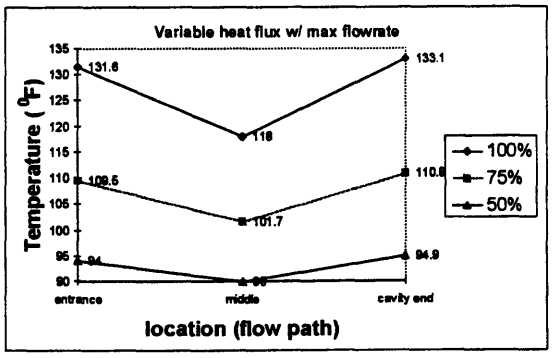

a) Variable heat flux with max. flowrates.

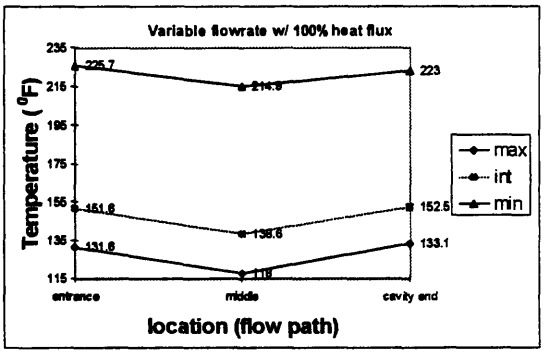

b) Variable flowrate with max. heat flux.

Figure VI.3.12: Steady state temperatures for various voltages and water flow rate.

Figure VI.3.13 displays the difference between the male and female bolsters. The female has a smaller mass and a greater surface area contact with the injection molding machine than the male bolster. This causes an imbalance between the thermal inertias of the male and the female die halves which is evident from the data from Table VI.3.2. If the thermal inertia was the same between the two mold halves then the temperatures as well as the thermal response from channels A and B should be relatively close. However, Table VI.3.2 shows that as the voltage level increases or as the flow rate decreases there is a greater divergence between the temperature readings of channels A and B, with B channel temperatures consistently higher than those of channel A. Thus, the male mudframe had a much higher thermal inertia which made cooling down a lengthy process. Consequently, rapid unbalanced thermal cycling from low thermal injection molds can induce distortions.

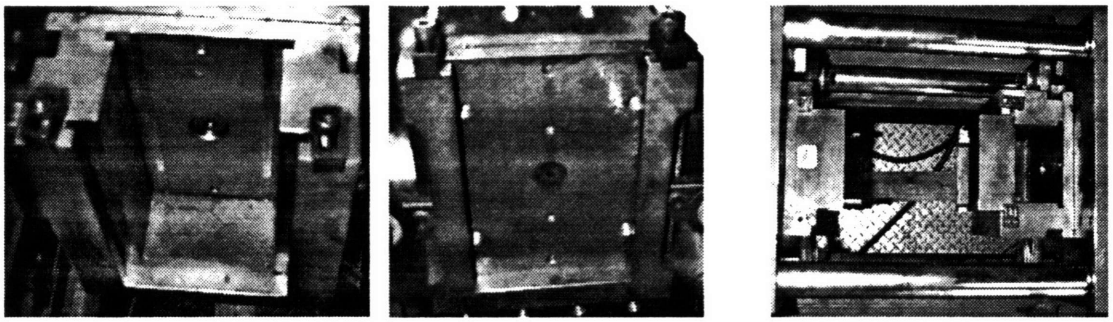

a) Male bolster. b) Female bolster. c) Mudframes in bolster.

Figure VI.3.13: Bolster and mudframe assembly.

Experiments 1, 2, and 3 set up a correlation of temperature effects of varying the voltage while maintaining maximal waterline flow.

Experiments 4, 5, 6 and 7 complete the picture of the effects of flow rate at 100% voltage setting and can be extended to the other two voltage level percentages (75% and 50%).

Figures VI.3.14 and VI.3.15 display the thermal profile leading to the steady state temperatures in Table VI.3.2 as well as the temperature decay after power shutoff. The numbers in the figures correspond to the labels in the legend with 1 referring to the top label in the legend and subsequent numbers refer to labels from top to bottom. For

example, in Figures VI.3.14 the number 4 refers to 75%-1(2 and 3)B. Channel assignments were previously discussed.

From the above experiments it was determined that the minimal flow rate provides the best profile based on the trade-off between being close to but not too close the glass transition temperature (400°F)and high enough to produce an appreciable gradient so the gradient effects can best be seen. The objective is to produce a uniform melt/plastic temperature decay not heating up the mold to the glass transition temperature. Thus, the temperature range around 200°F (provided by the minimal flow rate) was assumed to provide the most desirable thermal profile in terms of relaxation of the skin layer and sufficient retarding of heat diffusion to effect a semi balanced cooling.

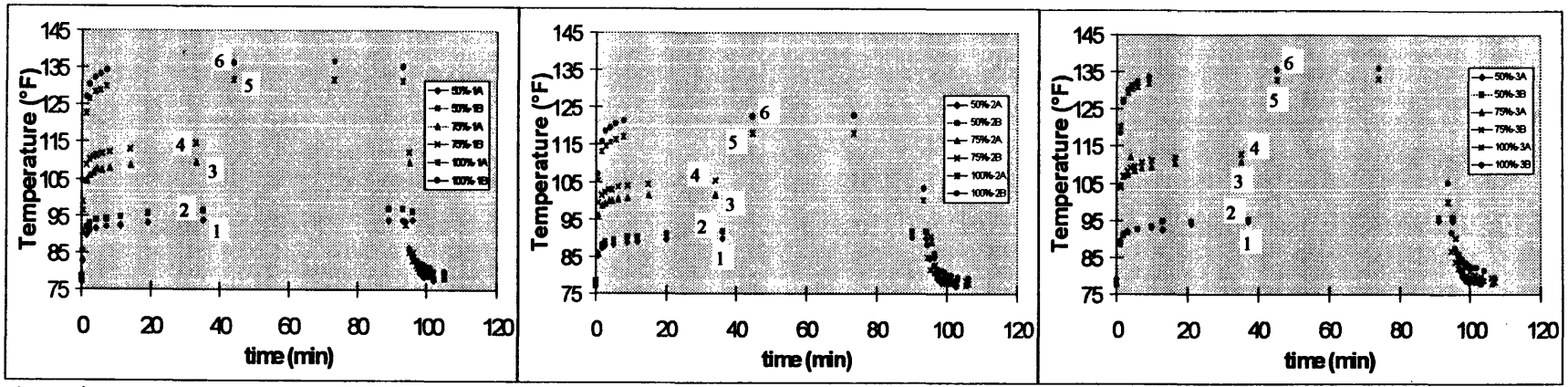

a) Region nearest the sprue (top). b) Middle region. c) Region furthest from the sprue (bottom).

Figure VI.3.14: Temperature response curves for maximum flow rates and varying voltages - 50%, 75%, and 100% of V_{max} (120V).

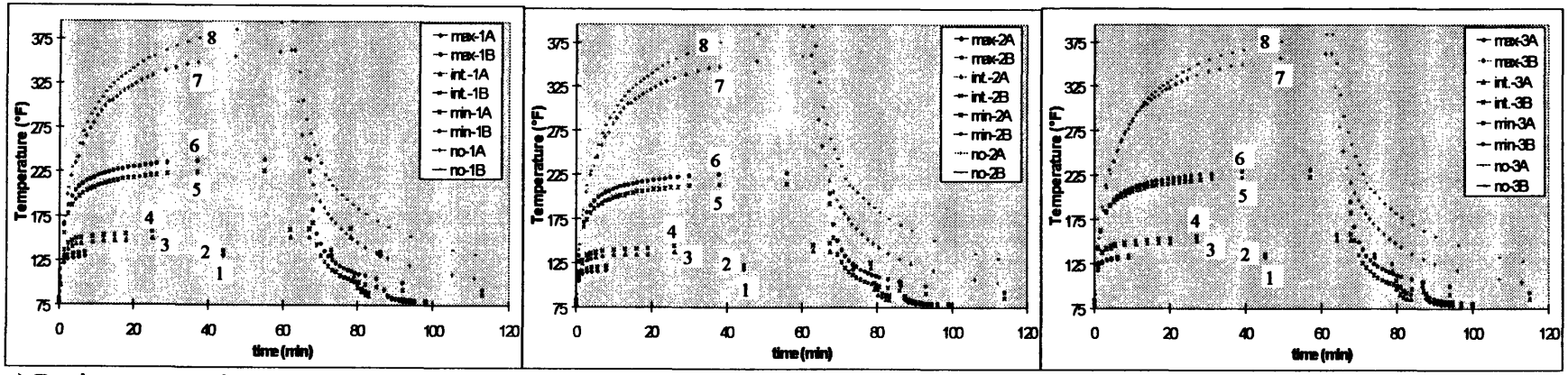

a) Region nearest the sprue (top). (b) Middle region. (c) Region furthest from the sprue (bottom).

Figure VI.3.15: Temperature response curves for 100% voltage setting but varying flow rates - max, intermediate, minimal, and no flow.

The next set of experiments will establish the basis of an exaggerated profile and will not maintain balanced cooling while keeping the flow rate at the minimal level.

The numbers in the grid are heater numbers and only the shaded portions indicate the heater voltage level and the nomenclature of Table VI.3.3 is as follows:

Experiment number. Shape of thermal profile

Steady state temperatures- 1A, 1B, 2A, 2B, 3A, 3B (°F)

For example, (area shaded in Table VI.3.3)

9. skewed parabolic (hottest near end of cavity)

155.2, 178.7, 165.3, 183.2, 176.8, 191.9

indicates that experiment 9 has heaters 1 and 3 at 50%, and heaters 2 and 4 at 100% of V_{max} (120V) with minimal flow rate and the steady state temperatures are 155.2°F, 178.7°F, 165.3°F, 183.2°F, 176.8°F, and 191.9°F from thermocouple channels 1A, 1B, 2A, 2B, 3A, and 3B, respectively.

Table VI.3.3: Steady state temperatures for minimum flow rates but varying thermal profiles.

Experiment number. Shape of thermal profile Steady state temperatures (°F) - 1A, 1B, 2A, 2B, 3A, 3B	heater voltage level (% of 120V) 100		50		0	
8. skewed parabolic (hottest near sprue) 186.6, 205.6, 164.5, 180, 160.2, 174.8	1 3	2 4	1 3	2 4	1 3	2 4
9. skewed parabolic (hottest near end of cavity) 155.2, 178.7, 165.3, 183.2, 176.8, 191.9	1 3	2 4	1 3	2 4	1 3	2 4
10. linear (sprue region hottest) 167.6, 187.2, 142.4, 158.6, 137, 150.6	1 3	2 4	1 3	2 4	1 3	2 4
11. linear (end of the cavity hottest) 138.2, 156.1, 153.9, 169.3, 166.4, 179.1	1 3	2 4	1 3	2 4	1 3	2 4
12. unbalanced heating of female only 195.5, 103.1, 193.9, 102.9, 192.5, 102.5	1 3	2 4	1 3	2 4	1 3	2 4
13. unbalanced heating of male only 101.3, 216.9, 93.9, 199.3, 101.6, 205.6	1 3	2 4	1 3	2 4	1 3	2 4

The thermal profile in experiment 8 was not a skewed parabolic as expected. It was a decay in temperature with the top region hottest. Furthermore, experiment 9 displayed the same trend except the decay start from the end of the cavity. Thus, the water flow rate must be increased to establish a stronger heat sink in the middle of the

cavity. The variacs at the 100% level overwhelmed the waterline heat removal capability. Thus, the effect of the waterline was obscured.

The linear profiles for experiments 10 and 11 are actually two separate linearly profiles for two different sloped regions. The region where the heaters are at the 100% variac setting to the waterline has a very steep drop in temperature while the region from the waterline to the end with the heaters set at the 0% variac setting has a fairly flat slope.

Experiments 12 and 13 were included to observe the maximum temperature difference between the two mold halves. Using these profiles, the expected warpage is in the direction of the hotter mold.

Figures VI.3.16 and VI.3.17 displays the thermal profile leading to the steady state temperatures in Table VI.3.3 as well as the temperature decay after power shutoff. The numbers in the figures refer to the top label in the legend and subsequent numbers refer to labels from top to bottom. For example, in Figures VI.3.16 the number 4 refers to 1,3X.5;2,4X1-1(2 and 3)B which represent heaters 1 and 3 at the 50% variac setting and heater 2 and 4 at the 100% variac setting. Channel assignments were previously discussed.

The B channels (male side) all have higher temperatures than the A channels (female side) which, as discussed earlier, resulted from the higher thermal inertia of the male side. The higher male side temperatures resulted from the retention of heat from previous experiments. The female side dissipates the heat much faster relative to the male side; thus, the male side heats up faster upon subsequent experiments.

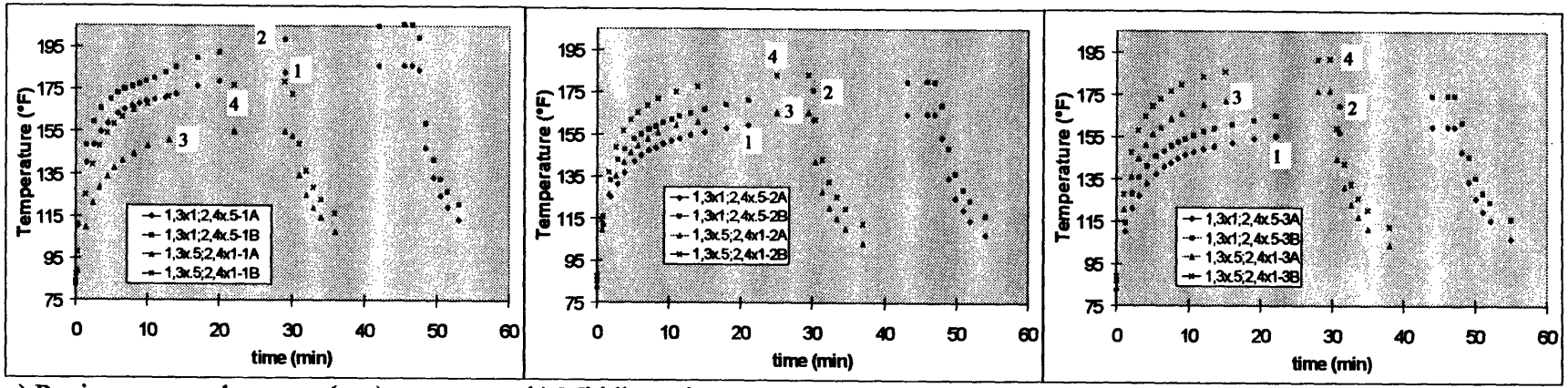

a) Region nearest the sprue (top). b) Middle region. c) Region furthest from the sprue (bottom).

Figure VI.3.16: Temperature response curves for min flow rates and skewed parabolic thermal profiles 1,3 - 2,4 100% or 50% of V_{max}.

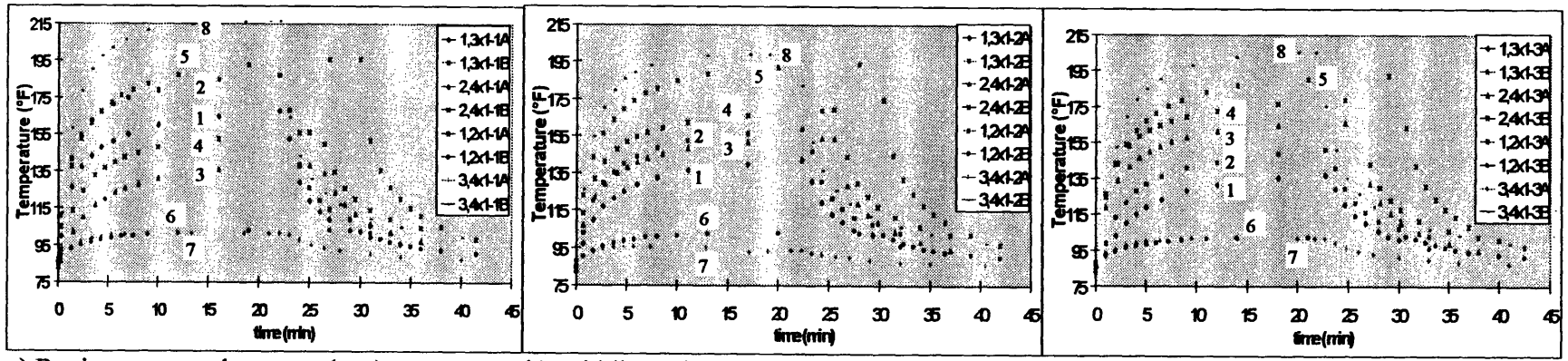

a) Region nearest the sprue (top). b) Middle region. c) Region furthest from the sprue (bottom).

Figure VI.3.17: Temperature response curves for minimum flow rates and 100% voltage (V_{max}) setting for 1,3; 2,4; 1,2; and 3,4.

Part III: Direct measurement of thermal profile effects on the part.

Eight 6 mm thick parts were molded with dynamic thermal boundaries. These eight will be compared to the seven molded conventionally in Section VI.2.

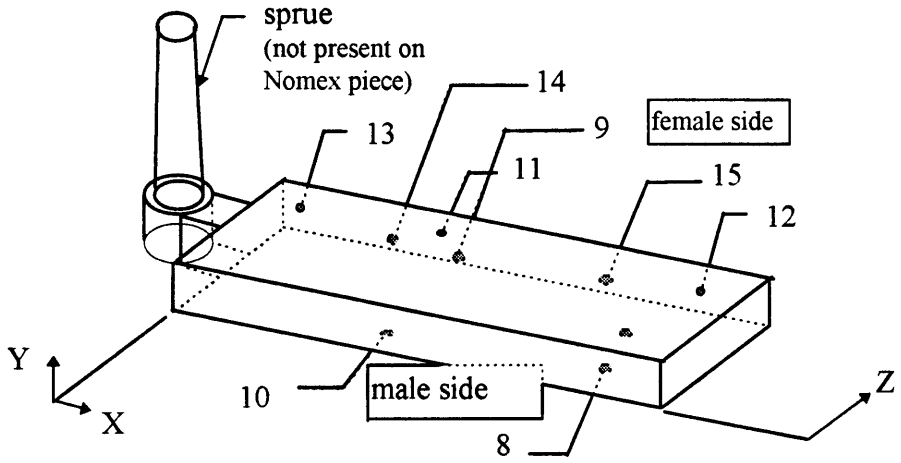

Figure VI.3.18: Final thermocouple locations for experiment sample numbers 8 to 15.

The results in Table VI.3.4 and Figure VI.3.19 can be compared to those given in Table VI.2.1 and Figure VI.2.9 (Section VI.2 b).

Table VI.3.4: Coordinate of thermocouple tip in the dynamic thermal boundary parts.

Thermocouple final location	Comments	Region (entrance, middle, end)
8. 2.285 x 0.196 x 0.064	1, 3 100%; 2, 4 50% min flow 6mm; badly warped	end
9. 1.208 x 0.043 x 0.529	1, 3 50%; 2, 4 100% min flow 6mm	middle
10. 1.130 x 0.066 x 0.170	1, 3 100% min flow 6mm	middle
11. 1.003 x 0.113 x 0.587	1, 3 100% max flow 6mm	middle
12. 2.168 x 0.082 x 0.615	1, 3 100% max flow 6mm; (extreme side)	end
13. 0.175 x 0.111 x 0.645	1, 2 100% min flow 6mm	entrance
14. 0.950 x 0.020 x 0.618	1, 2 100% min flow 6mm	middle
15. 1.771 x 0.043 x 0.582	2, 4 100% min flow 6 mm	end

Figure VI.3.19 shows the temperature decay of the respective thermocouples. Experiment number nine gave erroneous values of constant temperatures due the a short

in the thermocouple, so those values were excluded from the figure. Figure VI.3.19 a) shows the effect of the two parabolic and the two linear profiles on the polymer temperature decay. Figures VI.3.19 b) through d) show these decays for the three different regions discussed earlier. These profiles are shown only as references. The analyses of these profiles are compared to the no thermal control profiles in Figure VI.3.20.

The part was sectioned into three equal volume regions as discussed previously. The top region accounts for the region near the sprue. The middle region accounts for the following one third region. The end region accounts for the last third region which includes the end of the cavity. The experiment numbers are included for reference, and coordinates of the thermocouple tip are also listed.

It has been observed that the majority of the residual stress buildup occurs during solidification (after filling). Therefore, the temperature of concern is the temperature after the polymer fills the mold. The polymer temperature profile for the two skewed parabolics and the two linear profiles are all shown in Figure VI.3.20 a). The average temperature for all the profiles (190°F). The elevated mean temperature reduced the quenching effect of the hot polymer entering a cold mold. Consequently, the polymer temperature gradient should decrease regardless of the temperature gradient imposed on the mold. This reduced quenching effect can be seen in Figures VI.3.20 b) through d). The various polymer temperature profiles had a smaller maximum deviation than those without increasing the mold temperature. Therefore, to obtain more conclusive results it is necessary to reduce the mean temperature of the polymer and produce substantially larger temperature gradients than those that were achieved with the current system.

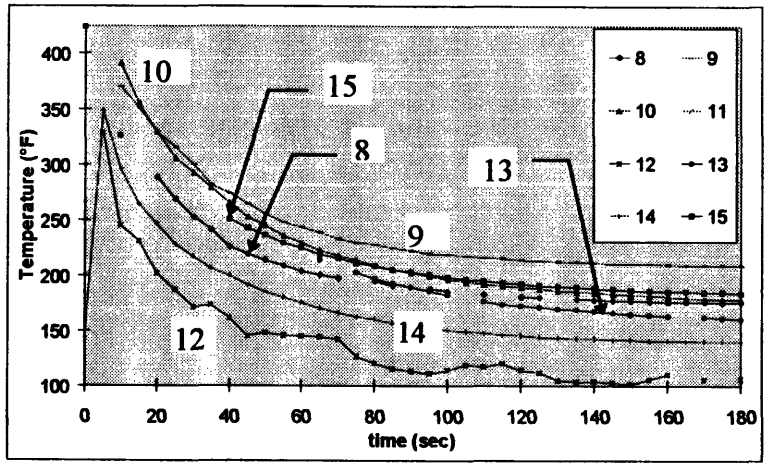

a) Comparison between different profiles for all regions.

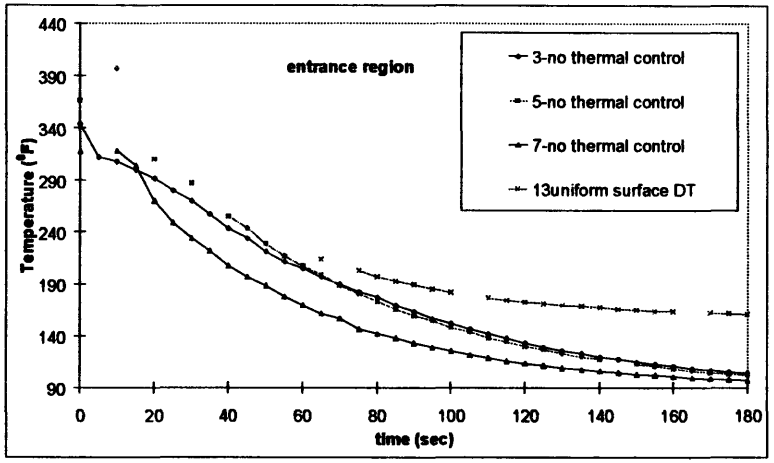

b) Comparison between different profiles for the entrance region.

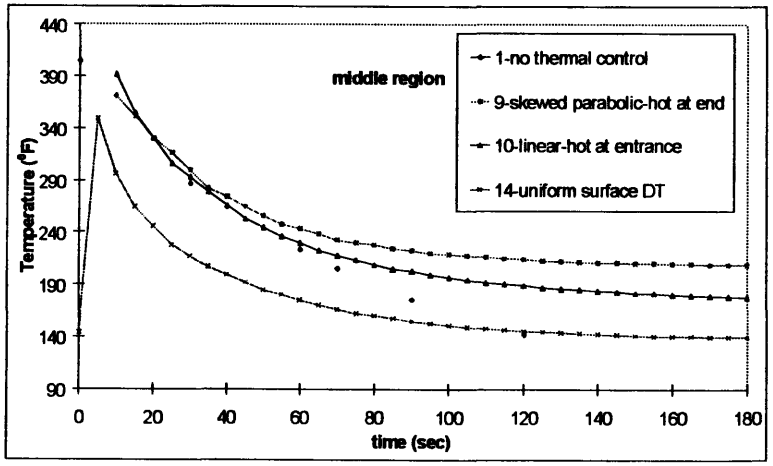

c) Comparison between different profiles for the middle region.

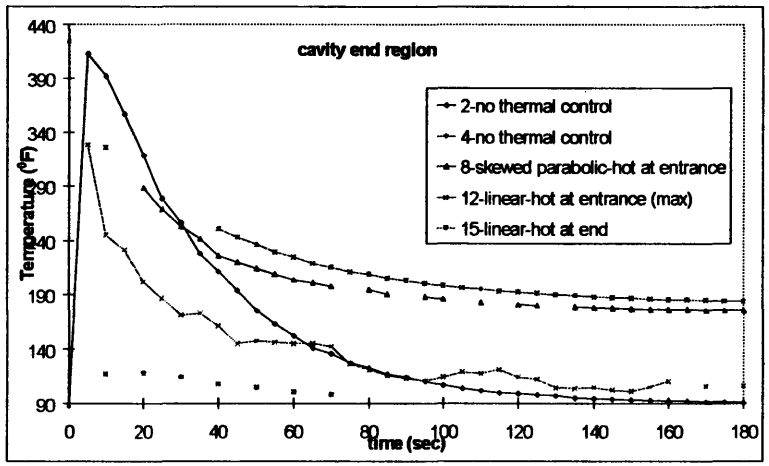

d) Comparison between different profiles for the end region.

Figure VI.3.19: Solidifying plastic thermal response in dynamic thermal boundary molding.

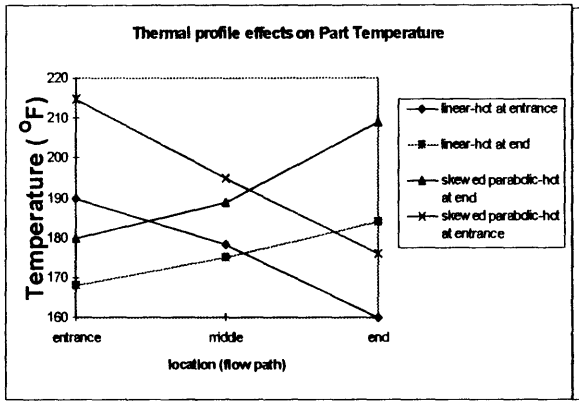

a) Two skewed parabolic and two linear.

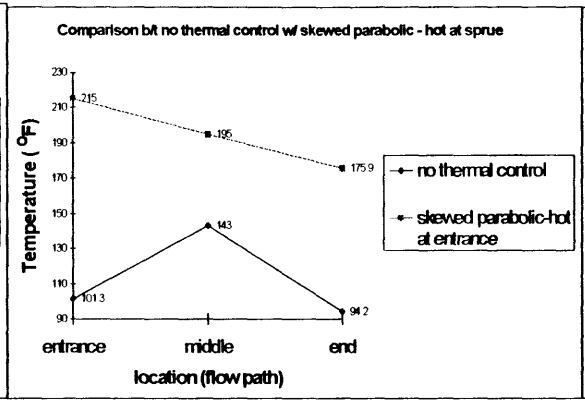

b) Skewed parabolic (hot near entrance).

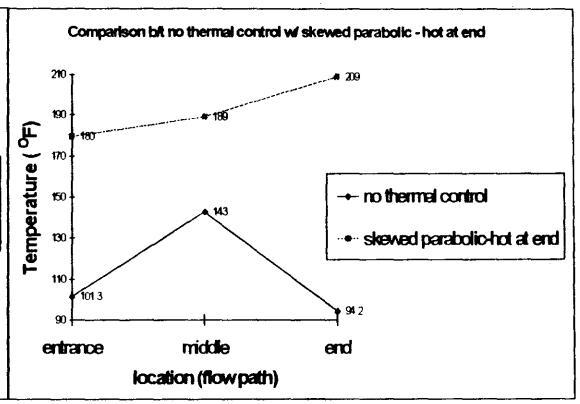

c) Skewed parabolic (hot near end).

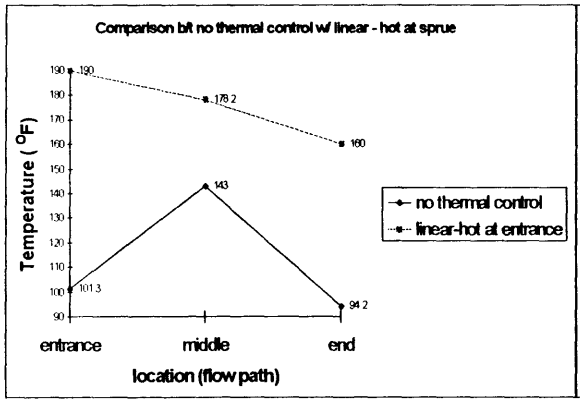

d) Linear (hot near entrance).

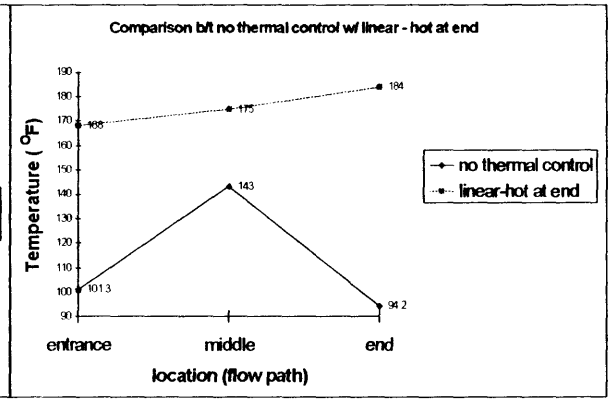

e) Linear (hot near end).

Figure VI.3.20: Polymer temperature comparison between no thermal control with two skewed parabolic or two linear profiles.

Experiment samples 8 and 9 both had large sink marks of comparable sizes on the surface facing the female mold except sample 8 had its sink mark start from the middle region to the end while sample 9 had its start from the top region to the middle. Comparing this observation to the steady state temperatures in Table VI.3.3, the hottest side of the cavity fills more completely and the colder side produced the sink marks. The sink marks appeared on the colder side because greater shrinkage occurred there and without pressure the plastic detached from the walls to relieve the stress buildup in that region. The desired skewed parabolic profile was not generated only an exponentially decaying profile was created with the variac settings.

Experiment sample 10 had a uniform sinking of the surface facing the female mold, but the higher flow rates experienced by samples 11 and 12 produced smaller uniform sink surface not only on the side facing the female but also on the male side of the part. These sink surfaces were comparable to those found in samples 1 through 7 from conventional molding. A hypothesis was made as to how these sink marks and sink surfaces are produced. Higher flow rates produce cooler and more balanced male and female mold surface temperatures. The lower surface temperatures produce the sink surfaces as evidenced by the more pronounced sink surface of sample 10. Thus, a minimum temperature is needed to prevent these sink surfaces which can be determined by adjusting the variac settings.

Experiment samples 13 and 14 provide further evidence that sink surfaces are caused by the cooler mold face. In these experiments only the heaters in the female mold were on, and the observed sink surface is now only on the male side.

Experiment sample 15 had a uniform sinking of the surface facing the female mold comparable to that of sample 10. Samples 15 and 10 had inverse mold temperature profiles where sample 15 had the end region hottest and sample 10 had the top region hottest. Sample 15 exhibited greater birefringence near the gate (top) region than sample 10; however sample 10 exhibited greater birefringence near the end region than sample 15.

These established steady state gradients might eliminate the need for low thermal inertia injection molding as it maintains the plastic at a uniform temperature during the

solidification portion of injection molding. However, low thermal inertia injection molds are needed for thermal profile manipulations. These gradients slow the heat transfer in some areas so that the overall process can produce parts that solidifies near the same temperatures. Again note that the melt is initially nonuniform in temperature as measured directly by the thermocouple so a constant surface temperature will not remedy the problem of warpage.

Figure VI.3.21 shows the thought process behind the implementation. Because the skin layer thickness is thicker near the entrance and acts as an insulator, the expected polymer temperature must be monotonically increasing. However, during the subsequent cooling phase the melt temperature was determined to have the profile shown in Figure VI.3.21 b). The hypothesis is that a mold thermal profile inverse to that of the polymer will produce a spatially isothermal part. The spatially isothermal part is hypothesized to minimize residual stresses.

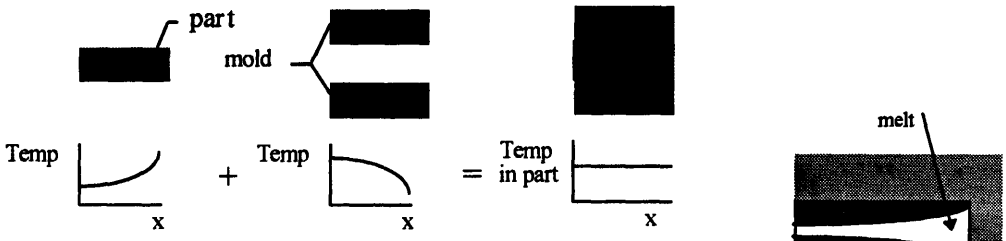

a) Temperature profiles during the filling phase.

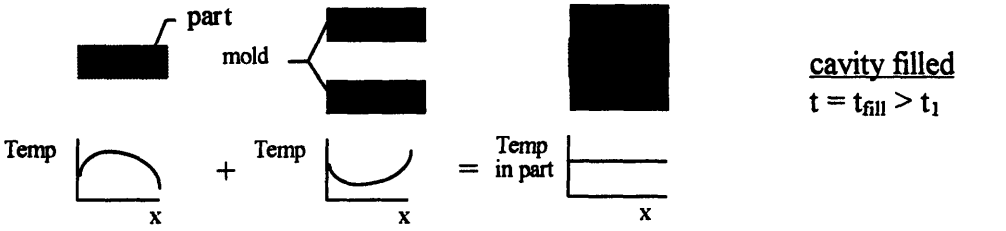

b) Temperature profiles during the post-filling (cooling) phase.
Figure VI.3.21: Temperature profiles during the filling and post-filling (cooling) phases.

The inverse mold thermal profile hypothesis has not been verfied because of the inability to generate mold temperature gradients higher than those observed in the polymer. The mold temperature gradients must be higher because the polymer is an insulator with respect to the metal mold; thus, the polymer has a higher thermal resistance.

Part IV Correlation of birefringence to residual stresses.

The following birefringence patterns shown in Figure VI.3.22 were taken using the optical system described in Section VI.2. The part observed was 2 mm thick. Selected regions (all near the sprue) were focused on to provide a comparison of the different patterns observable in the part.

a) Corner birefringence.

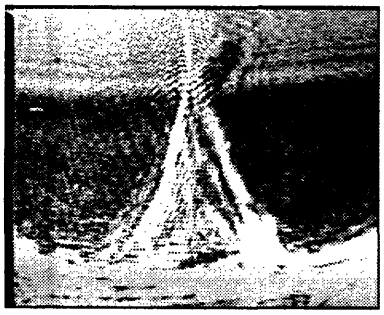

b) Gate birefringence.

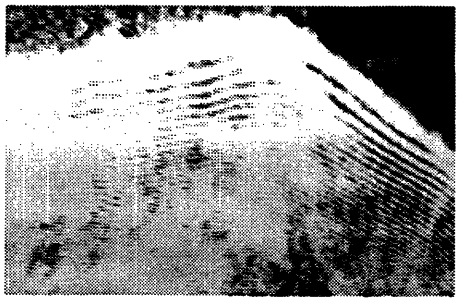

c) Opposite corner birefringence.

d) Center region birefringence.

Figure VI.3.22: Birefringence patterns of various locations in a part.

Figure VI.3.22 a) shows gradual disappearance of fringe patterns away from the corner. Similar patterns were observed in the opposite corner in Figure VI.3.22 c). The gate region (near the sprue) shows an unusual pattern. This pattern might be a result of the flow turning 90° (stagnation flow). The center region in Figure VI.3.22 d) is relatively free of residual stresses.

CHAPTER VII

Conclusions

VII.1 Summary Of Observations And Results

The end goal of injection molding research is to optimize the process to produce parts of consistently high quality. The focus of this research was on the manipulations of mold temperatures to achieve the goal. From the formulations developed in this thesis and backed by experimental evidence, a skewed parabolic thermal profile using warm temperatures near the gate region, colder temperatures in the middle region, and relatively hot temperatures at the end of the cavity maximally reduces the temperature gradients in the part; thus, maximally reduces the temperature nonuniformities that lead to residual stresses or warpage. The remainder of this thesis focused on quantifying this skewed parabolic profile and observing the effects of other thermal profile on final part characteristics. This chapter provides a overview of the results obtained in this investigation and discusses areas where potential for further research may lie.

- Formulations were derived for three thermal resistance considerations. These cases provide insight into the requirements of a specific low thermal inertia mold to the particular plastic being molded. The original equation numbers were used.

  - Case I: $\frac{T_m(\delta,t)-T_c}{T_c-T_o} << 1$ all the thermal resistance is in the mold

$$\frac{ds}{dt} = -\frac{k_m(T_m-T_o)}{\rho_p h_{sfp}\sqrt{\pi\alpha_m t}} \quad \Rightarrow \quad s(x) = s(x(t=0)) + \frac{2k_m(T_m-T_o)}{\rho_p h_{sfp}\sqrt{\pi\alpha_m}}\sqrt{\frac{x_{front}-x}{V_{inj}}} \qquad (22)$$

$$\text{for } t \le \frac{L_1}{V_{inj}} \text{ and } \delta_{99} \le L_1$$

This s(x) overpredicts the thickness since the melt is at a temperature higher than the solidification temperature T_m. At $t = \frac{L_1}{V_{inj}}$ the flow front has reached the end of the cavity and for $\delta_{99} > L_1$ the semi infinite body solution is no longer valid. After the plastic stops flowing and packing, the plastic will start to shrink; thus, perfect plastic and mold contact is no longer valid. These air gaps represent thermal contact resistant regions which hampers heat transfer. Therefore, warpage is a greater problem in a part with greater shrinkage capacity and possibly thinner section parts. Once the flow completely stops birefringence patterns disappear in the interior sections indicating a relaxation of stresses in the core region of the plastic. Intuitively this observation is reasonable since the core region is the unsolidified plastic no longer subjected to the shearing stress induced by the flow.

- Case II: $\frac{T_m(\delta,t) - T_c}{T_c - T_o} >> 1$ all the thermal resistance is in the plastic

This case considers a thermally controlled mold surface temperature. The formulations developed for this case provides a heat transfer lower limit for low thermal inertia injection molding.

$$\frac{ds}{dt} = (\frac{\zeta}{2})\sqrt{\frac{\alpha}{t}} \text{ and } s = \zeta\sqrt{\alpha_p t} \qquad (26)$$

where ζ is found from $Ja \equiv \frac{Cp_p(T_m - T_c)}{h_{sfp}} = \sqrt{\pi}(\frac{\zeta}{2}) \quad e^{(\frac{\zeta}{2})^2} \; erf(\frac{\zeta}{2})$.

which is valid for $t \geq 0^+$

$t=0^+$ when the front has reached that location in the mold ($x_{front} = x$)

The concept of variable wall temperatures can be applied to better simulate actual conditions of the thermally controlled mold surface. This case would best model thin sections where large ratios of thermal gradients to the thickness of the part exists.

- Case III: $\frac{T_m(\delta,t)-T_c}{T_c-T_o} \cong 1$

thermal resistance of solidifying material $\cong$ thermal resistance of the mold

$$\frac{ds}{dt} = (\frac{\zeta}{2})\sqrt{\frac{\alpha}{t}} \text{ and } s = \zeta\sqrt{\alpha_p t} \qquad (33)$$

where $$\zeta \cong \sqrt{\frac{2Cp_p(T_m-T_c)}{h_{sfp}}} \qquad (32)$$

and $$T_c = T_o - \frac{A}{2}(1-\sqrt{1-\frac{4(T_m-T_o)}{A}}) \qquad (31)$$

and $$A \equiv \frac{\pi\rho_p{}^2 h_{sfp} Cp_p \alpha_p (T_m-T_c)\alpha_m}{2k_m{}^2} \qquad (30)$$

- Furthermore, a formulation for warpage was also developed incorporating the calculated skin layer thickness calculated in one of the three above cases.

$$\Lambda_{net} = |\Lambda_1 - \Lambda_2| \qquad (46)$$

where Λ is the warpage induced by the solidified skin layer and the additional solidified layer at the point when the two flow fronts meet.

There is one on each side of the mold just prior to the meeting of the two solidification fronts. (Λ is the y direction thickness measured from the surface of the mold)

where $$\Lambda = \frac{L_1{}^2}{8y}(\frac{\sigma_x}{E}+\alpha\Delta T) \qquad (45)$$

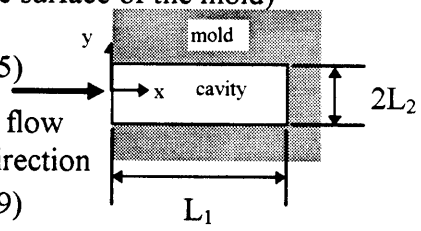

where $\sigma_x(y) = -\alpha E\Delta T(y) + C_1 y + C_2$ (39)

$$\Rightarrow C_1 = \frac{12}{L_2{}^3}\int_{-\frac{L_2}{2}}^{\frac{L_2}{2}} \alpha E y \Delta T(y)\ dy \quad \text{and} \quad C_2 = \frac{1}{L_2}\int_{-\frac{L_2}{2}}^{\frac{L_2}{2}} \alpha E \Delta T(y)\ dy \qquad (42)$$

More accurately, s (skin layer thickness at the time the solidification fronts meet) should be used but $s \approx L_2$ (half thickness of the part) and $s = L_2$ for a completely balanced cooling. An accurate calculation of s is needed to compute the final warpage of the part.

This formulation is restricted to rectangular parts $L_1 >> 2L_2 (=2s) >> W$

where W is the width of the rectangular part into the page and the temperature gradient is in the y direction only ($\Delta T(y)$ only):

This analysis explains the phenomenon of the plastic bends towards the hotter side after the mold opens. The hotter side has a smaller Λ, so Λ_{net} pushes the plastic towards the hotter side.

Figure VI.3.21 shows the thought process behind the thermal implementation. Because the skin layer thickness is thicker near the entrance and acts as an insulator, the expected polymer temperature must be monotonically increasing. However, during the subsequent cooling phase the melt temperature was determined to have the profile shown in Figure VI.3.21 b). The hypothesis is that a mold thermal profile inverse to that of the polymer will produce a spatially isothermal part. The spatially isothermal part is hypothesized to minimize residual stresses.

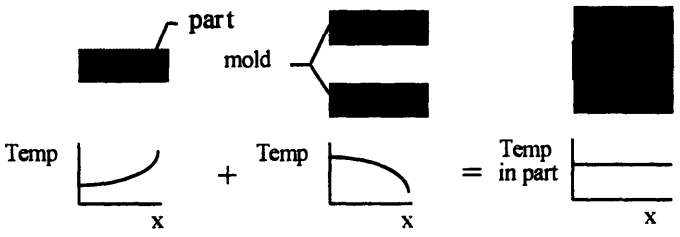

a) Temperature profiles during the filling phase.

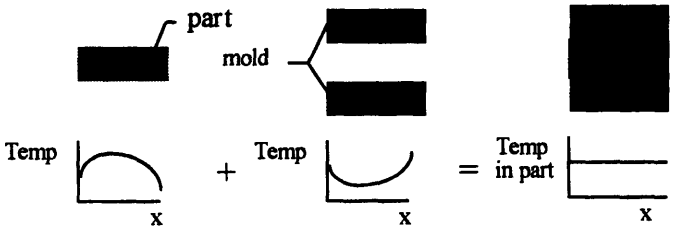

b) Temperature profiles during the post-filling (cooling) phase.

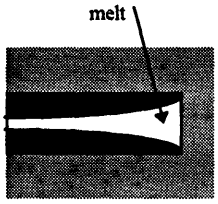

cavity filled
$t = t_{fill} > t_1$

Figure VI.3.21: Temperature profiles during the filling and post-filling (cooling) phases.

The inverse mold thermal profile hypothesis has not been verfied because of the inability to generate mold temperature gradients higher than those observed in the

polymer. The mold temperature gradients must be higher because the polymer is an insulator with respect to the metal mold; thus, the polymer has a higher thermal resistance.

A summary of observations and results obtained from the conventional molding follows:

- Utilizing the stepped lamination layer method to obtain part temperatures during solidification, the middle region of a rectangular molded part was determined to be the hottest, followed by top region, then the end region was the coldest by directly measuring the part's temperature.

A summary of observations and results obtained from the dynamic thermal boundary molding follows:

- The melt temperature distribution entering the mold from the injection unit nozzle is nonuniform because the melt temperature distribution in the nozzle and barrel of the injection unit is nonuniform prior to injection. The temporal and spatial temperature variations can be as great as 10°F, 15°F respectively
- Typical heaters can have heat flux nonuniformities; thus, rapid cycling of the mold may present a detriment to part qualities.
- Thermal inertia of the two mold halves might be unbalanced; thus, inputting the same heat flux will not produce the same effects. A simple test was developed in this thesis to quantify the degree of imbalance using a thermocouple—mold—Nomex (insulator) sandwich.
- Arbitrary thermal profiles can be generated using linear combinations of independent bases of thermal profiles generated from different voltage levels and water flow rates (Table VI.3.2).
- Using the stepped lamination layer method, which exaggerates distortions, allows the relaxation of stresses to be directly observed on the part (no packing pressure). Thus, different combinations of temperature profiles and flow rates can be investigated to produce parts without sink marks or surfaces and provide reduced residual stresses.

VII.2 Future Research

Mold temperature gradients in the mold must be greater than those in the polymer. These mold thermal gradients were not achieved with the present thermal control system. It is possible to achieve higher gradients using conformal heating and cooling passages.

It might be possible to design an optical sensor that can detect the onset of polymer solidification and residual stress levels using fibre optic techniques similar to those developed by Bur, Wang, Thomas, and Rose[104]. Then an optical controls algorithm could be developed where the level of energy input would be proportional to the residual stresses recorded (register the total intensity of birefringence of an area) as well as switch the type of thermal profiles used during the switch for filling, just prior to complete solidification and cooling. The higher intensity correlates with more fringe patterns which is an area of greater stress concentration. These higher intensity areas can be mapped out and heating units can become more active or cooling water flow rates can be reduced in these areas.

A more detailed model of heat transfer effects can lead to not only producing reduced residual stresses in injection molded parts, but also the thermal profiles might be used to manipulate the plastic into complex shapes (preferential warpage) that cannot be realized by current injection molding methods. An example would be a burst of heat flux might induce convection in a local region allowing the incorporation of air bubble in the plastic; therefore, the part will have a bubble or any complex enclosed shape at a preset location. This phenomenon was observed in Earl Sun's research.[105]

---

[104] Bur, A.J., F.W. Wang, C.L. Thomas, and J.L. Rose, "In-Line Optical Monitoring of Polymer Injection Molding," Polymer Engineering and Science, 34, 8, (April 1994).

[105] Sun, E.S., *Implementation of Low Thermal Inertia Injection Molds Using Conformal Passages*, Master of Science Thesis, M.I.T., 1995.

A. Property Data

A collection of property data for polystyrene was gathered from various technical papers. They can be used to compare and/or corroborate the formulations given in this thesis. Mold properties are also included.

Table of Rheological Parameters for Dow Styron 685D[106]

Power law fit: $\eta = A\ e^{\frac{B}{T}} \dot{\gamma}^{-(n-1)}$

$A = 80.1$ poise s^{n-1}

$B = 3635$ (K)

$n = 0.32$

$N_1 = A'\sigma_{12}^{\beta}$

$A' = 1.432 \times 10^3$ (dyn cm^2)$^{1-\beta}$

Constitutive law: $\eta_o = 1.05 \times 10^5$ poise

$a_M = 0.07$

$\tau_o = 0.94$ s

WLF constants ($T < 205°C$): $C_1 = 24.26$ $C_2 = 309.4°C$

Arrhenius constants ($T > 205°C$): $D = 6.131 \times 10^{-11}$ $\Delta E = 2.26$ kcal

Stress-optical coefficient: $C = 4.5 \times 10^{-10}$ cm^2 dyn^{-1}

Table of Rheological Parameters for Dow Styron 678E[107]

Leonov: $N = 2$ $s = 0.009$ $T_{ref} = 190°C$

$\eta_1 = 5142$ Pas $\theta_1 = 0.66$ s

$h_2 = 1622$ Pas $q_2 = 0.025$ s

Tait: $v_{g,0} = 0.9758$ cm^3/g; $T_{g,0} = 100°C$

	b_1 (Pa)	b_2 (1/°C)	b_3 (m^3/kg°C)
solid	3.5×10^8	3.0×10^{-3}	2.3×10^{-7}
fluid	2.4×10^8	3.6×10^{-3}	5.8×10^{-7}

Spencer Gilmore: $(p + \hat{p})(v - \hat{v}) = R\,T$

$\hat{p} = 1.86 \times 10^8$ N/m^2; $\hat{v} = 8.2 \times 10^{-4}$ m^3/kg; $R = 80$ J/kg K

---

[106] Greener, J. and Pearson, G.H. "Orientation Residual Stresses and Birefringence in Injection Molding"

[107] Flaman A.A.M. "Buildup and Relaxation of Molecular Orientation in Injection Molding. Part I: Formulation"

W.L.F.: $C_1 = 24.26$ $C_2 = 309.4°C$ $T_{ref} = 190°C$

Thermal: $k = 0.17$ W/m K $c_p = 2100$ J/kg K

Stress optical coefficient: $C = -4.8 \times 10^{-9}$ N/m^2

Power law with pressure dependence[108]: $\eta = m\ e^{\beta P} e^{CT} \dot{\gamma}^{n-1}$

$m = 3873.9$ Pa sec $C = -0.0136379$ $\beta = 3.5 \times 10^{-8}$ m^2/ N $n = 0.395$

Tait $\rho = V_o^{-1} [1 - C \ln(1 + \frac{P}{B(T)})]^{-1}$

$v_o(T) = b_1 + b_2(T - b_5)$

$B(T) = b_3 e^{-b_4 T}$

$b_1 = 9.6 \times 10^{-4}$ m^3/kg, $b_2 = 2.2 \times 10^{-7}$ m^3/kg K, $b_3 = 2.44 \times 10^8$ N/m^2, $b_4 = 4.14 \times 10^{-3}$ 1/°C and $b_5 = 100°C$

Isotropic Material Properties of an Amorphous polymer (polystyrene)[109]

Mechanical properties of solid polystyrene:

elastic modulus E	2.431×10^9 N/m^2
Poisson's ratio ν	0.35

Thermal Properties

thermal expansion coefficient α	50×10^{-6} m /m K
glass transition temperature T_g	100°C
heat conductivity k	0.126 J/s m K
material density ρ	1.05×10^3 kg/m^3
heat capacity C	2100.0 J/kg K

Thermophysical Data Of The Mold.

Mold material	Mold Temp. [°C]	Thermal conductivity [W/mK]	Specific Heat [J/Kg K]	Density [kg/m^3]	Thermal Diffusivity [m^2/s]
Aluminum	27	237	903	2702	97.1×10^{-6}
Stainless Steel (AISI 304)	27	14.9	477	7900	3.95×10^{-6}

[108] Chen, S.-C., Cheng, N.-T., and Jeng, K.-K., "Post-Filling Simulation and Analyses of Shrinkage and Warpage of the Injection Molded Parts"

[109] Rietveld, J.X., and Liu, S.-J., "Simulation of Warpage Caused by Thermal and Geometric Asymmetries in Injection Molded Articles"

B. Optics Background and Calibration Procedure

The calibration procedures and the background theory for the optical instruments are as follows:

The polarizer plane of vibration should be at 45° to the optic axis of the quarter-wave plate for an emerging circularly polarized light. The second quarter-wave plate should be aligned with the first so that without the sample a phase difference of either zero or 180° emerges. In either case the light will now be plane-polarized and can be made to suffer complete extinction by rotating a polarizer in its path. Circularly polarized light cannot produce interference effects (the intensity of the resultant light wave, averaged over one or more cycles of oscillation, is the same no matter what phase difference exists between the two waves).

If linear polarized light passes through a transparent polymer, the light will interact with the electrons of the polymer. Under the influence of the electric field E, the mobility of the electrons relative to the positive core creates a dipole moment p. The coefficient $\alpha = p / E$ is called the polarizability, which is directly related to the refractive index n of the polymer. Birefringence materials are characterized by the fact that the polarizability has different values in different Cartesian coordinate directions and, therefore, α is a tensor.

By definition, the refractive index is linked to the phase velocity c as well as to the wavelength λ: Increase in refractive index results in a decrease of phase velocity and a shortening of the wavelength:

$n = n/n_o = c_o/c = \lambda_o/\lambda$

n_o, , c_o, λ_o :in vacuum (air), $n_o = 1$

n, c, λ.: in polymer

For a circularly polarized light the electric vectors are equal in magnitude and are oriented orthogonally in x- and y- directions and the light propagates in the z-direction. As the light pass through the sample, the electric vectors see different polarization of the electrons, and experience different refractive indices n_x and n_y . This results in a phase difference in the waves as they pass through the medium. This phase difference remains constant after both beams leave the medium and depends on the difference between n_x and n_y as well as the path length d through the medium. Its sign may be positive or negative.[110]

[110] Siebourg, W., et al. Birefringence-An Important Property of Plastic Substrates for Magneto-Optical Storage Disks.

C. Machine Drawings Of Test Mold Components

The components of the test mold consist of the female and the male molds, and the 6, 4, or 2 mm laminations layers with the accompanying Plexiglas windows. Drawings of the jig plate to hold the optical equipment and a drawing of the laser components are also included.

The drawing for the female part includes a view of section A-A which cut the plane where the sprue hole sits.

The drawing for the 2 mm lamination layers is included but the drawings for the 4 mm and the 6 mm lamination layers were excluded. The latter drawings are redundant except for the change in thickness of the lamination layer.

(Note: 2 mm = 0.07874 inches, 4 mm = 0.15748 inches, and 6 mm = 0.23622 inches.)

The autocad drawings of the jig plate hole locations generated the coordinates and the hole sizes for the CNC machine. The precision of the maching was ±0.0005. Thus only the fourth decimal (±0.0001) was specified for the dimensions. The dimensions had to be accurate to ensure proper alignment to each other as well as through the sample.

The dimensions of the drawings on the following pages are all in inches. Furthermore, the drawings are not to scale.

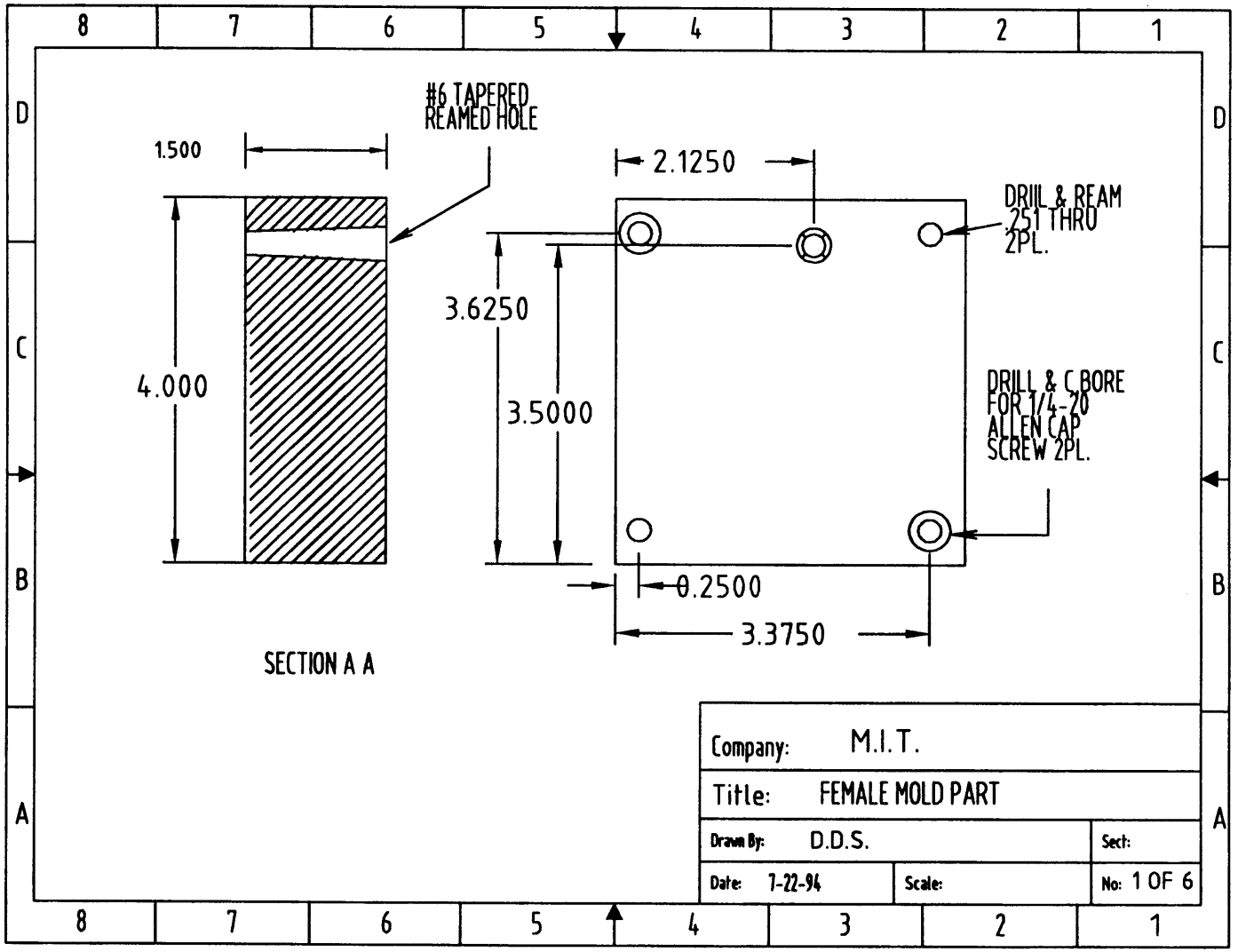
8
7
6
5
4
3
2
1
D
C
B
A
#6 TAPERED
REAMED HOLE
1.500
2.1250
DRILL & REAM
.251 THRU
2PL.
3.6250
4.000
3.5000
DRILL & C'BORE
FOR 1/4-20
ALLEN CAP
SCREW 2PL.
0.2500
3.3750
SECTION A A
Company: M.I.T.
Title: FEMALE MOLD PART
Drawn By: D.D.S.
Sect:
Date: 7-22-94
Scale:
No: 1 OF 6

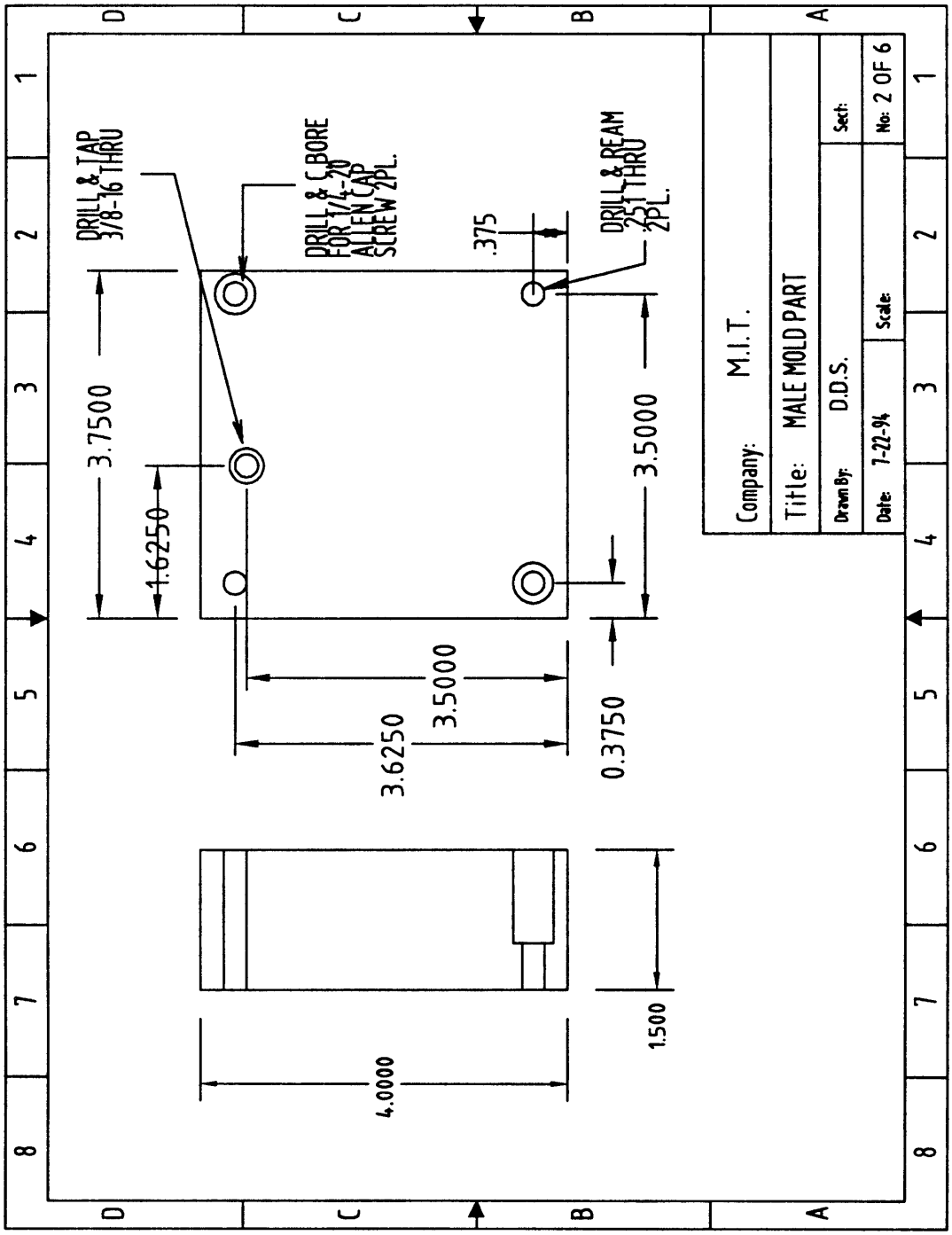
DRILL & TAP
3/8-16 THRU
DRILL & C'BORE
FOR 1/4-20
ALLEN CAP
SCREW 2PL.
.375
DRILL & REAM
.251 THRU
2PL.
3.7500
1.6250
3.5000
3.5000
3.6250
0.3750
4.0000
1.500
Company: M.I.T.
Title: MALE MOLD PART
Drawn By: D.D.S.
Sect:
Date: 7-22-94
Scale:
No: 2 OF 6

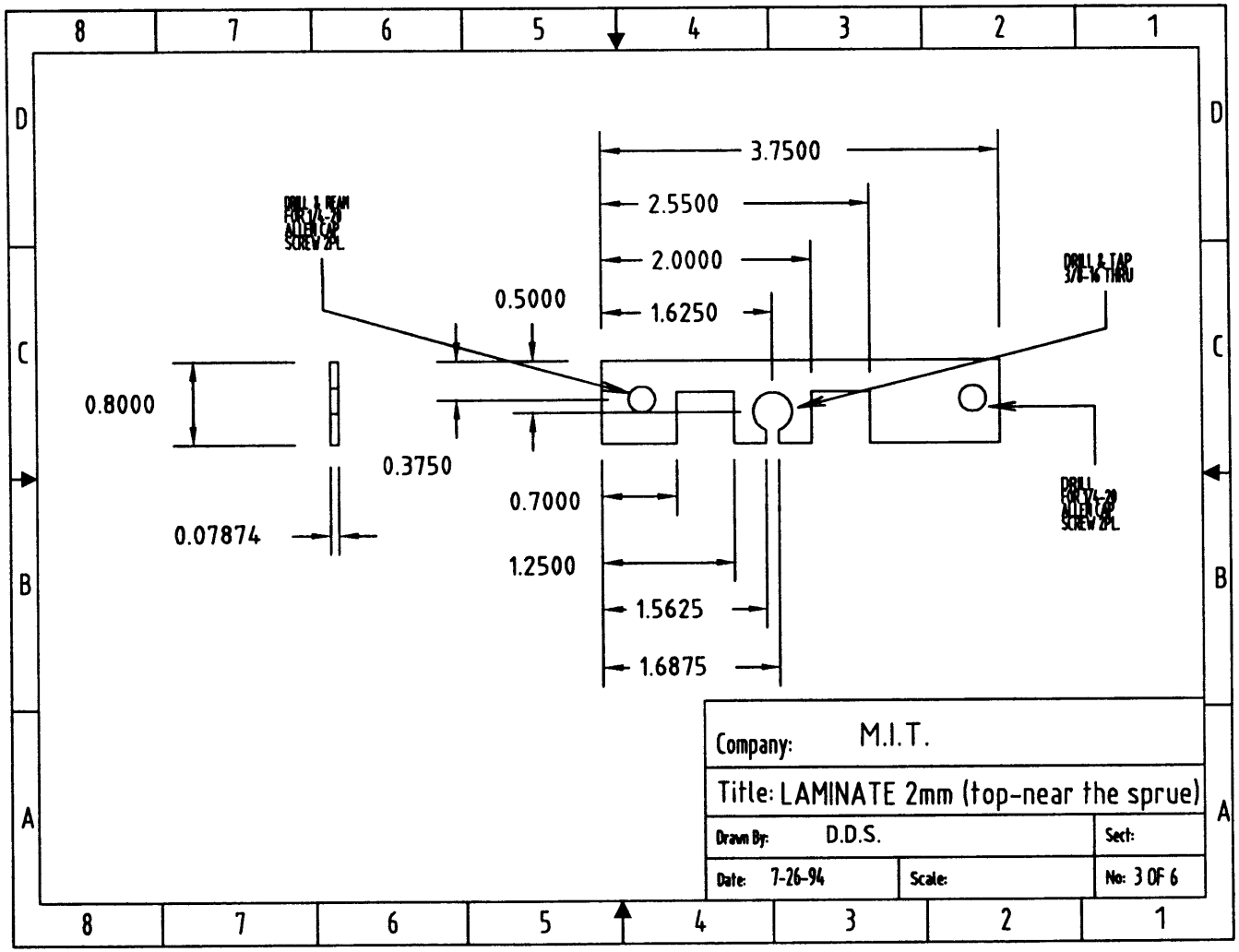
8
7
6
5
4
3
2
1
D
C
B
A
3.7500
2.5500
2.0000
1.6250
0.5000
0.8000
0.3750
0.07874
0.7000
1.2500
1.5625
1.6875
DRILL & REAM FOR 1/4-20 ALLEN CAP SCREW 2PL
DRILL & TAP 5/16-18 THRU
DRILL FOR 1/4-20 ALLEN CAP SCREW 2PL
Company: M.I.T.
Title: LAMINATE 2mm (top-near the sprue)
Drawn By: D.D.S.
Sect:
Date: 7-26-94
Scale:
No: 3 OF 6

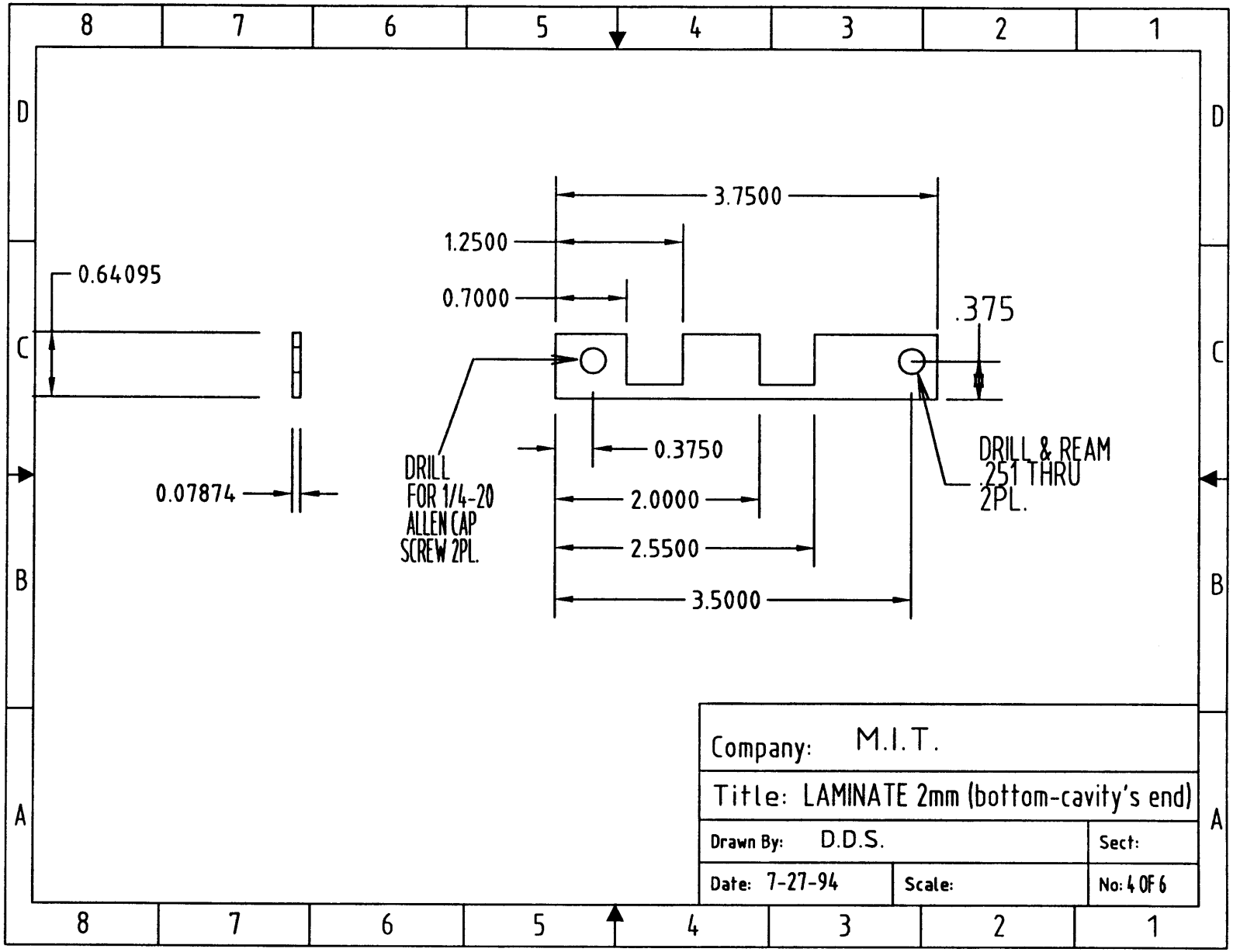
8
7
6
5
4
3
2
1
D
C
B
A
3.7500
1.2500
0.7000
0.64095
.375
0.3750
2.0000
2.5500
3.5000
0.07874
DRILL
FOR 1/4-20
ALLEN CAP
SCREW 2PL.
DRILL & REAM
.251 THRU
2PL.
Company: M.I.T.
Title: LAMINATE 2mm (bottom-cavity's end)
Drawn By: D.D.S.
Sect:
Date: 7-27-94
Scale:
No: 4 OF 6

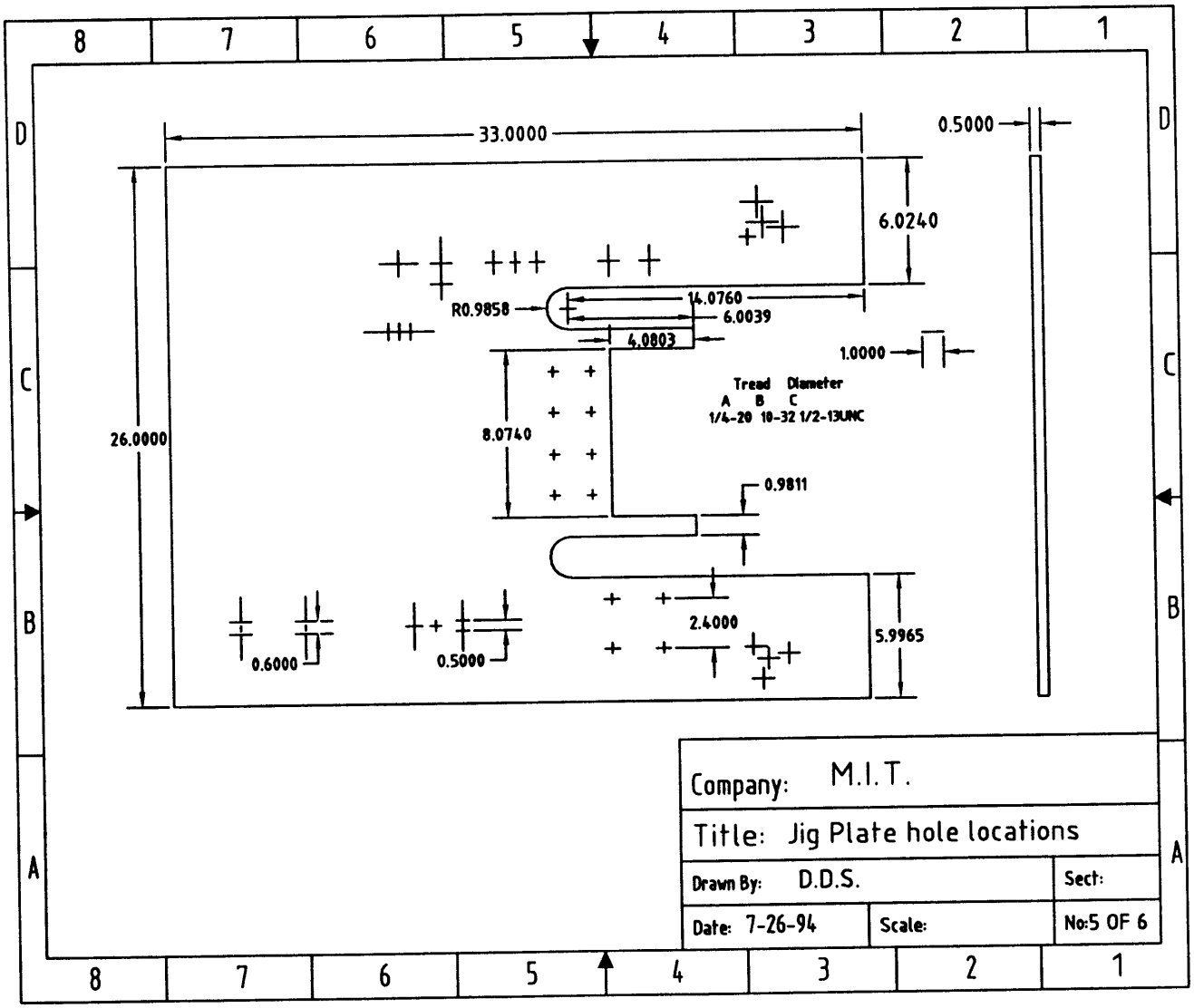
8
7
6
5
4
3
2
1
D
C
B
A
33.0000
0.5000
6.0240
R0.9858
14.0760
6.0039
4.0803
1.0000
Tread Diameter
A B C
1/4-20 10-32 1/2-13UNC
26.0000
8.0740
0.9811
2.4000
5.9965
0.6000
0.5000
Company: M.I.T.
Title: Jig Plate hole locations
Drawn By: D.D.S.
Sect:
Date: 7-26-94
Scale:
No:5 OF 6

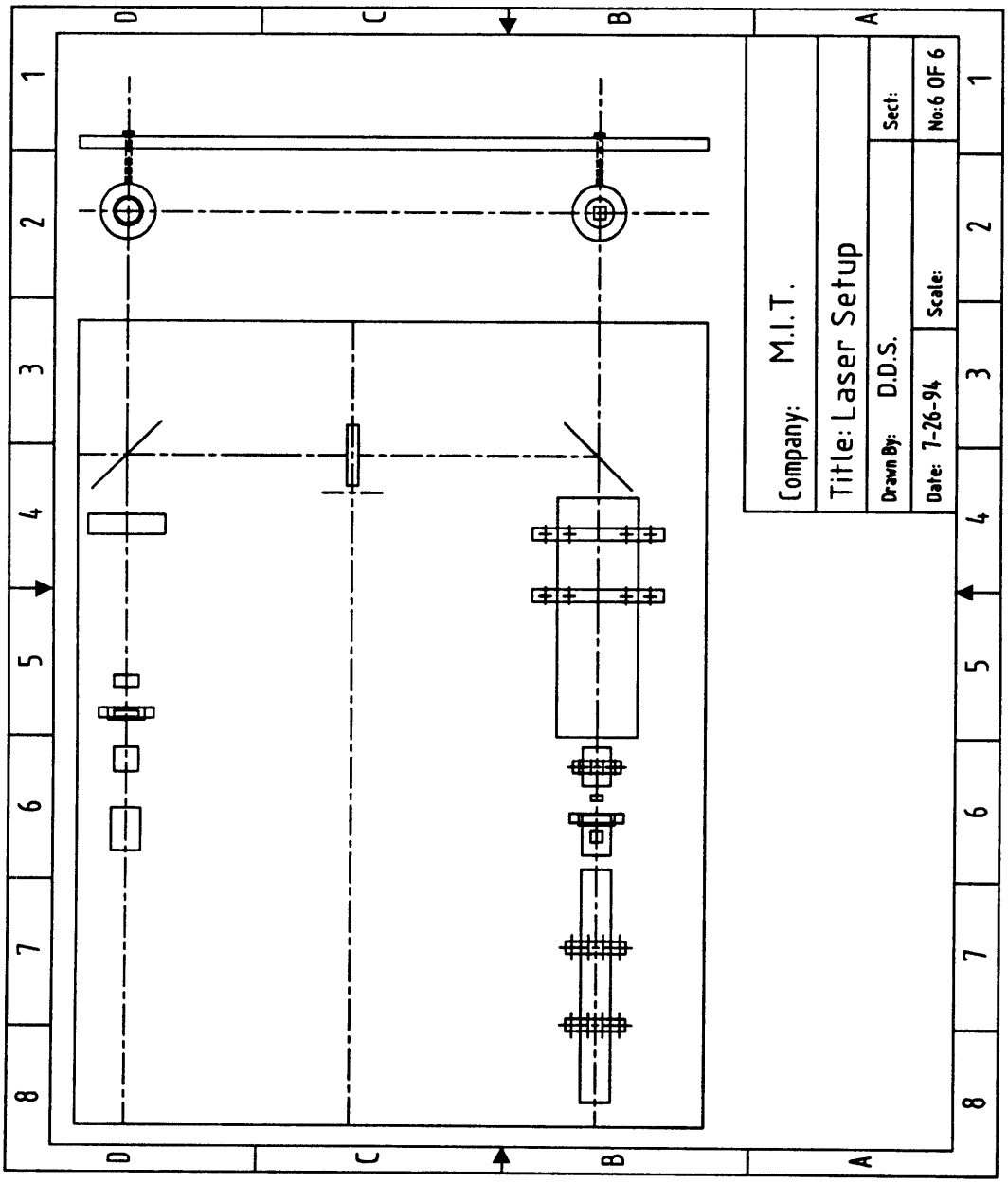
Company: M.I.T.
Title: Laser Setup
Drawn By: D.D.S.
Date: 7-26-94
Sect:
Scale:
No:6 OF 6